Journal of Archaeological Science 137 (2022) 105474

Contents lists available at ScienceDirect

Journal of Archaeological Science

journal homepage: www.elsevier.com/locate/jas

New findings of ancient Greek silver sources

Markos Vaxevanopoulos [a,*], Janne Blichert-Toft [a], Gillan Davis [b], Francis Albarède [a]

[a] Ecole Normale Supérieure de Lyon, CNRS, And Université de Lyon, France
[b] Australian Catholic University, Sydney, Australia

ARTICLE INFO

Keywords:
Lead isotopes
Ancient mining
Lavrion
Dysoron
Greece
Model ages
Silver

ABSTRACT

Over the last 60 years, much analytical research has sought to determine the ore sources of ancient Greek silver artefacts. Lead isotopic analysis has played a key role in this endeavor. While most studies so far have limited their search to places mentioned in historical sources, the present study takes a different approach by first identifying Ag-bearing ore sources in the Aegean world based on their geological characteristics and then using Pb isotopes to determine whether they were exploited in antiquity. To this end, we have geolocated, sampled, and measured high-precision Pb isotopic compositions of 17 Ag-bearing mineralizations in Greece for which we have evidence of ancient mining activity, and a further 10 exhibiting minor Ag occurrences that may also have been exploited in ancient times. We found that Pb model ages provide better discrimination of ore sources than the more conventional plots of raw Pb isotope data.

Our study establishes Lavrion, northeast Chalkidiki, Pangaeon, Thasos, Siphnos, Palaea Kavala, Angistron, and south Euboea as the most important ancient silver mining districts in Greece. Two previously undiscovered ancient mining areas in Pelion and in the Kroussia mountain range are also documented. The latter may be identified with ancient Mount Dysoron, from which King Alexander I of Macedon reportedly extracted the fabulous sum of a talent of silver per day. For the first time, we isotopically differentiate some of the mining districts in Thraco-Macedonia, and show that the mines of Thasos include geologically different silver-bearing ore sources. We further identify the hitherto unrealized importance of Euboean silver mines and demonstrate that they isotopically overlap those of Siphnos, with major implications for our understanding of ancient Greek history.

1. Introduction

Understanding metal production and circulation in antiquity is directly related to our knowledge of ore sources, but, for the most part, these are uncertain. The main reasons for these uncertainties derive from the primary tool used to track ore sources, namely Pb isotopes. First and foremost, similar Pb isotopic compositions can be found in more than one locality, especially if provenance is determined exclusively with the help of two-dimensional Pb isotope plots. Coincidence in full-fledged three-dimensional space is required to robustly establish a source (Albarède et al., 2020). Other reasons are the analytical quality of the Pb isotope data, the mineralogy of the ore in question (e.g. galena, chalcopyrite), and the nature of the object (e.g. artefact, slag) used to represent a given locality. Lead isotopic analysis (LIA) has long been widely used for Pb–Cu–Ag-bearing ore deposits to assign provenance to copper/lead/silver artefacts as it has proved to be the most reliable analytical technique for providing coherent provenance signatures, especially in coin provenance studies (Gentner et al., 1978; Gale, 1979; Chamberlain and Gale, 1980; Gale et al., 1980; Wagner et al., 1980; Wagner and Weisgerber, 1985; Artioli et al., 2020; Killick et al., 2020). During the 1960s, sampling and Pb isotopic measurement established Pb isotopic signatures for some major ancient mining districts including Lavrion (in Attica, Greece), Asia Minor, southern Iberia (Spain), and Roman Britain (Brill and Wampler, 1965, 1967; Grögler et al., 1966). A major study of Greek ore deposits published by Gale et al. (1980) for Lavrion, the Cyclades, and northern Greece, as well as many silver coinages, using different Pb isotopic ratios has underpinned most subsequent historical understandings of silver extraction and usage in archaic Greek coin production.

The identification of ancient metal sources is based on the study of ancient mining territories and sampling of the related mineralizations combined with the study of the archeometallurgical remains and applied metallurgical processes. Provenance studies using LIA may encounter problems such as mixing during smelting, cupellation, or refining

* Corresponding author.
E-mail addresses: Markos.vaxevanopoulos@ens-lyon.fr, Vaxevanopoulos@gmail.com (M. Vaxevanopoulos).

https://doi.org/10.1016/j.jas.2021.105474
Received 4 June 2021; Received in revised form 17 August 2021; Accepted 24 August 2021
Available online 8 December 2021

(though unlikely for small operations), as well as isotopic overlap between different ore deposits. Nevertheless, LIA is a powerful tool for *excluding* a given ore district as a raw silver-lead provider (Stos-Gale and Gale, 2009). To help avoid erroneous source assignments using LIA, complementary archeological evidence obtained from mining/metallurgical operations and artefacts should be taken into consideration as well. However, the exact periods of ancient exploitation may be difficult to establish as it is not always possible to find archeologically datable material in a mine. Additionally, long-lasting exploitation poses interpretative difficulties because subsequent mining activity has often superimposed and hence obliterated earlier mining phases - an acute problem especially for Lavrion and Siphnos.

In this study, we first geolocated the Ag occurrences in Greece and obtained samples from those areas where the archeological and geological features indicate the existence or likelihood of ancient mining (Fig. 1). Our approach relies on understanding the geological processes that determine where silver ores could have formed, rather than reckoning with largely anecdotal information provided by ancient writers that has happened to survive. The geological context of Greece can be described as the subduction of the African (tectonic) plate under continental Europe over the last 200 million years. During this period, convergence, obduction, collision, and subduction of geotectonic units, nappe stacking, slab retreats, and tearing processes constituted the main compounds of the geotectonic processes in the Aegean (Pe-Piper and Piper, 2002; Schmid et al., 2008, 2020; Jolivet and Brun, 2010; Jolivet et al., 2013; Menant et al., 2016). Numerous Ag-bearing mineralizations in Greece are associated with intrusion-related veins, skarns, carbonate replacements, and epithermal systems (Melfos and Voudouris, 2017; Voudouris et al., 2019; Ross et al., 2020). The different types of Ag occurrences located mainly in the Rhodope massif, the Serbo-Macedonian zone, the Circum-Rhodope Belt, and the Attic-Cycladic crystalline complex are listed in Table 1 and shown in Fig. 2. Further information on the geotectonic evolution of Greece and its relationship with mineralizations found in ancient mining areas, as well as detailed descriptions of the archeological settings, are included in the supplementary material (Appendices I-II).

Following this first step which underpins our sample selection, we undertook a broad, high-precision Pb isotopic survey of the ores found at ancient mining localities in Greece with the expectation that improved state-of-the-art analytical quality would help associate Ag-bearing ores with metal use. The acquired high-precision Pb isotope data were used to calculate 'Pb model ages' using the parameters of Albarède and Juteau (1984) and the equations of Albarède et al. (2012). The advantage of Pb model ages is that they define ore provenance better than conventional two-dimensional plots of unprocessed (raw) Pb isotopic ratios by supplying additional information and clarity. Lead model ages establish the geological age of initial Pb segregation from the crustal source to form the ore precursor. The U/Pb (μ) and Th/U (κ) ratios, also deduced from the measured Pb isotopic abundances of the ores, constitute two additional sensitive parameters characteristic of their crustal source (Albarède et al., 2012, 2021). Lead model ages tend to be distributed in well-defined frequency peaks which represent a useful and strongly visual tool (Milot et al., 2021). By contrast, plots of conventional raw Pb isotopic ratios normalized to ^{204}Pb show strong

Fig. 1. Geographic map depicting the Ag-bearing mineralizations of Greece (base map modified after SRTM worldwide elevation data 3-arc-second resolution).

Table 1
Characteristics of Ag-bearing mineralizations in Greece.

	Ore District	Geotectonic Unit	Other Major Metal Compounds	Host Geology	Deposit Type/Style	mineralization Age	Indicative References
1	Lavrion	Attic-Cycladic Massif	Pb, Zn, Fe, Cu, As, Sn, Au	Marble, schist, granodiorite	Carbonate replacement, veins, intrusion related	Upper Miocene	Marinos and Petracheck (1956); Conophagos (1980); Voudouris et al (2008a; b); Bonsall et al (2011); Voudouris et al (2021)
2	South Euboea	Attic-Cycladic Massif	Pb, Zn, Cu, Fe, As, Au	Schist, gneiss, marble	Detachment fault	Miocene	Perlikos (1989); Voudouris et al (2011)
3	Central Euboea (Almyropotamos)	Attic-Cycladic Massif	Fe, Pb, Zn, As	Marble, schist	Fault controled, veins		Vryniotis (1978); this study
4	Siphnos	Attic-Cycladic Massif	Fe, Mn, Cu, Pb, Zn, Au	Marble, gneiss, schist	Detachment fault/ Carbonate replacement	Miocene	Wagner and Weisgerber (1985); Vavelidis (1988); this study
5	Seriphos	Attic-Cycladic Massif	Fe, Pb, Zn, As, Cu	Schist, marble	Detachment fault/ Carbonate replacement	Upper Miocene	Gale and Stos-Gale (1981b); Ducoux et al (2017)
6	Melos	Attic-Cycladic Massif	Pb, Zn, Cu, Au	Rhyolite, dacite, andesites, pyroclastic rocks	Epithermal	Pliocene to Pleistocene	Alfieris et al (2013)
7	Syros	Attic-Cycladic Massif	Fe, Pb, Zn, Cu, Sn, Au	Marble, schist	Detachment fault/ Carbonate replacement, veins	Upper Miocene	Melidonis and Constantinides (1983); Voudouris et al (2014)
8	Kythnos	Attic-Cycladic Massif	Fe, Pb, Zn, Cu, Au	Marble, schist	Detachment fault/ Carbonate replacement		Stos-Gale (1998); Bassiakos and Philaniotou (2007); this study
9	Antiparos	Attic-Cycladic Massif	Pb, Zn, Fe, Cu	Marble, schist	Epithermal	Miocene	Gale and Stos-Gale (1981b); Voudouris et al (2019)
10	Polyaigos	Attic-Cycladic Massif	Pb, Zn	Ignimbrite, andesite	Epithermal		Fytikas and Vougioukalakis (1992); this study
11	Thera	Attic-Cycladic Massif	Pb, Fe, Cu, Zn	Phyllitic schist	Epithermal		Gale (1998)
12	Anaphi	Attic-Cycladic Massif	Pb, Zn	Marble, granodiorite	Epithermal		Voudouris et al (2019); this study
13	Kos	Pelagonic zone	Pb, Zn	Marble breccia	Veins		IGME (1965)
14	Samos	Attic-Cycladic Massif	Pb, Fe, Au	Pyroclastics, conglomerates and carbonates	Epithermal	Miocene	IGME (1965); Voudouris et al (2019)
15	Mykonos	Attic-Cycladic Massif	Fe, Pb, Zn, Cu, Au	Monzogranite, schist	Veins	Miocene	IGME (1965); Voudouris et al (2019)
16	Tinos	Attic-Cycladic Massif	Pb, Zn, Au	Marble, schist	Epithermal	Miocene	Tombros et al (2007); Voudouris et al (2019)
17	Kea	Attic-Cycladic Massif	Pb, Fe	Marble	Veins		Gale (1998)
18	Tyros	Gavrovo Unit	Pb, Zn	Marble	VMS	Triassic	IGME (1965); Skarpelis (2020)
19	Molaoi	Gavrovo Unit	Pb, Zn	Tuffs, tuffites lavas and pyroclastics	VMS	Triassic	Grossou-Valta et al (1990)
20	Taygetus	Ionian Zone	Pb, Zn, Fe, Cu, Au	Schist	Veins/VMS?		Maratos (1956)
21	Hymettus	Attic-Cycladic Massif	Fe, Pb, As, Cu	Schist, marble	Carbonate replacement	Upper Miocene	IGME (1965); Stouraiti et al (2019)
22	Chios	Sakarya Block	Pb, Zn, Au	Clastic sediments	Epithermal	Mid-Miocene	Skarpelis (1999)
23	Pelion	Pelagonic zone	Fe, Pb, Zn, Cu	Schist, marble	Veins/Carbonate replacement		Tataris (1960); this study
24	Lesbos (Argenos)	Rhodope Massif-Sakarya	Fe, Pb, Zn, Cu, Au	Dacite, trachyandesite	Epithermal	Upper Miocene	Kontis et al (1994); Pernicka et al (2003); Voudouris et al (2019)
25	Limnos (Fakos)	Rhodope Massif	Pb, Zn, Cu, As, Au	Sandstone, monzodiorite	Epithermal	Lower Miocene	Voudouris and Skarpelis (1998); Voudouris and Alfieris (2005); Voudouris et al (2019)
26	Samothrace	Circum Rhodope Belt	Pb, Fe, Cu	Granite	Epithermal	Miocene	Voudouris et al (2019)
27	Sykia Chalkidiki	Circum Rhodope Belt	Pb, Cu, Zn, Fe	Granodiorite	Veins		IGME (1965; Wagner et al (1986)
28	NE Chalkidiki (Olympiada, Madem Lakkos, Mavres Petres)	Rhodope Massif	Pb, Zn, Cu, As, Au	Marble, gneiss, amphibolite	Carbonate replacement, intrusion related	Oligocene	Wagner et al (1986); Kalogeropoulos et al (1989); Siron et al. (2018)
29	Thasos	Rhodope Massif	Fe, Mn, Pb, Zn, Cu, As, Au	Marble, gneiss, schist	Carbonate replacement, intrusion related	Miocene	Vavelidis and Amstutz (1983); Wagner and Weisgerber (1988)
30	Kilkis (Drakontio, Stefania, Koronouda)	Vertiskos Unit	Pb, Zn, Cu, Fe, Au	Gneiss, schist, amphibolite	Intrusion related	Oligocene-Miocene	Melfos and Voudouris (2017)
31	Kroussia	Vertiskos Unit	Pb, Zn, Cu, Fe, Au	Schist, gneiss, marble	Veins/Carbonate replacement/ Porphyry		IGME (1965); Veranis and Tsamantouridis (1991); Stergiou et al. (2016); this study

(*continued on next page*)

Table 1 (*continued*)

	Ore District	Geotectonic Unit	Other Major Metal Compounds	Host Geology	Deposit Type/Style	mineralization Age	Indicative References
32	Skra	Circum Rhodope Belt	Pb, Zn	Rhyodacitic lavas, pyroclastics, porphyries and cherty tuffs	VMS	Upper Jurassic	Skarpelis (2020)
33	Angistron	Rhodope Massif	Fe, Mn, Pb, Zn, Cu, Au	Marble	Veins/ Carbonate replacement		Chiotis et al. (1996); this study
34	Pangaeon	Rhodope Massif Serbomacedonian Zone	Pb, Zn, Cu, Fe, Mn, Au	Marble, schist, gneiss, amphibolite	Intrusion related/ Carbonate replacement	Miocene	Vaxevanopoulos (2017; 2018)
35	Palaea Kavala	Rhodope Massif	Fe, Mn, Pb, Zn, Cu, Au	Marble, gneiss, schist, granodiorite	Intrusion related/ Carbonate replacement	Miocene	Vavelidis et al. (1996); Fornadel et al.(2011)
36	Thermes	Rhodope Massif	Fe, Pb, Zn, Cu, Au	Marble, gneiss, amphibolite	Carbonate replacemement	Oligocene	Gialoglou and Drymniotis (1983); Kalogeropoulos et al. (1996); Nesbitt et al. (1998)
37	Perama Hill	Circum Rhodope Belt	Cu, Pb, Au	Andesite, breccia, sandstone	Epithermal	Oligocene	Voudouris and Skarpelis (1998)
38	Kallintiri	Circum Rhodope Belt	Pb, Zn, Au	Marble, schist	Pollymetalic	Oligocene	Kanellopoulos et al. (2014); Melfos and Voudouris (2017)
39	Sappes	Circum Rhodope Belt	Fe, Cu, Pb, Zn, Au	Monzodiorite	Epithermal	Oligocene	Voudouris et al. (2006)
40	Kirki	Circum Rhodope Belt	Fe, Cu, Pb, Zn, As, Sn, Au	Andesite	Epithermal	Oligocene	Nesbitt et al. (1988); Melfos and Voudouris (2017)
41	Aisymi	Circum Rhodope Belt	Fe, Pb, Zn, Cu,	Granodiorite	Epithermal	Oligocene	Voudouris et al. (2006)
42	Neda (King Arthur)	Rhodope Massif	Fe, Pb, Cu, Zn	Andesite-Gneiss	Epithermal	Oligocene	Nesbitt et al. (1988); Voudouris et al. (2019)
43	Pefka	Circum Rhodope Belt	Pb, Cu, Zn, As, Bi, Sn, Au	Rhyodacitic lavas and pyroclastics	Epithermal	Oligocene	Voudouris (2005); Melfos and Voudouris (2017)
44	Loutros	Circum Rhodope Belt	Fe, Pb, As	Rhyolite	Epithermal	Miocene	Melfos and Voudouris (2016); 2017

correlations which obscure the true data relationships. This correlation is due to the much larger statistical noise on the small ^{204}Pb peak with respect to the peaks of the other more abundant Pb isotopes. Correlation coefficients were calculated by Albarède et al. (2004) and are approximately 0.94 in $^{207}Pb/^{204}Pb$ versus $^{206}Pb/^{204}Pb$ plots and 0.96 in $^{208}Pb/^{204}Pb$ versus $^{206}Pb/^{204}Pb$ plots, which are statistically highly significant. Slanted, narrow elliptic error surfaces in two-dimensional space (such as those commonly used for U–Pb dating) and ellipsoidal volumes in three-dimensional space therefore are more appropriate than the simple 'error boxes' often used in LIA. To give an example (e.g. Artioli et al., 2020; Wind et al., 2020), in a plot of $^{207}Pb/^{204}Pb$ versus $^{206}Pb/^{204}Pb$, or, as would be the case in another plot also widely used in archeometry, $^{208}Pb/^{206}Pb$ versus $^{207}Pb/^{206}Pb$, different groups of points overlap to some extent. In addition to better error treatment as outlined above, improving the overall analytical quality of Pb isotopic data will be certain to enhance provenance resolution. Moreover, as will be shown here, a one-dimensional T_{mod} histogram based on the new high-precision Pb isotope data from this study shows several well-defined peaks, which, when compared to the broader peaks based on older, often less precise literature data, confirms the necessity of focusing on data collected with modern quality standards, in particular those acquired by MC-ICP-MS for which analytical mass bias is well controlled.

2. Materials and methods

We have identified 44 Ag-rich mineralizations in Greece (Table 1). Of these, we obtained samples from 17 for which we could find evidence of ancient mining activity (Fig. 1). We sampled another 10 districts with minor Ag occurrences for each of which there is no proof of ancient mining activity, but for which, based on the local geology, it seems a reasonable possibility that future archeological research may uncover such evidence. These areas present sparse and unidentified mining traces, such as from chisel and pick, that might date to antiquity, but pottery or organic material that could provide reliable dating is absent. In some cases, modern exploitation has obliterated probable ancient mining phases. The remaining 17 minor Ag ore deposits with no evidence or geological likelihood of ancient mining were not sampled and are not described in the present study. The field investigations were conducted from March to July 2019, and from June to July 2020.

Silver and Pb concentrations and Pb isotopic compositions of 149 samples from the above mentioned mineralizations were analyzed by, respectively, quadrupole inductively-coupled plasma mass spectrometry (Q-ICP-MS) and multiple-collector inductively-coupled plasma mass spectrometry (MC-ICP-MS) at the Ecole Normale Supérieure in Lyon (ENS Lyon). Further information on sample preparation, analytical techniques, and accuracy and precision can be found in the supplementary material (Appendix III). The geological characteristics and latitude and longitude are listed in Table 2 and the Ag and Pb concentrations, Pb isotopic compositions, Pb model ages T_{mod}, and apparent $^{238}U/^{204}Pb$ (μ) and $^{232}Th/^{238}U$ (κ) values are listed in Table 3.

Lead model ages (T_{mod}) (Table 3) were calculated from the measured Pb isotopic compositions according to Albarède and Juteau (1984) and would differ by 30 Ma at most from those calculated from the parameters of Stacey and Kramer (1975) but have the advantage of eliminating most negative values. The values of μ ($^{238}U/^{204}Pb$) and κ ($^{232}Th/^{238}U$) also were computed (Table 3) from the measured Pb isotopic compositions. Table 4 lists Pb isotopic data from previous studies of Greek Pb–Zn mineralizations, which have been used in this paper though they are, in general, less precise that the Pb isotopic data acquired in the present study. Data on slags, litharge, and copper mineralizations were not included.

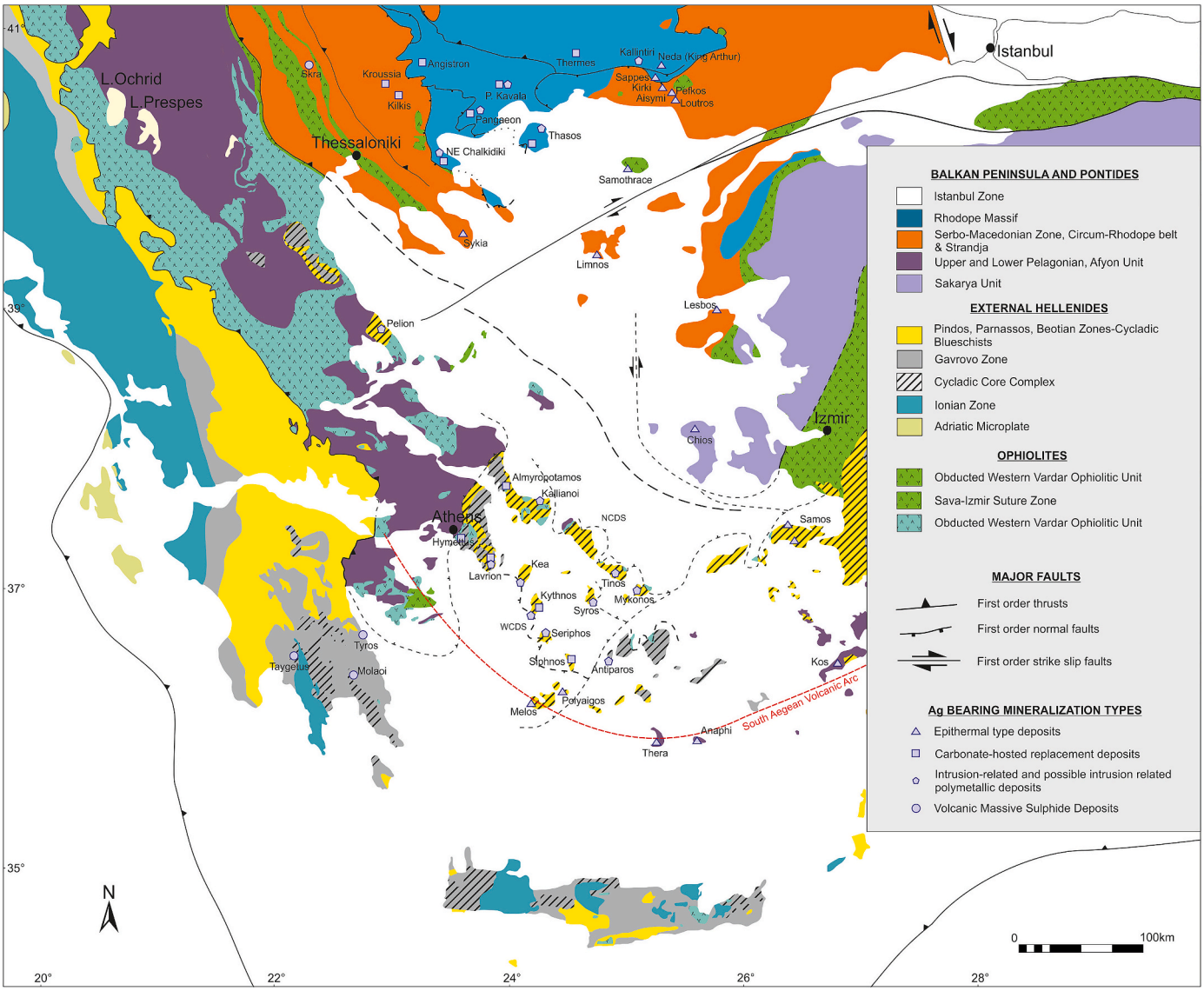

Fig. 2. Simplified geotectonic map of the Aegean region showing the main tectonic zones within the Hellenide orogen (modified after Schmid et al., 2008; 2020). Silver-bearing mineralizations are shown (Tables 1 and 4 and references therein). The North Cycladic Detachment System (NCDS) and the West Cycladic Detachment System (WCDS) are also depicted.

3. Results and discussion

3.1. On-site investigation and Ag grades of ancient Aegean mining districts

Field observations of ancient mining territories allow the documentation of the extent of mining activity, distinguishing between different exploitation phases, recording the extent of the metallurgical processes, and evaluating the relative importance of each mining area (Table 5). In the following, the investigated mining districts are described according to their geological context and their archeological importance. Silver concentrations are listed in Table 3.

3.1.1. Attic-Cycladic core complex (central Greece and southern Aegean)

Lavrion. Mining galleries span kilometers of underground workings with >2 km in the Esperanza mine in east Kamareza (Fig. 3a). The exploitation is extensive at the numerous mantos (horizontal) Ag occurrences mainly in the Kamareza, Soureza, Botsari, and Ari areas. The Plaka area presents numerous modern exploitation adits, but only scarce remains of ancient mines are found at the surface. The ancient mining areas closest to the Plaka granodiorite are at Ari and Dimoliaki with numerous adits and shafts that explore the contact between the Lavrion schists and Pounta marble (Fig. 3b). The Sounion area has shafts and ancient mines at the south edge of the Lavreotiki. The consistently high Ag yields reveal the importance of Lavrion with Ag concentrations varying from 1673 ppm in Kamareza to 5872 ppm in the modern mines of Plaka. A galena sample (L-17) found at the metallurgical area of Poundazeza (southeast coast of Lavrion) has a Ag concentration of 4220 ppm, which is representative of the ores being processed from these metallurgical areas.

Mount Hymettus. Situated to the east of Athens, the mountain hosts argentiferous galena veins (Stouraiti et al., 2019) exploited by three modern adits and a shaft in Agios Ioannis Kynigos and two adits in the Kamini area. No ancient mining has been recorded in the underground exploitations. Concentrations of Ag are low (0–6.3 ppm), whereas Stouraiti et al. (2019) mention Ag concentrations from 6 to >1500 ppm.

South Euboea. There are three Ag-bearing ore districts: the Kallianou valley, the Schinodavli site escarpment in the Agios Dimitrios gorge, and the Gialpides gorge. Mining activity and prospecting are recorded at the Kallianou valley with 11 modern adits and two ancient workings. The Ag

Table 2
Geological description and location of the sampled ores. The existence of ancient mining phases is also noted.

Sample	Region	District/mine	Mining Phase	Main minerals*	Host Rock	x	y
L-01	Lavrion	Hilarion	Ancient	Gn, Conich, Gth	Marble	37° 42′ 57.7866″ N	24° 00′ 49.5334″ E
L-02A	Lavrion	Porto-09	Modern-Ancient	Gn	Schist	37° 47′ 27.5781″ N	24° 04′ 55.6097″ E
L-02B	Lavrion	Porto-09	Modern-Ancient	Gn	Schist	37° 47′ 27.5781″ N	24° 04′ 55.6097″ E
L-03	Lavrion	Ari	Ancient	Gn	Marble	37° 45′ 42.8612″ N	23° 59′ 28.2221″ E
L-04	Lavrion	Esperanza	Ancient	Cer, Ang	Marble	37° 43′ 34.3682″ N	24° 01′ 58.0272″ E
L-05	Lavrion	Dimoliaki	Ancient	Gth, Gn	Marble	37° 45′ 11.1933″ N	24° 00′ 06.0348″ E
L-06	Lavrion	Jean Vaptiste	Modern-Ancient	Gn, Cer, Mlc, Conich	Marble	37° 43′ 42.7689″ N	24° 00′ 38.2815″ E
L-07	Lavrion	Esperanza	Modern-Ancient	Gn, Cer	Marble	37° 43′ 34.3682″ N	24° 01′ 58.0272″ E
L-08	Lavrion	Plaka-80	Modern	Gn, Sp	Marble	37° 45′ 36.1342″ N	24° 01′ 59.6156″ E
L-09	Lavrion	Plaka-80	Modern	Gn, Sp	Marble	37° 45′ 35.8797″ N	24° 01′ 57.0971″ E
L-10	Lavrion	Dimoliaki	Ancient	Cer, Gn, Gth	Marble	37° 45′ 11.1933″ N	24° 00′ 06.0347″ E
L-11	Lavrion	Plaka-145	Modern	Gn	Marble	37° 45′ 35.5808″ N	24° 02′ 01.0620″ E
L-12	Lavrion	Esperanza	Ancient	Gn, Sp	Marble	37° 43′ 34.1947″ N	24° 02′ 01.7645″ E
L-13	Lavrion	Esperanza	Ancient	Gn, Sp	Marble	37° 43′ 34.1947″ N	24° 02′ 01.7645″ E
L-14	Lavrion	Esperanza	Ancient	Sp, Gn	Marble	37° 43′ 34.4729″ N	24° 02′ 01.3349″ E
L-15	Lavrion	Esperanza	Ancient	Sp, Gn	Marble	37° 43′ 34.4729″ N	24° 02′ 01.3349″ E
L-16	Lavrion	HIL-24	Ancient	Gn, Cer	Marble	37° 43′ 13.2700″ N	24° 00′ 41.5551″ E
L-17	Lavrion	Poundazeza	Ancient	Gn	Marble	37° 40′ 51.8589″ N	24° 04′ 03.8284″ E
L-26	Lavrion	Sounio-06	Modern-Ancient	Cer	Marble	37° 40′ 51.6458″ N	24° 01′ 02.4408″ E
L-32	Lavrion	Elafos	Modern-Ancient	Gth, Cer	Marble	37° 42′ 41.4758″ N	24° 01′ 27.2640″ E
L-34	Lavrion	Dimoliaki	Ancient	Cer, Gn, Gth, Smith	Marble	37° 45′ 11.1933″ N	24° 00′ 06.0347″ E
L-40	Lavrion	Sykia	Ancient	Cer	Marble	37° 41′ 58.1481″ N	24° 00′ 38.6262″ E
L-41	Lavrion	Mpotsari	Ancient	Gn, Cer	Marble	37° 41′ 37.6138″ N	24° 01′ 36.2949″ E
L-42	Lavrion	Christiana	Modern-Ancient	Gn, Cer	Marble	37° 44′ 02.4144″ N	24° 01′ 10.9848″ E
L-43	Lavrion	MAN-HOR-1	Ancient	Cer, Gth	Marble	37° 46′ 10.1912″ N	23° 59′ 53.8461″ E
L-47	Lavrion	Thorikos mine	Ancient	Gth, Cer	Marble	37° 44′ 17.0548″ N	24° 03′ 15.7263″ E
E-01	Euboea	Kordelas	Modern	Gn	Marble	38° 06′ 49.4600″ N	24° 30′ 47.7804″ E
E-02	Euboea	St Barbara	Modern	Gn	Marble	38° 06′ 48.7526″ N	24° 30′ 40.3656″ E
E-03	Euboea	St Barbara	Modern	Gn	Marble	38° 06′ 48.7526″ N	24° 30′ 40.3656″ E
E-05	Euboea	Moskies	Ancient	Gn	Marble	38° 06′ 15.6060″ N	24° 30′ 38.9232″ E
E-06	Euboea	Moskies	Ancient	Gn, Py	Marble	38° 06′ 17.2800″ N	24° 30′ 39.5208″ E
GIA-02A	Euboea	Gialpides	Ancient	Ccp, Cer	Marble	38° 08′ 32.1909″ N	24° 32′ 14.6206″ E
GIA-02B	Euboea	Gialpides	Ancient	Ccp, Cer	Marble	38° 08′ 32.1909″ N	24° 32′ 14.6206″ E
SCHI-01A	Euboea	Schinodavli mine	Ancient	Gth, Cer	Schist	38° 08′ 38.4173″ N	24° 26′ 52.0365″ E
SCHI-01B	Euboea	Schinodavli mine	Ancient	Gth, Cer	Schist	38° 08′ 38.4173″ N	24° 26′ 52.0365″ E
AL-01	Euboea	Almyropotamos mine-01	Modern-Ancient	Cer, Gth	Marble	38° 15′ 00.9759″ N	24° 10′ 14.4010″ E
AL-02	Euboea	Almyropotamos mine-02	Modern-Ancient	Cer, Gth	Marble	38° 15′ 11.1816″ N	24° 10′ 15.4272″ E
AL-03	Euboea	Almyropotamos mine-07	Modern-Ancient	Cer, Gth	Marble	38° 15′ 19.3932″ N	24° 10′ 30.7668″ E
SI-02	Siphnos	Ai Sostis	Ancient	Gth, Cer, Hem, Pyrol	Marble	37° 00′ 48.9132″ N	24° 42′ 49.2732″ E
SI-03	Siphnos	Ai Sostis	Ancient	Gth, Hem, Pyrol, Cer	Marble	37° 00′ 45.6151″ N	24° 42′ 49.0187″ E
SI-10	Siphnos	Agios Silvestros	Ancient	Gth, Hem, Pyrol, Gn, Cer	Marble	37° 00′ 22.4271″ N	24° 42′ 23.6622″ E
SI-11	Siphnos	Xero Xylo	Ancient	Cer, Gth, Hem	Marble	36° 58′ 32.6352″ N	24° 41′ 21.3432″ E
SI-13	Siphnos	Kapsalos-Frase	Ancient-Modern	Cer, Gth, Hem	Marble	36° 58′ 50.7396″ N	24° 41′ 25.9548″ E
SI-14	Siphnos	Ai Sostis	Ancient	Cer, Gth, Hem	Marble	37° 00′ 48.9132″ N	24° 42′ 49.2732″ E
SI-15	Siphnos	Xero Xylo	Ancient-Modern	Cer, Gth, Hem	Marble	36° 58′ 32.6352″ N	24° 41′ 21.3432″ E
SE-02	Seriphos	Moutoula-07	Ancient	Gn	Marble	37° 11′ 12.1704″ N	24° 30′ 06.5340″ E
SE-03	Seriphos	Moutoula-08	Ancient	Gn	Marble	37° 11′ 12.1704″ N	24° 30′ 06.5340″ E
M-01A	Melos	Agios Nikolaos	Modern-Ancient	Gn	Tuff	36° 42′ 23.5944″ N	24° 20′ 47.9112″ E
M-01B	Melos	Agios Nikolaos	Modern-Ancient	Gn	Tuff	36° 42′ 23.5944″ N	24° 20′ 47.9112″ E
M-03A	Melos	Triades	Modern-Ancient	Gth, Cer	Tuff	36° 43′ 58.2240″ N	24° 22′ 02.5392″ E
M-03B	Melos	Triades	Modern-Ancient	Gth, Cer	Tuff	36° 43′ 58.2240″ N	24° 22′ 02.5392″ E
SYR-04	Syros	Azolimnos	Modern	Gn, Cer	Marble	37° 24′ 50.1300″ N	24° 57′ 50.3700″ E
SYR-06	Syros	Rozos	Ancient	Gn, Cer	Marble	37° 22′ 29.9928″ N	24° 54′ 15.0552″ E
SYR-07	Syros	Rozos	Ancient	Gn, Cer	Marble	37° 22′ 28.8372″ N	24° 54′ 16.1100″ E
SYR-08	Syros	Rozos	Ancient	Gn, Cer	Marble	37° 22′ 29.9928″ N	24° 54′ 15.0552″ E
SYR-09	Syros	Rozos	Ancient	Gn, Cer	Marble	37° 22′ 29.9928″ N	24° 54′ 15.0552″ E
SYR10	Syros	Rozos	Modern	Gn, Cer	Marble	37° 22′ 29.9928″ N	24° 54′ 15.0552″ E
KY-01	Kythnos	Agios Dimitrios mine	Ancient	Gth, Cer	Marble	37° 18′ 07.3233″ N	24° 21′ 51.8554″ E
KY-02	Kythnos	Agios Dimitrios	Modern	Gth, Cer	Marble	37° 18′ 03.8231″ N	24° 21′ 57.7715″ E
KY-05	Kythnos	Katafyki mine	Modern	Gth, Cer	Marble	37° 22′ 53.2584″ N	24° 25′ 47.5470″ E
KY-08	Kythnos	Kastellas	Ancient	Gth, Cer	Marble	37° 21′ 29.9736″ N	24° 23′ 22.3764″ E
KY-10	Kythnos	Tourkala	Modern	Gth, Cer	Marble	37° 22′ 44.6990″ N	24° 27′ 21.9268″ E
AN-02	Antiparos	Monastiria mine 1	Modern-Ancient	Cer, Gn	Gneiss	37° 00′ 10.7244″ N	25° 02′ 00.1500″ E
AN-03	Antiparos	Chatzovounia mine 1	Modern	Cer, Gth	Marble	36° 59′ 41.0712″ N	25° 03′ 21.9744″ E
AN-04A	Antiparos	Agios Georgios mine 3	Modern	Gn	Marble	36° 59′ 07.6596″ N	25° 01′ 49.6668″ E
AN-04B	Antiparos	Agios Georgios mine 4	Modern	Gn	Marble	36° 59′ 07.6596″ N	25° 01′ 49.6668″ E
PO-01A	Polyaigos	Modern mine	Modern	Gn, Bar	Marble	36° 47′ 07.8527″ N	24° 36′ 43.7007″ E
PO-01B	Polyaigos	Modern mine	Modern	Gn, Bar	Marble	36° 47′ 07.6344″ N	24° 36′ 43.7904″ E
PO-01C	Polyaigos	Modern mine	Modern	Gn, Bar	Marble	36° 47′ 07.8527″ N	24° 36′ 43.7007″ E
ANA-01	Anaphi	Ntoumparia	Modern	Gn, Sp	Marble	36° 21′ 59.5620″ N	25° 45′ 45.8244″ E
HYM-01	Hymettus	Kynigos-1 mine	Modern	Gth, Cer	Marble	37° 59′ 58.5700″ N	23° 50′ 12.4600″ E
HYM-02	Hymettus	Hymittos-2 (Kamini)	Modern	Gth, Cer	Marble	37° 58′ 58.6619″ N	23° 50′ 28.0622″ E
HYM-03	Hymettus	Kynigos-1 mine	Modern	Gth, Cer	Marble	37° 59′ 58.5700″ N	23° 50′ 12.4600″ E
HYM-04	Hymettus	Hymittos-2 (Kamini)	Modern	Gth, Cer	Marble	37° 58′ 58.3285″ N	23° 50′ 27.7016″ E

(*continued on next page*)

Table 2 (*continued*)

Sample	Region	District/mine	Mining Phase	Main minerals*	Host Rock	x	y
PE-01	Pelion	Gourounotrypa	Ancient	Gth, cer	Marble	39° 21′ 29.9987″ N	23° 11′ 03.9587″ E
PE-02	Pelion	Gourounotrypa	Ancient	Gth, cer	Marble	39° 21′ 29.9987″ N	23° 11′ 03.9587″ E
PE-03A	Pelion	Souvria	Ancient	Gth, cer	Marble	39° 23′ 53.2373″ N	23° 10′ 13.2839″ E
PE-03B	Pelion	Souvria	Ancient	Gth, cer	Marble	39° 23′ 53.2373″ N	23° 10′ 13.2839″ E
PE-04	Pelion	Souvria	Ancient	Gth, cer	Marble	39° 23′ 53.2373″ N	23° 10′ 13.2839″ E
LES-01	Lesbos	Argenos	Modern	Gn	Andesite	39° 22′ 38.7120″ N	26° 15′ 04.8636″ E
SAM-01	Samothrace	Pachia Ammos	Modern	Gn	Granite	40° 23′ 46.0527″ N	25° 33′ 38.9740″ E
MP-01A	Chalkidiki	Mavres Petres	Modern	Gn	Marble	40° 31′ 01.2847″ N	23° 42′ 29.5980″ E
MP-01B	Chalkidiki	Mavres Petres	Modern	Gn	Marble	40° 31′ 01.2847″ N	23° 42′ 29.5980″ E
MP-01C	Chalkidiki	Mavres Petres	Modern	Gn	Marble	40° 31′ 01.2847″ N	23° 42′ 29.5980″ E
OL-01A	Chalkidiki	Olympiada	Modern	Gn	Marble	40° 35′ 11.0020″ N	23° 45′ 00.6924″ E
OL-01B	Chalkidiki	Olympiada	Modern	Gn	Marble	40° 35′ 11.0020″ N	23° 45′ 00.6924″ E
OL-02A	Chalkidiki	Olympiada	Ancient	Cer, Fe-Mn	Marble	40° 35′ 51.5256″ N	23° 44′ 50.0640″ E
OL-02B	Chalkidiki	Olympiada	Ancient	Gth, Cer, Pyrol	Marble	40° 35′ 51.5256″ N	23° 44′ 50.0640″ E
C-01A	Chalkidiki	Stratoni	Modern	Gn, Cer	Marble	40° 31′ 46.8264″ N	23° 46′ 10.0920″ E
C-01B	Chalkidiki	Stratoni	Modern	Gn, Cer	Marble	40° 31′ 46.8264″ N	23° 46′ 10.0920″ E
C-02	Chalkidiki	Fterouda	Ancient	Gth, Cer	Marble	40° 31′ 46.8264″ N	23° 46′ 10.0920″ E
T-01	Thasos	Acropolis mine	Ancient	Gn, Cer	Marble	40° 46′ 32.4552″ N	24° 43′ 04.8144″ E
T-02	Thasos	Rachoni mine	Ancient	Gth, Cer	Marble	40° 47′ 02.0371″ N	24° 37′ 19.6057″ E
T-03	Thasos	Sotiros mine	Ancient	Gth, Cer	Marble	40° 43′ 16.8707″ N	24° 34′ 17.5007″ E
T-04	Thasos	Koumaria	Ancient	Gth, Cer	Marble	40° 39′ 54.1540″ N	24° 34′ 09.6350″ E
T-06	Thasos	Rachoni mine	Ancient	Gth, Cer	Marble	40° 47′ 02.0371″ N	24° 37′ 19.6057″ E
T-07	Thasos	Vouves	Modern	Smith, Cer	Marble	40° 38′ 05.3052″ N	24° 35′ 40.6320″ E
T-08	Thasos	Vouves	Modern	Gth, Cer	Marble	40° 38′ 05.3052″ N	24° 35′ 40.6320″ E
T-10	Thasos	Acropolis mine	Ancient	Gth, Cer	Marble	40° 46′ 32.4552″ N	24° 43′ 04.8144″ E
T-11	Thasos	Acropolis mine	Ancient	Gth, Cer	Marble	40° 46′ 32.4552″ N	24° 43′ 04.8144″ E
T-12	Thasos	Acropolis mine	Ancient	Gth, Cer	Marble	40° 46′ 32.4552″ N	24° 43′ 04.8144″ E
D-01	Kroussia	Kerkini	Ancient	Cer	Marble	41° 09′ 34.8722″ N	23° 10′ 07.6496″ E
D-02	Kroussia	Agios Markos	Modern	Gn	Gneiss	41° 08′ 14.1108″ N	23° 04′ 10.9271″ E
D-03	Kroussia	Agios Markos	Modern	Gn	Gneiss	41° 08′ 14.1108″ N	23° 04′ 10.9271″ E
D-04	Kroussia	Koulachli mine	Ancient	Cer	Gneiss	41° 09′ 02.6280″ N	23° 06′ 59.0255″ E
D-05	Kroussia	Koulachli mine	Ancient	Cer	Gneiss	41° 09′ 02.6280″ N	23° 06′ 59.0255″ E
D-06	Kroussia	Koulachli mine	Ancient	Cer	Gneiss	41° 09′ 02.6280″ N	23° 06′ 59.0255″ E
D-07	Kroussia	Vathi Ancient mine	Ancient	Cer	Rhyolite	41° 08′ 47.1732″ N	22° 58′ 06.3695″ E
D-10	Kroussia	Myriophyto outcrop	Modern Quarry	Gth, Cer	Marble	41° 12′ 21.0816″ N	22° 49′ 59.8978″ E
LE-01	Angistron	Lechovo	Ancient-Modern	Cer	Marble	41° 22′ 27.0300″ N	23° 29′ 16.1016″ E
LE-02	Angistron	Lechovo	Ancient-Modern	Cer	Marble	41° 22′ 27.0300″ N	23° 29′ 16.1016″ E
LE-03	Angistron	Lechovo	Ancient-Modern	Cer	Marble	41° 22′ 27.0300″ N	23° 29′ 16.1016″ E
LE-04	Angistron	Lechovo	Ancient-Modern	Cer	Marble	41° 22′ 27.0300″ N	23° 29′ 16.1016″ E
PA-01	Pangaeon	Nerostria	Modern-Ancient	Gth, Cer	Granodiorite	40° 55′ 34.9248″ N	24° 07′ 15.4128″ E
PA-02	Pangaeon	Asimotrypes	Ancient-Modern	Pyr, Apy, Gn. Sp, Ccp	Marble	40° 54′ 56.0765″ N	24° 06′ 37.9461″ E
PA-02B	Pangaeon	Asimotrypes	Ancient-Modern	Pyr, Apy, Gn. Sp, Ccp	Marble	40° 54′ 56.0765″ N	24° 06′ 37.9461″ E
PA-03	Pangaeon	Agia Triada-1	Ancient	Gth, Mlc, Cer	Marble	40° 55′ 12.7038″ N	24° 12′ 43.2706″ E
PA-04A	Pangaeon	Asimotrypes	Ancient-Modern	Pyr, Apy, Gn. Sp, Ccp	Marble	40° 54′ 56.0765″ N	24° 06′ 37.9461″ E
PA-04B	Pangaeon	Asimotrypes	Ancient-Modern	Pyr, Apy, Gn. Sp, Ccp	Marble	40° 54′ 56.0765″ N	24° 06′ 37.9461″ E
PA-05	Pangaeon	Avgo peak	Ancient-Modern	Gth, Cer	Marble	40° 54′ 30.6504″ N	24° 06′ 26.9100″ E
PA-06	Pangaeon	Avgo peak	Ancient-Modern	Gth, Cer	Marble	40° 54′ 30.6504″ N	24° 06′ 26.9100″ E
PA-07A	Pangaeon	Ofrynio-2	Ancient	Gth, Cer	Marble	40° 49′ 01.4746″ N	23° 54′ 29.9437″ E
PA-07B	Pangaeon	Ofrynio-2	Ancient	Gth, Cer	Marble	40° 49′ 01.4746″ N	23° 54′ 29.9437″ E
PA-11	Pangaeon	Asimotrypes	Ancient-Modern	Cer, Gth	Marble	40° 54′ 56.0765″ N	24° 06′ 37.9461″ E
PA-15	Pangaeon	Asimotrypes	Ancient-Modern	Gn	Marble	40° 54′ 56.0765″ N	24° 06′ 37.9461″ E
SY-04	Pangaeon	Kokkinochoma-1 Symvolon	Ancient	Gth, Cer	Marble	40° 55′ 24.6557″ N	24° 18′ 58.6504″ E
PK-01	Palaea Kavala	Agia Eleni mine	Ancient	Cer, Gth, Hem	Marble	41° 01′ 06.9872″ N	24° 23′ 41.6675″ E
PK-02	Palaea Kavala	Agia Eleni mine	Ancient	Cer, Gth, Hem	Marble	41° 01′ 06.9872″ N	24° 23′ 41.6675″ E
PK-03	Palaea Kavala	Agia Eleni mine	Ancient	Cer, Gth, Hem	Marble	41° 01′ 06.9872″ N	24° 23′ 41.6675″ E
PK-04	Palaea Kavala	Agia Eleni mine	Ancient	Cer, Gth, Hem	Marble	41° 01′ 06.9872″ N	24° 23′ 41.6675″ E
PK-06	Palaea Kavala	Mavri Trypa mine	Ancient	Cer	Marble	41° 01′ 14.2529″ N	24° 23′ 35.2166″ E
PK-07	Palaea Kavala	Lazaros-1 mine	Ancient	Cer	Marble	41° 01′ 57.9359″ N	24° 23′ 37.8996″ E
PK-08	Palaea Kavala	Lazaros-1 mine	Ancient	Cer	Marble	41° 01′ 57.9359″ N	24° 23′ 37.8996″ E
PK-09	Palaea Kavala	Peristerionas mine	Ancient	Cer	Marble	41° 02′ 06.8675″ N	24° 23′ 52.8720″ E
PK-11	Palaea Kavala	Kel-Tepe	Ancient	Gth, Cer	Marble	41° 01′ 47.8883″ N	24° 24′ 19.5587″ E
THE-01	Thermes	Loutra	Modern	Gn	Marble	41° 22′ 44.8599″ N	24° 56′ 00.5299″ E
THE-02	Thermes	Razul	Modern	Gn	Marble	41° 22′ 44.8599″ N	24° 56′ 00.5299″ E
THE-03	Thermes	Razul	Modern	Gn	Marble	41° 20′ 56.9417″ N	25° 00′ 09.1599″ E
KIR-01	Kirki	Saint-Philippos	Modern	Gn	Andesite	41° 01′ 16.1292″ N	25° 49′ 03.5579″ E
KIR-02	Kirki	Saint-Philippos	Modern	Gn, Ccp	Andesite	41° 01′ 16.1292″ N	25° 49′ 03.5579″ E
KIR-03	Kirki	Saint-Philippos	Modern	Gn, Ccp	Andesite	41° 01′ 16.1292″ N	25° 49′ 03.5579″ E
KIR-04	Kirki	Saint-Philippos	Modern	Gn, Ccp	Andesite	41° 01′ 16.1292″ N	25° 49′ 03.5579″ E
SAP-01	Sappes	Sappes	Modern	Gn	Diorite	41° 00′ 39.7079″ N	25° 44′ 40.8443″ E
SAP-02	Sappes	Sappes	Modern	Gn	Diorite	41° 00′ 46.5444″ N	25° 44′ 31.1711″ E
AIS-01	Aisymi	Aisymi	Modern	Gn	Marble	41° 02′ 05.6658″ N	25° 59′ 00.0348″ E
NED-01	Neda (King Arthur)	Neda (King Arthur)	Modern	Gn	Marble	41° 03′ 26.5571″ N	25° 49′ 11.7299″ E
NED-02	Neda (King Arthur)	Neda (King Arthur)	Modern	Gn	Marble	41° 03′ 26.5571″ N	25° 49′ 11.7299″ E
NED-03	Neda (King Arthur)	Neda (King Arthur)	Modern	Gn	Marble	41° 03′ 26.5571″ N	25° 49′ 11.7299″ E
PEF-02	Pefkos	Pefkos	Modern	Gn	Rhyolite	40° 54′ 32.0399″ N	26° 02′ 14.8559″ E

* Abbreviations: Apy = Arsenopyrite; Bar = Barite; Ccp = Chalcopyrite; Cer = Cerussite; Conich = Conichalcite; Fe-Mn = Iron-Manganese oxides; Gn = Galena; Gth = Goethite; Hem = Hematite; Jrs = Jarpsite; Lm = Limonite; Mlc = Malachite; Smith = Smithsonite; Sp = Sphalerite; Py = Pyrite; Pyrol = Pyrolusite

Table 3
High-precision Pb isotopic compositions of Ag-bearing localities in Greece.

Sample	Ag (ppm)	Pb (wt %)	$^{206}Pb/^{204}Pb$	2s	$^{207}Pb/^{204}Pb$	2s	$^{208}Pb/^{204}Pb$	2s	$^{204}Pb/^{206}Pb$	2s	$^{207}Pb/^{206}Pb$	2s	$^{208}Pb/^{206}Pb$	2s	T_{mod} (Ma)	μ	k
L-01	321	19.6	18.8401	0.0007	15.6852	0.0006	38.820	0.002	0.0531	0.0007	0.83254	0.00001	2.06048	0.00003	43	9.855	3.858
L-02A	124	18.1	18.8591	0.0010	15.6938	0.0011	38.939	0.003	0.0530	0.0010	0.83216	0.00001	2.06471	0.00008	46	9.885	3.908
L-02B	107	12.9	18.8593	0.0008	15.6939	0.0008	38.938	0.003	0.0530	0.0008	0.83216	0.00001	2.06471	0.00005	46	9.885	3.908
L-03	295	15.7	18.8635	0.0011	15.6936	0.0008	38.884	0.002	0.0530	0.0011	0.83194	0.00003	2.06127	0.00008	43	9.883	3.878
L-04	182	1.14	18.8688	0.0008	15.6925	0.0009	38.865	0.003	0.0530	0.0008	0.83165	0.00001	2.05975	0.00009	36	9.878	3.865
L-05	20.9	3.49	18.8744	0.0009	15.6916	0.0011	38.884	0.004	0.0530	0.0009	0.83136	0.00002	2.06013	0.00010	31	9.873	3.870
L-06	1673	70.7	18.8599	0.0008	15.6837	0.0009	38.825	0.003	0.0530	0.0008	0.83158	0.00001	2.05856	0.00007	26	9.846	3.848
L-07	1978	67.9	18.8607	0.0007	15.6872	0.0007	38.824	0.002	0.0530	0.0007	0.83175	0.00001	2.05845	0.00005	32	9.859	3.848
L-08	1656	52.0	18.8906	0.0032	15.7093	0.0026	38.938	0.006	0.0529	0.0032	0.83160	0.00001	2.06122	0.00006	54	9.938	3.893
L-09	3029	65.7	18.8845	0.0019	15.7034	0.0016	38.923	0.003	0.0530	0.0019	0.83155	0.00001	2.06112	0.00005	46	9.917	3.888
L-10	1182	32.5	18.8741	0.0007	15.6921	0.0006	38.878	0.002	0.0530	0.0007	0.83141	0.00001	2.05984	0.00008	32	9.875	3.868
L-11	5872	65.7	18.8762	0.0008	15.6918	0.0007	38.893	0.002	0.0530	0.0008	0.83131	0.00001	2.06040	0.00005	30	9.874	3.874
L-12	1959	79.3	18.8649	0.0007	15.6901	0.0006	38.838	0.002	0.0530	0.0007	0.83171	0.00001	2.05874	0.00004	35	9.869	3.853
L-13	2005	69.8	18.8670	0.0012	15.6905	0.0011	38.837	0.003	0.0530	0.0012	0.83164	0.00001	2.05850	0.00006	34	9.870	3.852
L-14	330	0.972	18.8594	0.0010	15.6845	0.0010	38.857	0.003	0.0530	0.0010	0.83166	0.00001	2.06033	0.00009	28	9.849	3.864
L-15	333	0.982	18.8625	0.0006	15.6865	0.0005	38.860	0.001	0.0530	0.0006	0.83163	0.00001	2.06021	0.00002	46	9.837	3.886
L-16	17.6	0.023	18.8220	0.0007	15.6795	0.0007	38.858	0.002	0.0531	0.0007	0.83305	0.00001	2.06450	0.00006	34	9.883	3.884
L-17	4220	55.6	18.8764	0.0009	15.6941	0.0010	38.913	0.003	0.0530	0.0009	0.83142	0.00002	2.06148	0.00010	29	9.856	3.864
L-26	2.41	0.289	18.8238	0.0005	15.6925	0.0004	38.882	0.001	0.0531	0.0005	0.83367	0.00001	2.06561	0.00003	70	9.886	3.902
L-32	0.000	0.717	18.8515	0.0007	15.6850	0.0006	38.874	0.002	0.0530	0.0007	0.83202	0.00001	2.06207	0.00002	34	9.852	3.877
L-34	2464	22.2	18.8637	0.0025	15.6861	0.0031	38.860	0.010	0.0530	0.0025	0.83154	0.00005	2.06003	0.00023	28	9.854	3.863
L-40	1037	42.9	18.8602	0.0006	15.6995	0.0006	38.889	0.002	0.0530	0.0006	0.83240	0.00001	2.06195	0.00004	57	9.906	3.885
L-41	3670	70.5	18.8504	0.0009	15.6946	0.0008	38.886	0.003	0.0530	0.0009	0.83256	0.00001	2.06280	0.00007	54	9.889	3.887
L-42	3951	70.4	18.8642	0.0015	15.6840	0.0014	38.830	0.004	0.0530	0.0015	0.83143	0.00002	2.05841	0.00010	23	9.846	3.848
L-43	40.2	10.8	18.8792	0.0007	15.6896	0.0006	38.858	0.002	0.0530	0.0007	0.83105	0.00001	2.05827	0.00003	23	9.865	3.854
L-47	0.000	3.64	18.8727	0.0009	15.6942	0.0007	38.921	0.002	0.0530	0.0009	0.83159	0.00001	2.06231	0.00005	37	9.884	3.891
E-01	19.9	2.24	18.6864	0.0006	15.6977	0.0005	38.908	0.001	0.0535	0.0006	0.84006	0.00001	2.08217	0.00003	181	9.933	4.005
E-02	583	1.62	18.6935	0.0006	15.6957	0.0005	38.912	0.002	0.0535	0.0006	0.83963	0.00001	2.08156	0.00003	172	9.924	4.002
E-03	86.9	0.879	18.7024	0.0006	15.7009	0.0005	38.927	0.002	0.0535	0.0006	0.83952	0.00001	2.08141	0.00003	176	9.943	4.005
E-05	731	40.8	18.6893	0.0007	15.7011	0.0006	38.916	0.002	0.0535	0.0007	0.84012	0.00001	2.08230	0.00004	186	9.946	4.009
E-06	509	29.9	18.6869	0.0006	15.6994	0.0005	38.913	0.002	0.0535	0.0006	0.84013	0.00001	2.08242	0.00005	184	9.940	4.008
GIA-02A	10.9	0.020	18.7279	0.0008	15.6943	0.0007	38.947	0.002	0.0534	0.0008	0.83802	0.00001	2.07966	0.00005	144	9.912	3.996
GIA-02B	48.8	0.023	18.6715	0.0006	15.6958	0.0005	38.669	0.001	0.0536	0.0006	0.84063	0.00001	2.07105	0.00004	189	9.929	3.892
SCHI-01A	0.000	0.041	18.6742	0.0009	15.6977	0.0008	38.675	0.002	0.0535	0.0009	0.84061	0.00001	2.07107	0.00004	190	9.936	3.894
SCHI-01B	0.919	0.042	18.7249	0.0007	15.6915	0.0007	38.941	0.002	0.0534	0.0007	0.83801	0.00001	2.07963	0.00006	141	9.902	3.994
AL-01	91.4	6.97	18.7987	0.0010	15.7059	0.0009	38.933	0.003	0.0532	0.0010	0.83549	0.00001	2.07112	0.00004	115	9.943	3.948
AL-02	65.3	14.1	18.7802	0.0011	15.7004	0.0010	38.912	0.003	0.0532	0.0011	0.83600	0.00001	2.07202	0.00005	118	9.925	3.947
AL-03	74.7	10.3	18.7929	0.0007	15.7048	0.0007	38.930	0.002	0.0532	0.0007	0.83569	0.00001	2.07155	0.00005	117	9.940	3.949
SI-02	13.2	6.44	18.7367	0.0009	15.7141	0.0010	38.960	0.003	0.0534	0.0009	0.83869	0.00001	2.07940	0.00011	176	9.987	4.004
SI-03	1.71	2.66	18.7291	0.0006	15.7045	0.0005	38.954	0.002	0.0534	0.0006	0.83851	0.00001	2.07985	0.00002	163	9.951	4.003
SI-10	4983	7.11	18.7361	0.0005	15.7040	0.0004	38.951	0.001	0.0534	0.0005	0.83817	0.00001	2.07894	0.00002	157	9.948	3.996
SI-11	126	0.430	18.7298	0.0005	15.7048	0.0004	38.955	0.001	0.0534	0.0005	0.83850	0.00001	2.07987	0.00002	163	9.952	4.003
SI-13	21.0	2.29	18.7273	0.0005	15.7018	0.0005	38.950	0.002	0.0534	0.0005	0.83843	0.00001	2.07987	0.00003	159	9.941	4.001
SI-14	3.20	0.761	18.7344	0.0006	15.7058	0.0006	38.961	0.002	0.0534	0.0006	0.83833	0.00001	2.07964	0.00004	161	9.955	4.003
SI-15	40.2	0.478	18.7265	0.0007	15.7009	0.0007	38.946	0.002	0.0534	0.0007	0.83846	0.00001	2.07974	0.00006	158	9.938	3.999
SE-02	162	70.0	18.9000	0.0008	15.7010	0.0008	39.009	0.003	0.0529	0.0008	0.83076	0.00001	2.06400	0.00006	30	9.905	3.919
SE-03	470	85.2	18.9024	0.0008	15.7030	0.0007	39.014	0.003	0.0529	0.0008	0.83075	0.00001	2.06394	0.00007	32	9.912	3.921
M-01A	2389	66.4	18.8601	0.0006	15.6892	0.0006	39.007	0.002	0.0530	0.0006	0.83188	0.00001	2.06829	0.00003	36	9.867	3.939
M-01B	2473	28.2	18.8619	0.0007	15.6896	0.0008	39.008	0.002	0.0530	0.0007	0.83181	0.00001	2.06810	0.00005	36	9.868	3.939
M-03A	1.48	0.014	18.8205	0.0006	15.6935	0.0006	38.971	0.002	0.0531	0.0006	0.83387	0.00001	2.07071	0.00004	74	9.891	3.948
M-03B	6.02	0.003	18.8200	0.0005	15.6954	0.0005	38.973	0.001	0.0531	0.0005	0.83398	0.00001	2.07082	0.00004	79	9.898	3.950
SYR-04	0.971	0.171	18.8401	0.0016	15.7186	0.0012	39.103	0.003	0.0531	0.0016	0.83431	0.00002	2.07551	0.00005	109	9.984	4.010
SYR-06	1.18	0.001	18.8178	0.0007	15.7099	0.0007	39.045	0.002	0.0531	0.0007	0.83486	0.00001	2.07495	0.00004	108	9.954	3.993
SYR-07	26.1	0.821	18.8296	0.0010	15.7141	0.0009	39.054	0.006	0.0531	0.0010	0.83455	0.00001	2.07419	0.00018	108	9.969	3.991

(*continued on next page*)

Table 3 (*continued*)

Sample	Ag (ppm)	Pb (wt %)	$^{206}Pb/^{204}Pb$	2s	$^{207}Pb/^{204}Pb$	2s	$^{208}Pb/^{204}Pb$	2s	$^{204}Pb/^{206}Pb$	2s	$^{207}Pb/^{206}Pb$	2s	$^{208}Pb/^{206}Pb$	2s	T_{mod} (Ma)	μ	k
SYR-08	0.781	0.128	18.8208	0.0016	15.7114	0.0014	39.056	0.003	0.0531	0.0016	0.83479	0.00002	2.07514	0.00005	109	9.960	3.997
SYR-09	23.2	0.418	18.8202	0.0019	15.7140	0.0009	39.064	0.004	0.0531	0.0019	0.83494	0.00001	2.07559	0.00004	114	9.970	4.002
SYR10	1.34	0.366	18.8376	0.0010	15.7196	0.0011	39.086	0.003	0.0531	0.0010	0.83450	0.00002	2.07494	0.00008	113	9.988	4.004
KY-01	0.000	0.187	18.9374	0.0010	15.7013	0.0009	39.025	0.003	0.0528	0.0010	0.82913	0.00001	2.06074	0.00005	3	9.899	3.904
KY-02	13.0	0.595	18.9225	0.0007	15.7018	0.0006	39.024	0.002	0.0528	0.0007	0.82980	0.00001	2.06227	0.00004	15	9.904	3.913
KY-05	0.772	0.003	18.8357	0.0007	15.7024	0.0007	39.008	0.002	0.0531	0.0007	0.83367	0.00001	2.07098	0.00003	26	9.903	3.916
KY-08	0.231	0.956	18.9053	0.0016	15.7009	0.0015	39.008	0.005	0.0529	0.0016	0.83050	0.00002	2.06330	0.00010	81	9.922	3.960
KY-10	16.2	0.035	18.8271	0.0009	15.7196	0.0007	39.123	0.002	0.0531	0.0009	0.83494	0.00001	2.07805	0.00003	120	9.990	4.029
AN-02	340	55.8	18.8392	0.0006	15.7258	0.0005	39.170	0.001	0.0531	0.0006	0.83475	0.00001	2.07920	0.00003	123	10.012	4.047
AN-03	2.30	0.126	18.8412	0.0008	15.7259	0.0008	39.173	0.002	0.0531	0.0008	0.83466	0.00001	2.07911	0.00006	122	10.012	4.047
AN-04A	386	67.0	18.8238	0.0007	15.7190	0.0006	39.118	0.002	0.0531	0.0007	0.83506	0.00001	2.07816	0.00003	121	9.988	4.029
AN-04B	238	61.6	18.8229	0.0007	15.7181	0.0006	39.117	0.002	0.0531	0.0007	0.83505	0.00001	2.07820	0.00006	120	9.985	4.028
PO-01A	80.6	33.2	18.8771	0.0006	15.6974	0.0006	39.015	0.001	0.0530	0.0006	0.83156	0.00001	2.06680	0.00003	40	9.895	3.936
PO-01B	67.6	54.6	18.8726	0.0009	15.6924	0.0011	39.003	0.004	0.0530	0.0009	0.83149	0.00002	2.06658	0.00012	33	9.877	3.931
PO-01C	116	89.2	18.8779	0.0009	15.6974	0.0008	39.017	0.002	0.0530	0.0009	0.83152	0.00001	2.06677	0.00004	39	9.895	3.936
ANA-01	81.2	36.9	18.8946	0.0011	15.7009	0.0014	39.031	0.004	0.0529	0.0011	0.83098	0.00002	2.06566	0.00011	34	9.905	3.919
HYM-01	1.86	1.16	18.4301	0.0015	15.6851	0.0013	38.597	0.004	0.0543	0.0015	0.85105	0.00001	2.09420	0.00005	345	9.942	4.010
HYM-02	0.000	0.191	18.4053	0.0007	15.6876	0.0007	38.575	0.002	0.0543	0.0007	0.85233	0.00001	2.09587	0.00004	367	9.958	4.016
HYM-03	6.30	1.02	18.4321	0.0006	15.6858	0.0005	38.597	0.001	0.0543	0.0006	0.85100	0.00001	2.09404	0.00003	345	9.944	4.009
HYM-04	0.715	0.259	18.4040	0.0006	15.6854	0.0006	38.574	0.001	0.0543	0.0006	0.85227	0.00001	2.09599	0.00003	364	9.950	4.015
PE-01	8.19	0.369	18.8707	0.0007	15.7090	0.0006	39.046	0.001	0.0530	0.0007	0.83246	0.00001	2.06912	0.00003	68	9.941	3.959
PE-02	13.0	1.40	18.8701	0.0006	15.7090	0.0006	39.048	0.002	0.0530	0.0006	0.83248	0.00001	2.06935	0.00003	68	9.941	3.960
PE-03A	2.95	0.061	18.8796	0.0008	15.7127	0.0007	39.067	0.002	0.0530	0.0008	0.83225	0.00001	2.06930	0.00003	68	9.953	3.965
PE-03B	11.0	0.059	18.8785	0.0006	15.7134	0.0005	39.070	0.001	0.0530	0.0006	0.83234	0.00001	2.06955	0.00002	71	9.956	3.967
PE-04	10.9	0.342	18.8696	0.0007	15.7112	0.0005	39.058	0.002	0.0530	0.0007	0.83262	0.00001	2.06993	0.00002	73	9.950	3.967
LES-01	155	38.0	18.6284	0.0008	15.6922	0.0007	39.010	0.002	0.0537	0.0008	0.84237	0.00001	2.09412	0.00004	213	9.924	4.078
SAM-01	471	58.6	18.3785	0.0007	15.6730	0.0006	38.538	0.002	0.0544	0.0007	0.85278	0.00001	2.09688	0.00003	360	9.906	4.009
MP-01A	2826	82.8	18.7966	0.0007	15.6656	0.0007	38.889	0.002	0.0532	0.0007	0.83343	0.00001	2.06895	0.00003	37	9.788	3.913
MP-01B	2880	82.4	18.8045	0.0007	15.6684	0.0006	38.900	0.002	0.0532	0.0007	0.83323	0.00001	2.06867	0.00003	37	9.797	3.914
MP-01C	2708	72.4	18.8076	0.0007	15.6707	0.0007	38.903	0.002	0.0532	0.0007	0.83322	0.00001	2.06855	0.00004	39	9.805	3.915
OL-01A	1536	55.0	18.7805	0.0008	15.6760	0.0008	38.877	0.003	0.0532	0.0008	0.83472	0.00001	2.07005	0.00007	70	9.831	3.921
OL-01B	1575	52.4	18.7801	0.0006	15.6751	0.0007	38.872	0.002	0.0532	0.0006	0.83467	0.00001	2.06986	0.00004	68	9.828	3.918
OL-02A	291	0.025	18.7878	0.0005	15.6790	0.0004	38.887	0.001	0.0532	0.0005	0.83453	0.00001	2.06978	0.00002	70	9.841	3.922
OL-02B	674	0.032	18.7928	0.0007	15.6836	0.0006	38.897	0.002	0.0532	0.0007	0.83456	0.00001	2.06979	0.00003	75	9.858	3.926
C-01A	14.2	0.195	18.8121	0.0013	15.6755	0.0011	38.920	0.003	0.0532	0.0013	0.83326	0.00001	2.06883	0.00004	45	9.823	3.922
C-01B	18.5	0.190	18.8147	0.0006	15.6733	0.0005	38.920	0.002	0.0532	0.0006	0.83303	0.00001	2.06860	0.00003	39	9.814	3.919
C-02	39.5	3.22	18.7061	0.0009	15.6712	0.0009	38.835	0.003	0.0535	0.0009	0.83777	0.00001	2.07602	0.00006	115	9.826	3.946
T-01	50.8	0.097	18.6928	0.0005	15.6842	0.0005	38.869	0.001	0.0535	0.0005	0.83905	0.00001	2.07935	0.00003	151	9.880	3.976
T-02	44.9	2.80	18.8502	0.0006	15.6898	0.0006	38.991	0.002	0.0530	0.0006	0.83235	0.00001	2.06848	0.00003	45	9.871	3.938
T-03	8.49	1.71	18.7992	0.0007	15.6841	0.0006	38.937	0.002	0.0532	0.0007	0.83429	0.00001	2.07121	0.00003	72	9.858	3.942
T-04	2.79	0.002	18.8010	0.0007	15.6853	0.0007	38.932	0.002	0.0532	0.0007	0.83428	0.00001	2.07072	0.00003	73	9.863	3.938
T-06	5.97	1.78	18.8468	0.0007	15.6870	0.0006	38.984	0.002	0.0531	0.0007	0.83233	0.00001	2.06848	0.00003	42	9.861	3.936
T-07	13.8	0.008	18.7902	0.0006	15.6838	0.0006	38.929	0.002	0.0532	0.0006	0.83467	0.00001	2.07173	0.00005	78	9.859	3.943
T-08	0.233	0.164	18.7820	0.0009	15.6845	0.0008	38.923	0.002	0.0532	0.0009	0.83506	0.00001	2.07235	0.00004	85	9.863	3.946
T-10	102	0.048	18.6901	0.0010	15.6848	0.0011	38.869	0.003	0.0535	0.0010	0.83919	0.00002	2.07958	0.00008	154	9.883	3.978
T-11	2.24	0.061	18.6886	0.0005	15.6802	0.0005	38.858	0.001	0.0535	0.0005	0.83902	0.00001	2.07923	0.00004	146	9.865	3.972
T-12	945	0.040	18.6921	0.0008	15.6836	0.0007	38.871	0.002	0.0535	0.0008	0.83905	0.00001	2.07953	0.00003	150	9.877	3.977
D-01	23.7	0.912	18.7909	0.0007	15.6608	0.0006	38.854	0.001	0.0532	0.0007	0.83341	0.00001	2.06767	0.00003	32	9.771	3.897
D-02	1364	13.7	18.8251	0.0006	15.6698	0.0006	38.932	0.002	0.0531	0.0006	0.83239	0.00001	2.06807	0.00003	24	9.799	3.917
D-03	215	13.6	18.8260	0.0006	15.6686	0.0006	38.923	0.002	0.0531	0.0006	0.83228	0.00001	2.06751	0.00004	21	9.794	3.912
D-04	8.93	0.752	18.8077	0.0005	15.6612	0.0005	38.905	0.001	0.0532	0.0005	0.83272	0.00001	2.06858	0.00004	20	9.769	3.912
D-05	4.73	0.095	18.8133	0.0010	15.6665	0.0008	38.923	0.002	0.0532	0.0010	0.83274	0.00001	2.06894	0.00003	26	9.788	3.919
D-06	18.8	0.160	18.8224	0.0008	15.6677	0.0007	38.926	0.002	0.0531	0.0008	0.83241	0.00001	2.06809	0.00004	22	9.791	3.915
D-07	0.000	0.082	18.8632	0.0006	15.6808	0.0005	38.970	0.001	0.0530	0.0006	0.83130	0.00001	2.06599	0.00004	17	9.834	3.916
D-10	0.700	0.021	18.3296	0.0006	15.6443	0.0006	38.428	0.001	0.0546	0.0006	0.85350	0.00001	2.09648	0.00002	343	9.804	3.973

(*continued on next page*)

Table 3 (*continued*)

Sample	Ag (ppm)	Pb (wt %)	$^{206}Pb/^{204}Pb$	2s	$^{207}Pb/^{204}Pb$	2s	$^{208}Pb/^{204}Pb$	2s	$^{204}Pb/^{206}Pb$	2s	$^{207}Pb/^{206}Pb$	2s	$^{208}Pb/^{206}Pb$	2s	T_{mod} (Ma)	μ	k
LE-01	11.4	4.49	18.7211	0.0006	15.6713	0.0004	38.827	0.001	0.0534	0.0006	0.83708	0.00001	2.07393	0.00003	104	9.824	3.932
LE-02	182	8.02	18.7250	0.0006	15.6721	0.0006	38.827	0.002	0.0534	0.0006	0.83696	0.00001	2.07351	0.00003	103	9.826	3.930
LE-03	11.8	3.84	18.7299	0.0007	15.6725	0.0005	38.837	0.002	0.0534	0.0007	0.83677	0.00001	2.07351	0.00002	100	9.827	3.932
LE-04	176	8.47	18.7283	0.0008	15.6710	0.0008	38.832	0.002	0.0534	0.0008	0.83675	0.00001	2.07342	0.00005	99	9.821	3.930
PA-01	1.32	0.008	18.7317	0.0005	15.6827	0.0005	38.841	0.001	0.0534	0.0005	0.83723	0.00001	2.07349	0.00002	119	9.866	3.936
PA-02	9697	22.4	18.7013	0.0008	15.6805	0.0007	38.819	0.002	0.0535	0.0008	0.83846	0.00001	2.07571	0.00003	137	9.863	3.944
PA-02B	9906	20.1	18.7044	0.0006	15.6827	0.0006	38.826	0.002	0.0535	0.0006	0.83845	0.00001	2.07575	0.00003	139	9.871	3.946
PA-03	124	0.302	18.7075	0.0005	15.6841	0.0007	38.862	0.002	0.0535	0.0005	0.83839	0.00001	2.07733	0.00002	140	9.876	3.963
PA-04A	5439	11.4	18.7012	0.0010	15.6835	0.0010	38.823	0.003	0.0535	0.0010	0.83864	0.00001	2.07599	0.00006	143	9.875	3.947
PA-04B	5042	10.6	18.6974	0.0008	15.6798	0.0009	38.812	0.002	0.0535	0.0008	0.83861	0.00001	2.07580	0.00005	139	9.862	3.943
PA-05	86.9	1.85	18.7013	0.0007	15.6819	0.0009	38.828	0.002	0.0535	0.0007	0.83855	0.00001	2.07623	0.00005	140	9.869	3.949
PA-06	145	5.70	18.6948	0.0007	15.6820	0.0006	38.826	0.002	0.0535	0.0007	0.83884	0.00001	2.07685	0.00004	145	9.871	3.952
PA-07A	20.2	1.25	18.7919	0.0006	15.6844	0.0005	38.917	0.001	0.0532	0.0006	0.83462	0.00001	2.07091	0.00002	78	9.861	3.936
PA-07B	23.8	1.09	18.7906	0.0007	15.6836	0.0006	38.914	0.002	0.0532	0.0007	0.83464	0.00001	2.07092	0.00003	77	9.858	3.936
PA-11	31.1	0.082	18.7051	0.0006	15.6835	0.0005	38.831	0.002	0.0535	0.0006	0.83846	0.00001	2.07595	0.00004	140	9.875	3.949
PA-15	7727	20.1	18.6936	0.0009	15.6772	0.0008	38.807	0.002	0.0535	0.0009	0.83862	0.00001	2.07596	0.00004	136	9.852	3.942
SY-04	10.1	0.007	18.7062	0.0006	15.6914	0.0005	38.937	0.002	0.0535	0.0006	0.83882	0.00001	2.08151	0.00004	155	9.905	4.005
PK-01	114	4.58	18.7606	0.0009	15.6817	0.0007	38.841	0.002	0.0533	0.0009	0.83589	0.00001	2.07039	0.00006	96	9.856	3.918
PK-02	147	3.91	18.7666	0.0006	15.6874	0.0004	38.869	0.001	0.0533	0.0006	0.83590	0.00001	2.07120	0.00003	102	9.877	3.930
PK-03	140	5.52	18.7675	0.0007	15.6882	0.0007	38.870	0.002	0.0533	0.0007	0.83593	0.00001	2.07116	0.00004	103	9.880	3.930
PK-04	57.1	5.25	18.7680	0.0008	15.6887	0.0007	38.872	0.002	0.0533	0.0008	0.83593	0.00001	2.07118	0.00004	104	9.882	3.931
PK-06	95.3	0.910	18.7565	0.0006	15.6838	0.0005	38.856	0.001	0.0533	0.0006	0.83617	0.00001	2.07162	0.00002	103	9.866	3.929
PK-07	213	4.68	18.7643	0.0008	15.6904	0.0007	38.881	0.002	0.0533	0.0008	0.83617	0.00001	2.07208	0.00002	110	9.889	3.938
PK-08	147	0.177	18.7570	0.0007	15.6868	0.0006	38.870	0.002	0.0533	0.0007	0.83633	0.00001	2.07230	0.00002	108	9.877	3.936
PK-09	80.5	13.0	18.7652	0.0007	15.6863	0.0006	38.867	0.001	0.0533	0.0007	0.83593	0.00001	2.07120	0.00002	101	9.874	3.929
PK-11	58.6	9.67	18.7595	0.0008	15.6893	0.0010	38.883	0.003	0.0533	0.0008	0.83631	0.00001	2.07271	0.00005	111	9.886	3.942
THE-01	13.9	0.010	18.6328	0.0008	15.6669	0.0007	38.815	0.002	0.0537	0.0008	0.84082	0.00001	2.08312	0.00003	162	9.825	3.982
THE-02	52.2	19.1	18.7138	0.0008	15.6749	0.0007	38.949	0.002	0.0534	0.0008	0.83760	0.00001	2.08125	0.00003	117	9.839	4.000
THE-03	3.74	0.004	18.7146	0.0006	15.6747	0.0005	38.935	0.001	0.0534	0.0006	0.83757	0.00001	2.08045	0.00004	116	9.839	3.992
KIR-01	949	2.00	18.7177	0.0006	15.6727	0.0006	38.886	0.002	0.0534	0.0006	0.83731	0.00001	2.07754	0.00006	110	9.830	3.965
KIR-02	97.4	0.538	18.7155	0.0006	15.6696	0.0006	38.881	0.002	0.0534	0.0006	0.83726	0.00001	2.07747	0.00003	105	9.819	3.962
KIR-03	1045	0.328	18.7170	0.0009	15.6691	0.0008	38.878	0.002	0.0534	0.0009	0.83716	0.00001	2.07718	0.00004	103	9.816	3.960
KIR-04	372	19.8	18.7146	0.0007	15.6695	0.0005	38.880	0.001	0.0534	0.0007	0.83728	0.00001	2.07752	0.00003	106	9.818	3.962
SAP-01	0.396	0.040	18.7549	0.0007	15.6715	0.0006	38.849	0.002	0.0533	0.0007	0.83559	0.00001	2.07139	0.00003	80	9.818	3.921
SAP-02	0.000	0.009	18.8143	0.0006	15.7137	0.0005	39.086	0.001	0.0532	0.0006	0.83521	0.00001	2.07747	0.00003	118	9.970	4.017
AIS-01	66.2	2.04	18.7430	0.0006	15.6644	0.0005	38.819	0.001	0.0534	0.0006	0.83574	0.00001	2.07109	0.00003	75	9.793	3.911
NED-01	38.7	19.6	18.7527	0.0011	15.6730	0.0010	38.845	0.003	0.0533	0.0011	0.83575	0.00002	2.07141	0.00008	84	9.824	3.921
NED-02	45.5	29.2	18.7482	0.0013	15.6687	0.0013	38.835	0.004	0.0533	0.0013	0.83575	0.00002	2.07139	0.00008	79	9.809	3.918
NED-03	17.7	7.50	18.7443	0.0013	15.6669	0.0012	38.830	0.003	0.0533	0.0013	0.83582	0.00001	2.07156	0.00005	78	9.802	3.917
PEF-02	1.30	0.112	18.7472	0.0008	15.6745	0.0007	38.875	0.002	0.0533	0.0008	0.83608	0.00001	2.07361	0.00003	92	9.831	3.941

Table 4
Lead isotope data from the literature.

Sample	District	mine	Ancient Mining	Collected by	Main minerals*	$^{206}Pb/^{204}Pb$	$^{207}Pb/^{204}Pb$	$^{208}Pb/^{204}Pb$	$^{204}Pb/^{206}Pb$	$^{207}Pb/^{206}Pb$	$^{208}Pb/^{206}Pb$	Reference
388	Lavrion	Esperanza	Yes		Gn	18.833	15.6709	38.817	0.0531	0.83210	2.06110	Barnes et al. (1974)
389	Lavrion	Esperanza	Yes		Gn	18.846	15.6703	38.823	0.0531	0.83149	2.06000	Barnes et al. (1974)
390	Lavrion	Esperanza	Yes		Gn	18.851	15.6705	38.844	0.0530	0.83128	2.06060	Barnes et al. (1974)
396	Lavrion	Kamareza	Yes		Gn	18.822	15.6633	38.760	0.0531	0.83218	2.05930	Barnes et al. (1974)
397	Lavrion	Kamareza	Yes		Gn	18.842	15.6699	38.803	0.0531	0.83165	2.05940	Barnes et al. (1974)
398	Lavrion	Kamareza	Yes		Gn	18.875	15.6983	38.845	0.0530	0.83170	2.05800	Barnes et al. (1974)
399	Lavrion	Kamareza	Yes		Gn	18.864	15.6728	38.820	0.0530	0.83083	2.05790	Barnes et al. (1974)
D1	Lavrion	Kamareza	Yes	Dayton	Gn	18.851	15.6867	38.806	0.0530	0.83214	2.05857	Stos-Gale et al. (1996)
TG60A-3	Lavrion	Kamareza	Yes	NHG/Gentner/Wagner	Gn/Cer?	18.830	15.6592	38.757	0.0531	0.83161	2.05825	Stos-Gale et al. (1996)
TG60A-2	Lavrion	Kamareza	Yes	NHG/Gentner/Wagner	Cer	18.895	15.7025	38.899	0.0529	0.83104	2.05871	Stos-Gale et al. (1996)
383	Lavrion	Plaka	No	V. Avdis	Gn	18.866	15.6827	38.864	0.0530	0.83127	2.06000	Barnes et al. (1974)
384	Lavrion	Plaka	No	V. Avdis	Gn	18.831	15.6567	38.799	0.0531	0.83143	2.06040	Barnes et al. (1974)
22252/91	Lavrion	Plaka	No	S. Papastavrou	Gn	18.923	15.7369	38.993	0.0528	0.83163	2.06059	OXALID unpublished data
Filon 80	Lavrion	Plaka	No	S. Papastavrou	Gn	18.916	15.7267	38.973	0.0529	0.83140	2.06033	OXALID unpublished data
PL1/90	Lavrion	Plaka	No	NHG&ZSG	Gn	18.906	15.7183	38.969	0.0529	0.83139	2.06119	Stos-Gale et al. (1996)
PL2	Lavrion	Plaka	No	NHG&ZSG	Gn	18.886	15.7069	38.940	0.0529	0.83167	2.06184	Stos-Gale et al. (1996)
385	Lavrion	Plaka 33	No	V. Avdis	Gn	18.831	15.6627	38.801	0.0531	0.83175	2.06050	Barnes et al. (1974)
386	Lavrion	Plaka 33	No	V. Avdis	Gn	18.820	15.6575	38.773	0.0531	0.83196	2.06020	Barnes et al. (1974)
387	Lavrion	Plaka 33	No	V. Avdis	Gn	18.832	15.6684	38.864	0.0531	0.83201	2.06370	Barnes et al. (1974)
391	Lavrion	Plaka-80	No	V. Avdis	Gn	18.857	15.6739	38.838	0.0530	0.83120	2.05960	Barnes et al. (1974)
392	Lavrion	Plaka-80	No	V. Avdis	Gn	18.874	15.6737	38.863	0.0530	0.83044	2.05910	Barnes et al. (1974)
393	Lavrion	Plaka-80	No	V. Avdis	Gn	18.877	15.6864	38.883	0.0530	0.83098	2.05980	Barnes et al. (1974)
394	Lavrion	Plaka-80	No	V. Avdis	Gn	18.849	15.6831	38.855	0.0530	0.83204	2.06140	Barnes et al. (1974)
A6	Lavrion	Plaka N.	No	NHG&ZSG	Gn	18.846	15.6933	38.893	0.0531	0.83271	2.06375	Stos-Gale et al. (1996)
A5	Lavrion	Plaka N.	No	NHG&ZSG	Gn	18.886	15.7137	38.959	0.0529	0.83203	2.06287	Stos-Gale et al. (1996)
A5B	Lavrion	Plaka N.	No	NHG&ZSG	Gn	18.897	15.7076	38.956	0.0529	0.83122	2.06150	Stos-Gale et al. (1996)
C3	Lavrion	Plaka S.	No	NHG&ZSG	Gn	18.911	15.7043	38.938	0.0529	0.83043	2.05902	Stos-Gale et al. (1996)
395	Lavrion	Plaka, Filon Sklives	No	V. Avdis	Gn	18.849	15.6831	38.855	0.0531	0.83204	2.06140	Barnes et al. (1974)
B2	Lavrion	Plaka	No	Dayton	Gn	18.882	15.6942	38.836	0.0530	0.83117	2.05676	Stos-Gale et al. (1996)
B5	Lavrion	Plaka	No	Dayton	Gn	18.857	15.6753	38.836	0.0530	0.83127	2.05951	Stos-Gale et al. (1996)
S12 published	Lavrion	Sounio	Yes	NHG&ZSG	Gn	18.910	15.7080	38.975	0.0529	0.83067	2.06110	Stos-Gale et al. (1996)
SOUL 7a	Lavrion	Soureza	Yes	NHG&ZSG	Gn in Lm	18.868	15.6989	38.889	0.0530	0.83204	2.06109	OXALID unpublished data
22364B	Makronisos	Central mines	Yes	S. Papastavrou	Gn	18.822	15.6445	38.717	0.0531	0.83118	2.05701	OXALID unpublished data
22354 KAM 354	Lavrion	Kamareza	Yes	S. Papastavrou	Gn	18.868	15.6870	38.862	0.0530	0.83141	2.05970	OXALID unpublished data
KAM 102	Lavrion	Kamareza	Yes	NHG&ZSG	Gn	18.872	15.6904	38.876	0.0530	0.83141	2.05997	OXALID unpublished data
22221 MP 221	Lavrion	Megala Pevka	Yes	S. Papastavrou	Gn	18.854	15.6907	38.847	0.0530	0.83222	2.06040	OXALID unpublished data
22235 PL 235	Lavrion	Plaka	No	S. Papastavrou	Gn	18.863	15.6819	38.842	0.0530	0.83136	2.05917	OXALID unpublished data
22251 PL 251	Lavrion	Plaka	No	S. Papastavrou	Gn	18.843	15.6794	38.830	0.0531	0.83211	2.06070	OXALID unpublished data
22252a PL 252A	Lavrion	Plaka	No	S. Papastavrou	Gn	18.848	15.6813	38.832	0.0531	0.83199	2.06027	OXALID unpublished data
22345 PL 345	Lavrion	Plaka	No	S. Papastavrou	Gn	18.850	15.6968	38.845	0.0531	0.83272	2.06073	OXALID unpublished data
PL 11	Lavrion	Plaka	No	NHG&ZSG	Gn	18.885	15.6951	38.891	0.0530	0.83109	2.05937	OXALID unpublished data
PL 16	Lavrion	Plaka Christiana	Yes	NHG&ZSG	Gn	18.856	15.6829	38.844	0.0530	0.83172	2.06005	OXALID unpublished data
PL 17	Lavrion	Plaka Christiana	Yes	NHG&ZSG	Gn	18.856	15.6774	38.844	0.0530	0.83143	2.06003	OXALID unpublished data
PL 13	Lavrion	Plaka-80	No	NHG&ZSG	Gn	18.884	15.6813	38.824	0.0530	0.83040	2.05590	OXALID unpublished data
PL 14	Lavrion	Plaka-80	No	NHG&ZSG	Gn	18.868	15.6840	38.840	0.0530	0.83125	2.05852	OXALID unpublished data
PL 15	Lavrion	Plaka-80	No	NHG&ZSG	Gn	18.882	15.6860	38.823	0.0530	0.83074	2.05610	OXALID unpublished data
PL F85	Lavrion	Plaka-80	No	NHG&ZSG	Gn	18.878	15.6840	38.841	0.0530	0.83081	2.05750	OXALID unpublished data
KALL 1	Euboea	Kallianou	Yes	NHG/ZSG	Gn	18.666	15.6714	38.805	0.0536	0.83957	2.07893	OXALID unpublished data
KALL 2 (TG59)	Euboea	Kallianou	Yes	NHG/ZSG	Gn	18.655	15.6821	38.851	0.0536	0.84064	2.08263	OXALID unpublished data
KALL3 (TG59)	Euboea	Kallianou	Yes	NHG/ZSG	Gn	18.668	15.6694	38.788	0.0536	0.83937	2.07779	OXALID unpublished data
KALL3 (TG59)	Euboea	Kallianou, Saliza mine	No	NHG/ZSG	Gn	18.667	15.6749	38.837	0.0536	0.83971	2.08054	OXALID unpublished data
TG-56A	Euboea	Almyropotamos	Yes		Gn	18.820	15.7000	38.980	0.0531	0.83422	2.07120	Wagner and Weisgerber (1985)
TG-56B	Euboea	Almyropotamos	Yes		Gn	18.850	15.7200	38.920	0.0531	0.83395	2.06472	Wagner and Weisgerber (1985)
AVE 1 (TG56)	Euboea	Almyropotamos	Yes	NHG/ZSG	Gn	18.827	15.7077	38.929	0.0531	0.83432	2.06772	OXALID unpublished data
AVE2 (TG56)	Euboea	Almyropotamos	Yes	NHG/ZSG	Gn	18.835	15.7176	38.920	0.0531	0.83449	2.06634	OXALID unpublished data

(*continued on next page*)

Table 4 (*continued*)

Sample	District	mine	Ancient Mining	Collected by	Main minerals*	$^{206}Pb/^{204}Pb$	$^{207}Pb/^{204}Pb$	$^{208}Pb/^{204}Pb$	$^{204}Pb/^{206}Pb$	$^{207}Pb/^{206}Pb$	$^{208}Pb/^{206}Pb$	Reference
TG43/9	Siphnos	Ay. Sostis Dump	Yes	Gale	Gn	18.714	15.6881	38.915	0.0534	0.83831	2.07945	Wagner and Weisgerber (1985)
TG43/10	Siphnos	Ay. Sostis	Yes	Gale	Cer	18.731	15.7159	38.986	0.0534	0.83903	2.08138	Wagner and Weisgerber (1985)
TG43/10	Siphnos	Ay. Sostis	Yes	Gale	Cer	18.731	15.7159	38.986	0.0534	0.83903	2.08138	Wagner and Weisgerber (1985)
TG54-4/2	Siphnos	Voreini	Yes		Jrs, Lm	18.720	15.6892	38.910	0.0534	0.83810	2.07850	Wagner and Weisgerber (1985)
TG55A-13	Siphnos	Kapsalos-Tsingoura	Yes			18.741	15.7141	38.977	0.0534	0.83849	2.07978	Wagner and Weisgerber (1985)
TG55A-14	Siphnos	Kapsalos-Tsingoura	Yes			18.723	15.6953	38.938	0.0534	0.83829	2.07970	Wagner and Weisgerber (1985)
TG55A-15	Siphnos	Kapsalos-Tsingoura	Yes			18.743	15.7158	38.984	0.0534	0.83849	2.07993	Wagner and Weisgerber (1985)
TG55A-16	Siphnos	Kapsalos-Tsingoura	Yes			18.735	15.6994	38.923	0.0534	0.83797	2.07757	Wagner and Weisgerber (1985)
TG55A-17	Siphnos	Kapsalos-Tsingoura	Yes			18.762	15.7310	39.070	0.0533	0.83845	2.08238	Wagner and Weisgerber (1985)
TG55A-18	Siphnos	Kapsalos-Tsingoura	Yes			18.757	15.7234	39.004	0.0533	0.83827	2.08238	Wagner and Weisgerber (1985)
TG55A-19	Siphnos	Kapsalos-Tsingoura	Yes			18.775	15.7430	39.063	0.0533	0.83851	2.07942	Wagner and Weisgerber (1985)
TG55A-20	Siphnos	Kapsalos-Tsingoura	Yes			18.752	15.7192	39.039	0.0533	0.83827	2.08060	Wagner and Weisgerber (1985)
TG55A-21	Siphnos	Kapsalos-Tsingoura	Yes			18.763	15.7305	38.988	0.0533	0.83838	2.08187	Wagner and Weisgerber (1985)
TG69-6	Siphnos	Xero Xylo	Yes		Jrs	18.730	15.6901	38.658	0.0534	0.83770	2.07790	Wagner and Weisgerber (1985)
SER21/TG52a2	Seriphos	Moutoula	Yes	NHG	Gn	18.920	15.7175	39.049	0.0529	0.83075	2.06394	OXALID unpublished data
SER1/96	Seriphos	Moutoula	Yes	ZSG/NHG	Gn	18.900	15.6977	38.969	0.0529	0.83055	2.06179	OXALID unpublished data
SER10/2	Seriphos	Moutoula	Yes	ZSG/NHG	Gn	18.903	15.7044	38.989	0.0529	0.83080	2.06260	OXALID unpublished data
SER2/2	Seriphos	Moutoula	Yes	ZSG/NHG	Gn	18.902	15.7020	38.983	0.0529	0.83070	2.06234	OXALID unpublished data
SER25/TG52b5	Seriphos	Moutoula	Yes	Gale	Gn	18.900	15.6948	38.961	0.0529	0.83042	2.06142	OXALID unpublished data
SER26/TG52b6	Seriphos	Moutoula	Yes	Gale	Gn	18.900	15.6960	38.964	0.0529	0.83048	2.06161	OXALID unpublished data
SER27/TG52b7	Seriphos	Moutoula	Yes	Gale	Gn	18.902	15.6977	38.972	0.0529	0.83050	2.06183	OXALID unpublished data
SER28/TG52 B8	Seriphos	Moutoula	Yes	Gale	Gn	18.901	15.6955	38.966	0.0529	0.83041	2.06160	OXALID unpublished data
SER29	Seriphos	Moutoula	Yes	Gale	Gn	18.896	15.6919	38.952	0.0529	0.83042	2.06133	OXALID unpublished data
SER31	Seriphos	Moutoula	Yes	Gale	Gn	18.899	15.6967	38.967	0.0529	0.83054	2.06182	OXALID unpublished data
SER33	Seriphos	Moutoula	Yes	Gale	Gn	18.901	15.6988	38.971	0.0529	0.83058	2.06183	OXALID unpublished data
SER34	Seriphos	Moutoula	Yes	Gale	Gn	18.895	15.6927	38.949	0.0529	0.83053	2.06137	OXALID unpublished data
SER35	Seriphos	Moutoula	Yes	Gale	Gn	18.912	15.7140	39.024	0.0529	0.83092	2.06349	OXALID unpublished data
SER36	Seriphos	Moutoula	Yes	Gale	Gn	18.894	15.6913	38.946	0.0529	0.83051	2.06134	OXALID unpublished data
SER37	Seriphos	Moutoula	Yes	Gale	Gn	18.896	15.6904	38.943	0.0529	0.83035	2.06090	OXALID unpublished data
SER39	Seriphos	Moutoula	Yes	Gale	Gn	18.897	15.6943	38.954	0.0529	0.83054	2.06146	OXALID unpublished data
SER40	Seriphos	Moutoula	Yes	Gale	Gn	18.896	15.6907	38.941	0.0529	0.83038	2.06081	OXALID unpublished data
SER41	Seriphos	Moutoula	Yes	Gale	Gn	18.898	15.6940	38.952	0.0529	0.83047	2.06122	OXALID unpublished data
SER42	Seriphos	Moutoula	Yes	Gale	Gn	18.894	15.6897	38.941	0.0529	0.83041	2.06105	OXALID unpublished data
SER45	Seriphos	Moutoula	Yes	Gale	Gn	18.900	15.6951	38.962	0.0529	0.83044	2.06153	OXALID unpublished data
SER7/4	Seriphos	Moutoula	Yes	Gale	Gn	18.894	15.6940	39.010	0.0529	0.83065	2.06474	OXALID unpublished data
SER8/2	Seriphos	Moutoula	Yes	Gale	Gn	18.898	15.7009	39.032	0.0529	0.83084	2.06543	OXALID unpublished data
SER9/2	Seriphos	Moutoula	Yes	Gale	Gn	18.895	15.6970	39.018	0.0529	0.83077	2.06503	OXALID unpublished data
SER 20	Seriphos	Moutoula	Yes	ZSG/NHG	Gn	18.879	15.6758	38.931	0.0530	0.83033	2.06213	OXALID unpublished data
SER14/2	Seriphos	Moutoula	Yes	NHG	Gn	18.902	15.7008	38.979	0.0529	0.83066	2.06219	OXALID unpublished data
SER18/2	Seriphos	Moutoula	Yes	NHG	Gn	18.899	15.7114	39.011	0.0529	0.83135	2.06422	OXALID unpublished data
SER20	Seriphos	Moutoula	Yes	NHG	Gn	18.895	15.6920	38.950	0.0529	0.83050	2.06144	OXALID unpublished data
TG 52 A2	Seriphos	Moutoula	Yes	Gale	Gn	18.919	15.7124	39.049	0.0529	0.83051	2.06400	OXALID unpublished data
TG 52 A4	Seriphos	Moutoula	Yes	Gale	Gn	18.892	15.6858	38.956	0.0529	0.83029	2.06202	Gale (1998)
TG 52 A5	Seriphos	Moutoula	Yes	Gale	Gn	18.885	15.6795	38.948	0.0530	0.83026	2.06238	Gale (1998)
SER1	Seriphos	Moutoula	Yes	ZSG/NHG	Gn	18.942	15.7397	39.086	0.0528	0.83094	2.06344	Gale and Stos-Gale (1981a)
SER10/1	Seriphos	Moutoula	Yes	ZSG/NHG	Gn	18.888	15.6898	38.980	0.0529	0.83069	2.06377	Stos-Gale et al. (1996)
SER12/1	Seriphos	Moutoula	Yes	ZSG/NHG	Gn	18.901	15.7039	39.017	0.0529	0.83087	2.06432	Stos-Gale et al. (1996)
SER12/2	Seriphos	Moutoula	Yes	ZSG/NHG	Gn	18.896	15.6980	38.968	0.0529	0.83075	2.06219	OXALID unpublished data
SER13/2	Seriphos	Moutoula	Yes	ZSG/NHG	Gn	18.901	15.7001	38.978	0.0529	0.83063	2.06216	OXALID unpublished data
SER14/1	Seriphos	Moutoula	Yes	ZSG/NHG	Gn	18.893	15.6937	38.989	0.0529	0.83066	2.06370	OXALID unpublished data
SER15/1	Seriphos	Moutoula	Yes	ZSG/NHG	Gn	18.899	15.7012	39.015	0.0529	0.83080	2.06441	Gale (1998)
SER16/2	Seriphos	Moutoula	Yes	ZSG/NHG	Gn	18.897	15.7007	39.003	0.0529	0.83088	2.06401	Stos-Gale et al. (1996)
SER17/1	Seriphos	Moutoula	Yes	ZSG/NHG	Gn	18.938	15.7446	39.160	0.0528	0.83138	2.06781	Gale (1998)
SER17/2	Seriphos	Moutoula	Yes	ZSG/NHG	Gn	18.879	15.6836	38.963	0.0530	0.83075	2.06384	Stos-Gale et al. (1996)
SER18/1	Seriphos	Moutoula	Yes	ZSG/NHG	Gn	18.909	15.7123	39.051	0.0529	0.83094	2.06520	Stos-Gale et al. (1996)
SER19	Seriphos	Moutoula	Yes	ZSG/NHG	Gn	18.895	15.6944	38.987	0.0529	0.83063	2.06340	Gale (1998)

(*continued on next page*)

Table 4 (*continued*)

Sample	District	mine	Ancient Mining	Collected by	Main minerals*	$^{206}Pb/^{204}Pb$	$^{207}Pb/^{204}Pb$	$^{208}Pb/^{204}Pb$	$^{204}Pb/^{206}Pb$	$^{207}Pb/^{206}Pb$	$^{208}Pb/^{206}Pb$	Reference
SER2/95 (TG52A)	Seriphos	Moutoula	Yes	Gale	Gn	18.920	15.7148	39.058	0.0529	0.83059	2.06437	Stos-Gale et al. (1996)
SER3 (TG52B)	Seriphos	Moutoula	Yes	Gale	Gn	18.893	15.6920	38.968	0.0529	0.83057	2.06255	Gale and Stos-Gale (1981a)
SER15/2	Seriphos	Moutoula	Yes	Gale	Gn	18.904	15.6986	38.977	0.0529	0.83044	2.06183	OXALID unpublished data
SER23/TG52b3	Seriphos	Moutoula	Yes	Gale	Gn	18.901	15.6968	38.967	0.0529	0.83048	2.06166	OXALID unpublished data
SER5/2	Seriphos	Moutoula	Yes	Gale	Gn	18.896	15.6943	39.009	0.0529	0.83056	2.06440	OXALID unpublished data
SER6/1	Seriphos	Moutoula	Yes	Gale	Gn	18.901	15.6917	38.980	0.0529	0.83021	2.06236	OXALID unpublished data
SER6/2	Seriphos	Moutoula	Yes	Gale	Gn	18.909	15.7116	39.001	0.0529	0.83092	2.06259	OXALID unpublished data
SER7/1	Seriphos	Moutoula	Yes	Gale	Gn	18.923	15.7331	39.120	0.0528	0.83143	2.06731	Stos-Gale et al. (1996)
SER8/1	Seriphos	Moutoula	Yes	Gale	Gn	18.906	15.7076	39.044	0.0529	0.83081	2.06512	OXALID unpublished data
SER9/1	Seriphos	Moutoula	Yes	Gale	Gn	18.904	15.7075	39.034	0.0529	0.83092	2.06489	Gale (1998)
TG 52 B1	Seriphos	Moutoula	Yes	Gale	Gn	18.890	15.6844	38.966	0.0529	0.83030	2.06280	Gale (1998)
TG 52 B2/1	Seriphos	Moutoula	Yes	Gale	Gn	18.927	15.7228	39.088	0.0528	0.83069	2.06514	OXALID unpublished data
TG 52 B2/2	Seriphos	Moutoula	Yes	Gale	Gn	18.856	15.6439	38.826	0.0530	0.82965	2.05909	OXALID unpublished data
TG 52 B3	Seriphos	Moutoula	Yes	Gale	Gn	18.861	15.6490	38.842	0.0530	0.82970	2.05937	OXALID unpublished data
TG 52 B6	Seriphos	Moutoula	Yes	Gale	Gn	18.916	15.7199	39.083	0.0529	0.83105	2.06618	Stos-Gale et al. (1996)
TG 52 B7	Seriphos	Moutoula	Yes	Gale	Gn	18.899	15.7009	39.017	0.0529	0.83079	2.06454	Gale (1998)
MIL1	Milos	Pilonisi		IGME	Gn	18.852	15.6673	38.901	0.0530	0.83107	2.06352	IGME unpublished data
IGMRII	Milos					18.882	15.7009	39.061	0.0530	0.83153	2.06871	Gale and Stos-Gale (1981a)
SYR 17A-1	Syros	Komito	No	ZSG/NHG	Gn	18.798	15.6678	38.936	0.0532	0.83348	2.07129	Stos-Gale et al. (1996)
SYR 17A-2	Syros	Komito	No	ZSG/NHG	Gn	18.800	15.6745	38.954	0.0532	0.83375	2.07202	Stos-Gale et al. (1996)
SYR 18A-1	Syros	Komito	No	ZSG/NHG	Gn	18.800	15.6781	38.953	0.0532	0.83394	2.07195	Stos-Gale et al. (1996)
SYR 18A-2	Syros	Komito	No	ZSG/NHG	Gn	18.854	15.7225	39.124	0.0530	0.83391	2.07509	Stos-Gale et al. (1996)
SYR 3A-1	Syros	Rozos	Yes	ZSG/NHG	Gn	18.785	15.6688	38.923	0.0532	0.83411	2.07203	Stos-Gale et al. (1996)
SYR 3A-2	Syros	Rozos	Yes	ZSG/NHG	Gn	18.780	15.6642	38.903	0.0532	0.83409	2.07153	Stos-Gale et al. (1996)
SYR 3A-3	Syros	Rozos	Yes	ZSG/NHG	Gn	18.803	15.6919	38.994	0.0532	0.83454	2.07384	Stos-Gale et al. (1996)
SYR 3A-4	Syros	Rozos	Yes	ZSG/NHG	Gn	18.807	15.6967	39.022	0.0532	0.83462	2.07487	Stos-Gale et al. (1996)
SYR 3B	Syros	Rozos	Yes	ZSG/NHG	Gn	18.781	15.6643	38.909	0.0532	0.83405	2.07171	Stos-Gale et al. (1996)
SYR 3C-2	Syros	Rozos	Yes	ZSG/NHG	Gn	18.802	15.6912	38.996	0.0532	0.83455	2.07404	Stos-Gale et al. (1996)
SYR 3C-3	Syros	Rozos	Yes	ZSG/NHG	Gn	18.788	15.6729	38.930	0.0532	0.83420	2.07208	Stos-Gale et al. (1996)
SYR 2B	Syros	Rozos	Yes	ZSG/NHG	Gn	18.818	15.7042	39.036	0.0531	0.83453	2.07438	Stos-Gale et al. (1996)
SYR 2C	Syros	Rozos	Yes	ZSG/NHG	Gn	18.806	15.6835	38.976	0.0532	0.83396	2.07251	Stos-Gale et al. (1996)
SYR 2D-1	Syros	Rozos	Yes	ZSG/NHG	Gn	18.803	15.6808	38.957	0.0532	0.83395	2.07186	Stos-Gale et al. (1996)
SYR 2D-2	Syros	Rozos	Yes	ZSG/NHG	Gn	18.842	15.7093	39.081	0.0531	0.83374	2.07415	Stos-Gale et al. (1996)
SYR 2D-3	Syros	Rozos	Yes	ZSG/NHG	Gn	18.805	15.6965	39.006	0.0532	0.83470	2.07425	Stos-Gale et al. (1996)
JK 5	Kythnos	Agios Dimitrios	Yes	Jansen, Utrecht	Gn	18.937	15.6959	39.002	0.0528	0.82885	2.05954	OXALID unpublished data
JK 4	Kythnos	Agios Dimitrios	Yes	Jansen, Utrecht	Gn	18.940	15.6980	39.013	0.0528	0.82883	2.05984	OXALID unpublished data
KYTG9	Kythnos	Agios Dimitrios	Yes	Jansen, Utrecht	Gn	18.927	15.6721	38.936	0.0528	0.82803	2.05716	OXALID unpublished data
KYTG10	Kythnos	Agios Dimitrios	Yes	Jansen, Utrecht	Gn	18.987	15.7465	39.180	0.0527	0.82933	2.06350	OXALID unpublished data
ANTI 5	Antiparos	Agios Georgios	No	Gale	Gn	18.817	15.7259	39.147	0.0531	0.83573	2.08039	Stos-Gale et al. (1996)
ANTI 6	Antiparos	Agios Georgios	No	Gale	Gn	18.822	15.7147	39.089	0.0531	0.83491	2.07679	Stos-Gale et al. (1996)
ANTI 7	Antiparos	Agios Georgios	No	Gale	Gn	18.815	15.7099	39.085	0.0531	0.83495	2.07727	Stos-Gale et al. (1996)
ANTI 8	Antiparos	Agios Georgios	No	Gale	Gn	18.809	15.7110	39.086	0.0532	0.83529	2.07804	Stos-Gale et al. (1996)
ANTI 9	Antiparos	Agios Georgios	No	Gale	Gn	18.820	15.7277	39.152	0.0531	0.83569	2.08033	Stos-Gale et al. (1996)
ANTI 10	Antiparos	Agios Georgios	No	Gale	Gn	18.815	15.7160	39.103	0.0531	0.83529	2.07830	Stos-Gale et al. (1996)
ANTI 11	Antiparos	Agios Georgios	No	Gale	Gn	18.820	15.7160	39.106	0.0531	0.83507	2.07788	Stos-Gale et al. (1996)
ANTI 12	Antiparos	Agios Georgios	No	Gale	Gn	18.816	15.7230	39.135	0.0531	0.83564	2.07993	Stos-Gale et al. (1996)
ANTI 13	Antiparos	Agios Georgios	No	Gale	Gn	18.814	15.7148	39.116	0.0532	0.83527	2.07910	Stos-Gale et al. (1996)
ANTI 14	Antiparos	Agios Georgios	No	Gale	Gn	18.815	15.7071	39.083	0.0531	0.83482	2.07722	Stos-Gale et al. (1996)
AP1/95	Antiparos	Agios Georgios	No	Gale	Gn	18.818	15.7134	39.093	0.0531	0.83502	2.07744	Stos-Gale et al. (1996)
AP4/95	Antiparos	Agios Georgios	No	Gale	Gn	18.813	15.7120	39.091	0.0532	0.83519	2.07794	Stos-Gale et al. (1996)
AP8	Antiparos	Agios Georgios	No	Gale	Gn	18.832	15.7339	39.162	0.0531	0.83549	2.07956	Gale and Stos-Gale (1981a)
AP9	Antiparos	Agios Georgios	No	Gale	Gn	18.827	15.7296	39.135	0.0531	0.83548	2.07864	Gale and Stos-Gale (1981a)
TG45D	Polyaigos	Tris Panagies	No	Gale/Gentner	Gn	18.914	15.7315	39.142	0.0529	0.83174	2.06946	Stos-Gale et al. (1996)
TG45E	Polyaigos	Tris Panagies	No	Gale/Gentner	Gn	18.917	15.7382	39.163	0.0529	0.83196	2.07026	Stos-Gale et al. (1996)
SN 12 B	Thera	Athinios	No	Gale/Bassiakos	Gn	18.983	15.7238	39.144	0.0527	0.82831	2.06203	Stos-Gale et al. (1996)
SN 12 C/1	Thera	Athinios	No	Gale/Bassiakos	Gn	18.995	15.7332	39.166	0.0526	0.82828	2.06190	Stos-Gale et al. (1996)

(*continued on next page*)

Table 4 (*continued*)

Sample	District	mine	Ancient Mining	Collected by	Main minerals*	$^{206}Pb/^{204}Pb$	$^{207}Pb/^{204}Pb$	$^{208}Pb/^{204}Pb$	$^{204}Pb/^{206}Pb$	$^{207}Pb/^{206}Pb$	$^{208}Pb/^{206}Pb$	Reference
SN 17 B	Thera	Athinios	No	Gale/Bassiakos	Gn	18.946	15.6670	38.947	0.0528	0.82693	2.05568	Stos-Gale et al. (1996)
SN 20 A	Thera	Athinios	No	Gale/Bassiakos	Gn	18.962	15.6895	39.020	0.0527	0.82742	2.05778	OXALID unpublished data
SN 20 B	Thera	Athinios	No	Gale/Bassiakos	Gn	18.974	15.7023	39.066	0.0527	0.82757	2.05892	Stos-Gale et al. (1996)
SN 21 A	Thera	Athinios	No	Gale/Bassiakos	Gn	18.975	15.7062	39.076	0.0527	0.82773	2.05935	Stos-Gale et al. (1996)
SN 21 C	Thera	Athinios	No	Gale/Bassiakos	Gn	18.970	15.6984	39.054	0.0527	0.82754	2.05871	Stos-Gale et al. (1996)
SN 21 D	Thera	Athinios	No	Gale/Bassiakos	Gn	18.968	15.6876	39.019	0.0527	0.82705	2.05707	Stos-Gale et al. (1996)
SN 21 E	Thera	Athinios	No	Gale/Bassiakos	Gn	18.972	15.7016	39.061	0.0527	0.82762	2.05889	OXALID unpublished data
360B/2	Thera	Cape Athinios	No	Karlsruhe	Gn	18.992	15.7089	39.088	0.0527	0.82713	2.05814	Stos-Gale et al. (1996)
PH30o/2	Thera	Cape Athinios	No	Karlsruhe	Gn	18.988	15.7099	39.091	0.0527	0.82737	2.05876	Stos-Gale et al. (1996)
ANAPHI1	Anaphi	Doumbaria	No	NHG&ZSG	Gn	18.883	15.7074	39.047	0.0530	0.83183	2.06783	OXALID unpublished data
ANA1/95	Anaphi	Stavros	No	NHG&ZSG	Gn	18.903	15.7008	39.026	0.0529	0.83060	2.06455	OXALID unpublished data
ANA11a	Anaphi	Stavros	No	NHG&ZSG	Gn	18.899	15.6960	39.010	0.0529	0.83052	2.06413	OXALID unpublished data
ANA11b	Anaphi	Stavros	No	NHG&ZSG	Gn	18.913	15.7119	39.068	0.0529	0.83076	2.06574	OXALID unpublished data
ANA13	Anaphi	Stavros	No	NHG&ZSG	Gn	18.894	15.7055	39.054	0.0529	0.83127	2.06705	OXALID unpublished data
ANA14	Anaphi	Stavros	No	NHG&ZSG	Gn	18.899	15.7060	39.099	0.0529	0.83105	2.06883	OXALID unpublished data
ANA15	Anaphi	Stavros	No	NHG&ZSG	Gn	18.946	15.7439	39.182	0.0528	0.83098	2.06804	OXALID unpublished data
ANA16	Anaphi	Stavros	No	NHG&ZSG	Gn	18.932	15.7271	39.128	0.0528	0.83071	2.06674	OXALID unpublished data
ANA17	Anaphi	Stavros	No	NHG&ZSG	Gn	18.896	15.6931	39.009	0.0529	0.83048	2.06438	OXALID unpublished data
ANA18	Anaphi	Stavros	No	NHG&ZSG	Gn	18.904	15.6938	39.015	0.0529	0.83017	2.06384	OXALID unpublished data
ANA4	Anaphi	Stavros	No	NHG&ZSG	Gn	18.916	15.7073	39.055	0.0529	0.83037	2.06464	OXALID unpublished data
ANA5	Anaphi	Stavros	No	NHG&ZSG	Gn	18.942	15.7421	39.181	0.0528	0.83108	2.06853	OXALID unpublished data
ANA6	Anaphi	Stavros	No	NHG&ZSG	Gn	18.913	15.7042	39.052	0.0529	0.83034	2.06483	OXALID unpublished data
ANA7	Anaphi	Stavros	No	NHG&ZSG	Gn	18.912	15.7039	39.045	0.0529	0.83038	2.06460	OXALID unpublished data
TG49	Samos	Ampelos (Nenedes)	No	Gentner	Gn	18.902	15.6862	38.896	0.0529	0.82987	2.05775	OXALID unpublished data
TG50B	Samos	Dhrakaioi, W. shore,Kalives	No	Gentner	Gn	18.853	15.6936	38.977	0.0530	0.83242	2.06740	OXALID unpublished data
TG50A	Samos	Dhrakaioi, W. shore, Mili	No	Gentner	Gn	18.867	15.6930	38.999	0.0530	0.83177	2.06704	OXALID unpublished data
TG47 published	Samos	Sikia, south shore	No	Gentner	Gn	17.833	15.6108	37.875	0.0561	0.87539	2.12386	OXALID unpublished data
TG46	Samos	Spatharaioi, galleries	No	Gentner	Gn	17.858	15.6199	37.982	0.0560	0.87467	2.12687	OXALID unpublished data
TG48	Samos	Zestos, N. Shore	No	Gentner	Gn	18.872	15.6796	38.868	0.0530	0.83084	2.05958	OXALID unpublished data
27711	Tinos	Apigania	No	Papastavrou	Gn	18.799	15.6833	38.949	0.0532	0.83426	2.07185	OXALID unpublished data
27798	Tinos	Apigania	No	Papastavrou	Gn	18.811	15.7000	38.999	0.0532	0.83462	2.07318	OXALID unpublished data
27708/2	Tinos	Apigania	No	Papastavrou	Gn	18.800	15.6860	38.947	0.0532	0.83436	2.07166	OXALID unpublished data
Ti1	Tinos	Apigania	No	Papastavrou	Gn	18.831	15.7216	39.079	0.0531	0.83488	2.07527	OXALID unpublished data
Ti2	Tinos	Apigania	No	Papastavrou	Gn	18.847	15.7269	39.100	0.0531	0.83445	2.07460	OXALID unpublished data
Ti27711	Tinos	Apigania	No	Papastavrou	Gn	18.827	15.7113	39.039	0.0531	0.83451	2.07354	OXALID unpublished data
Ti3	Tinos	Apigania	No	Papastavrou	Gn	18.839	15.7238	39.084	0.0531	0.83464	2.07463	OXALID unpublished data
Kea MEN 1	Kea	Schoinos	No	Mendoni	Gn	18.871	15.6922	38.970	0.0530	0.83156	2.06510	Gale (1998)
Kea MEN 4	Kea	Schoinos	No	Mendoni	Gn	18.868	15.6857	38.949	0.0530	0.83133	2.06423	Gale (1998)
F 1W/1	Kea	Faros	No	ZSG/NHG	Gn	18.905	15.7411	39.138	0.0529	0.83264	2.07022	OXALID unpublished data
F 1X/1 (TG 123B)	Kea	Faros	No	ZSG/NHG	Gn	18.881	15.7158	39.056	0.0530	0.83236	2.06854	OXALID unpublished data
F 1X/2 (TG 123B)	Kea	Faros	No	ZSG/NHG	Gn	18.860	15.6917	38.978	0.0530	0.83199	2.06666	OXALID unpublished data
FAR 1/3	Kea	Faros	No	ZSG/NHG	Gn	18.871	15.6977	39.006	0.0530	0.83186	2.06703	OXALID unpublished data
FAR 2/1	Kea	Faros	No	ZSG/NHG	Gn	18.868	15.6906	38.972	0.0530	0.83160	2.06553	OXALID unpublished data
FAR 5/1	Kea	Faros	No	ZSG/NHG	Gn	18.856	15.6734	38.915	0.0530	0.83122	2.06383	OXALID unpublished data
PET5	Kea	Faros	No	ZSG/NHG	Gn	18.861	15.6890	38.917	0.0530	0.83182	2.06338	OXALID unpublished data
PET6	Kea	Faros	No	ZSG/NHG	Gn	18.864	15.6892	38.947	0.0530	0.83170	2.06461	Gale (1998)
PET7	Kea	Faros	No	ZSG/NHG	Gn	18.861	15.6844	38.927	0.0530	0.83158	2.06390	Gale (1998)
KGP1	Kea	Faros	No	Jack Davis	Gn	18.839	15.6675	38.872	0.0531	0.83165	2.06338	OXALID unpublished data
KGP1	Kea	Faros	No	Jack Davis	Gn	18.858	15.6912	38.950	0.0530	0.83207	2.06544	OXALID unpublished data
KJD1A	Kea	Faros	No	Jack Davis	Gn	18.864	15.6832	38.946	0.0530	0.83138	2.06456	OXALID unpublished data
KJD1B	Kea	Faros	No	Jack Davis	Gn	18.883	15.7069	39.024	0.0530	0.83180	2.06662	OXALID unpublished data
KJD1C	Kea	Faros	No	Jack Davis	Gn	18.854	15.6718	38.868	0.0530	0.83122	2.06153	OXALID unpublished data
N 1W/1	Kea	Nikoleri	No	ZSG/NHG	Gn	18.893	15.7271	39.093	0.0529	0.83243	2.06919	OXALID unpublished data
N 1W/2	Kea	Nikoleri	No	ZSG/NHG	Gn	18.874	15.7026	39.015	0.0530	0.83197	2.06712	OXALID unpublished data
N 2C	Kea	Nikoleri	No	ZSG/NHG	Gn	18.873	15.7040	39.015	0.0530	0.83207	2.06720	OXALID unpublished data
N 2W	Kea	Nikoleri	No	ZSG/NHG	Gn	18.920	15.7539	39.181	0.0529	0.83266	2.07087	OXALID unpublished data

(*continued on next page*)

Table 4 (*continued*)

Sample	District	mine	Ancient Mining	Collected by	Main minerals*	$^{206}Pb/^{204}Pb$	$^{207}Pb/^{204}Pb$	$^{208}Pb/^{204}Pb$	$^{204}Pb/^{206}Pb$	$^{207}Pb/^{206}Pb$	$^{208}Pb/^{206}Pb$	Reference
N 2W	Kea	Nikoleri	No	ZSG/NHG	Gn	18.873	15.6961	38.995	0.0530	0.83167	2.06620	OXALID unpublished data
NI X	Kea	Nikoleri	No	ZSG/NHG	Gn	18.886	15.7111	39.042	0.0529	0.83189	2.06724	OXALID unpublished data
NIK 1C	Kea	Nikoleri	No	ZSG/NHG	Gn	18.905	15.7254	39.091	0.0529	0.83181	2.06775	OXALID unpublished data
PET10	Kea	Petroussa	No	ZSG/NHG	Gn	18.868	15.6918	38.976	0.0530	0.83168	2.06579	OXALID unpublished data
PET11	Kea	Petroussa	No	ZSG/NHG	Gn	18.872	15.6972	38.994	0.0530	0.83177	2.06624	OXALID unpublished data
PET12	Kea	Petroussa	No	ZSG/NHG	Gn	18.868	15.6935	38.983	0.0530	0.83175	2.06607	OXALID unpublished data
PET16	Kea	Petroussa	No	ZSG/NHG	Gn	18.875	15.7017	39.012	0.0530	0.83188	2.06684	OXALID unpublished data
PET19	Kea	Petroussa	No	ZSG/NHG	Gn	18.872	15.6985	38.998	0.0530	0.83184	2.06646	OXALID unpublished data
PET20	Kea	Petroussa	No	ZSG/NHG	Gn	18.881	15.7062	39.021	0.0530	0.83185	2.06670	OXALID unpublished data
PW 1	Kea	Petroussa	No	ZSG/NHG	Gn	18.890	15.7153	39.056	0.0529	0.83194	2.06757	OXALID unpublished data
PY 1	Kea	Petroussa	No	ZSG/NHG	Gn	18.892	15.7183	39.066	0.0529	0.83201	2.06784	OXALID unpublished data
PY 2	Kea	Petroussa	No	ZSG/NHG	Gn	18.865	15.6900	38.975	0.0530	0.83170	2.06597	OXALID unpublished data
D6a	Kea	Schoinos	No	Mendoni	Gn	18.864	15.7053	38.993	0.0530	0.83257	2.06710	Gale (1998)
G3	Kea	Schoinos	No	Mendoni	Gn	18.875	15.7091	39.025	0.0530	0.83226	2.06751	Gale (1998)
Kea MEN 2	Kea	Schoinos	No	Mendoni	Gn	18.896	15.7227	39.072	0.0529	0.83205	2.06767	Gale (1998)
Kea MEN 3	Kea	Schoinos	No	Mendoni	Gn	18.876	15.6937	38.978	0.0530	0.83139	2.06492	Gale (1998)
KG2	Kea	Spasmata	No	Photos	Gn	18.872	15.7002	38.995	0.0530	0.83192	2.06625	Gale (1998)
AT-1d	SW Peloponnesos	Ano Tiros	No	NHG/ZSG	Ccp /Gn	18.424	15.7190	38.683	0.0543	0.85319	2.09965	OXALID unpublished data
AT-1e	SW Peloponnesos	Ano Tiros	No	NHG/ZSG	Ccp /Gn	18.400	15.6881	38.582	0.0543	0.85260	2.09682	OXALID unpublished data
AT-1f	SW Peloponnesos	Ano Tiros	No	NHG/ZSG	Ccp /Gn	18.432	15.7274	38.715	0.0543	0.85326	2.10041	OXALID unpublished data
AT-1j	SW Peloponnesos	Ano Tiros	No	NHG/ZSG	Ccp /Gn	18.431	15.7259	38.712	0.0543	0.85321	2.10031	OXALID unpublished data
AT-1m	SW Peloponnesos	Ano Tiros	No	NHG/ZSG	Ccp /Gn	18.428	15.7220	38.701	0.0543	0.85316	2.10011	OXALID unpublished data
4541	SW Peloponnesos	Molai	No	IGME	Gn	18.400	15.6910	38.537	0.0543	0.85277	2.09441	OXALID unpublished data
4550	SW Peloponnesos	Molai	No	IGME	Gn	18.413	15.7076	38.588	0.0543	0.85307	2.09568	OXALID unpublished data
4543/94	SW Peloponnesos	Molai	No	IGME	Gn	18.404	15.6962	38.610	0.0543	0.85287	2.09792	OXALID unpublished data
MOL 11c	SW Peloponnesos	Molai	No	NHG/ZSG	Gn	18.400	15.6746	38.535	0.0543	0.85189	2.09432	OXALID unpublished data
MOL 11d	SW Peloponnesos	Molai	No	NHG/ZSG	Gn	18.421	15.6980	38.613	0.0543	0.85220	2.09621	OXALID unpublished data
MOL 11f	SW Peloponnesos	Molai	No	NHG/ZSG	Gn	18.426	15.7050	38.635	0.0543	0.85232	2.09674	OXALID unpublished data
MOL 11f	SW Peloponnesos	Molai	No	NHG/ZSG	Gn	18.426	15.7050	38.635	0.0543	0.85232	2.09674	OXALID unpublished data
4546	SW Peloponnesos	Molai	No	IGME	Gn	18.396	15.6795	38.505	0.0544	0.85233	2.09311	OXALID unpublished data
MOL 11b	SW Peloponnesos	Molai	No	NHG/ZSG	Gn	18.443	15.7270	38.708	0.0542	0.85272	2.09876	OXALID unpublished data
CH12	Chios		No	Papastavrou	Gn	18.211	15.6165	38.296	0.0549	0.85753	2.10292	OXALID unpublished data
CHI1	Chios	Agrelopos	No	Papastavrou	Gn	18.233	15.6439	38.385	0.0548	0.85800	2.10527	OXALID unpublished data
CHI3	Chios	Rosoja	No	Papastavrou	Gn	18.232	15.6423	38.352	0.0548	0.85796	2.10354	OXALID unpublished data
PIN 1A	Pelion	Agios Konstantinos	Yes	NHG/ZSG	Gn	18.799	15.6898	38.958	0.0532	0.83461	2.07232	OXALID unpublished data
PIN 5A	Pelion	Agios Konstantinos	Yes	NHG/ZSG	Gn	18.799	15.6956	38.972	0.0532	0.83492	2.07309	OXALID unpublished data
PIN 5A4	Pelion	Agios Konstantinos	Yes	NHG/ZSG	Gn	18.803	15.6951	38.974	0.0532	0.83472	2.07275	OXALID unpublished data
PIN 5A6	Pelion	Agios Konstantinos	Yes	NHG/ZSG	Gn	18.811	15.7062	39.018	0.0532	0.83497	2.07428	OXALID unpublished data
PIN 3A1	Pelion	Agios Konstantinos	Yes	NHG/ZSG	Gn	18.818	15.7138	39.034	0.0531	0.83503	2.07426	OXALID unpublished data
PIN 3A2	Pelion	Agios Konstantinos	Yes	NHG/ZSG	Gn	18.795	15.6896	38.957	0.0532	0.83477	2.07271	OXALID unpublished data
PIN 2A	Pelion	Agios Konstantinos	Yes	NHG/ZSG	Gn	18.801	15.6969	38.979	0.0532	0.83489	2.07321	OXALID unpublished data
PIN 5A2	Pelion	Agios Konstantinos	Yes	NHG/ZSG	Gn	18.822	15.7204	39.056	0.0531	0.83523	2.07505	OXALID unpublished data
PVORE-3	Pelion	Ksourichti	Yes	Vaxevanopoulos	Gth, Cer	18.867	15.7044	39.025	0.0530	0.83238	2.06840	Asderaki-Tzoumerkioti et al. (2017)
TG51	Lesbos	Argenos	Yes	Gentner	Gn	18.601	15.6702	38.977	0.0538	0.84244	2.09543	OXALID unpublished data
ML-A	Chalkidiki	Madem Lakkos	Yes		Gn	18.823	15.6890	38.989	0.0531	0.83350	2.07135	Frei (1992)
ML-A	Chalkidiki	Madem Lakkos	Yes		Gn	18.825	15.6940	38.991	0.0531	0.83368	2.07124	Frei (1992)
ML-A	Chalkidiki	Madem Lakkos	Yes		Gn	18.790	15.6810	38.959	0.0532	0.83454	2.07339	Frei (1992)
ML-A	Chalkidiki	Madem Lakkos	Yes		Gn	18.820	15.6870	38.966	0.0531	0.83353	2.07046	Frei (1992)
ML-B	Chalkidiki	Madem Lakkos	Yes		Gn	18.855	15.7310	39.113	0.0530	0.83431	2.07441	Frei (1992)
ML-B	Chalkidiki	Madem Lakkos	Yes		Gn	18.849	15.7210	39.073	0.0531	0.83405	2.07295	Frei (1992)
ML-B	Chalkidiki	Madem Lakkos	Yes		Gn	18.823	15.7250	39.106	0.0531	0.83541	2.07756	Frei (1992)
ML-B	Chalkidiki	Madem Lakkos	Yes		Gn	18.855	15.7300	39.115	0.0530	0.83426	2.07452	Frei (1992)
ML-Nr.3	Chalkidiki	Madem Lakkos	Yes		Gn	18.779	15.6690	38.913	0.0533	0.83439	2.07216	Frei (1992)
ML-Nr.5a	Chalkidiki	Madem Lakkos	Yes		Gn	18.778	15.6640	38.861	0.0533	0.83417	2.06950	Frei (1992)
ML-Nr.5b	Chalkidiki	Madem Lakkos	Yes		Gn	18.727	15.6590	38.881	0.0534	0.83617	2.07620	Frei (1992)
ML-Nr.5	Chalkidiki	Madem Lakkos	Yes		Gn	18.798	15.6640	38.894	0.0532	0.83328	2.06905	Frei (1992)

(*continued on next page*)

Table 4 (*continued*)

Sample	District	mine	Ancient Mining	Collected by	Main minerals*	$^{206}Pb/^{204}Pb$	$^{207}Pb/^{204}Pb$	$^{208}Pb/^{204}Pb$	$^{204}Pb/^{206}Pb$	$^{207}Pb/^{206}Pb$	$^{208}Pb/^{206}Pb$	Reference
B-97	Chalkidiki	Madem Lakkos	Yes		Gn	18.776	15.6570	38.875	0.0533	0.83388	2.07046	Frei (1992)
E-5	Chalkidiki	Madem Lakkos	Yes		Gn	18.768	15.6540	38.871	0.0533	0.83408	2.07113	Frei (1992)
E-27	Chalkidiki	Madem Lakkos	Yes		Gn	18.777	15.6670	38.908	0.0533	0.83437	2.07211	Frei (1992)
E-28	Chalkidiki	Madem Lakkos	Yes		Gn	18.773	15.6690	38.914	0.0533	0.83466	2.07287	Frei (1992)
E-37	Chalkidiki	Madem Lakkos	Yes		Gn	18.818	15.7030	39.045	0.0531	0.83447	2.07488	Frei (1992)
E-40	Chalkidiki	Madem Lakkos	Yes		Gn	18.782	15.6690	38.914	0.0532	0.83426	2.07188	Frei (1992)
7~1~5	Chalkidiki	Madem Lakkos	Yes		Gn	18.780	15.6700	38.910	0.0532	0.83440	2.07188	Nebel et al. (1991)
8~2~1	Chalkidiki	Madem Lakkos	Yes		Gn	18.780	15.6650	38.876	0.0532	0.83413	2.07007	Nebel et al. (1991)
7~10~1	Chalkidiki	Madem Lakkos	Yes		Gn	18.810	15.6700	38.880	0.0532	0.83307	2.06699	Nebel et al. (1991)
7~29~1	Chalkidiki	Madem Lakkos	Yes		Gn	18.795	15.6740	38.889	0.0532	0.83395	2.06911	Nebel et al. (1991)
AVE1	Chalkidiki	Madem Lakkos	Yes		Gn	18.780	15.6590	38.868	0.0532	0.83381	2.06965	Kalogeropoulos et al. (1989)
GRL1	Chalkidiki	Madem Lakkos	Yes		Gn	18.780	15.6600	38.880	0.0532	0.83387	2.07029	Wagner et al. (1986)
GRL3	Chalkidiki	Madem Lakkos	Yes		Gn	18.780	15.6600	38.910	0.0532	0.83387	2.07188	Wagner et al. (1986)
GRL4	Chalkidiki	Mavres Petres	Yes		Gn	18.810	15.6700	38.900	0.0532	0.83307	2.06805	Wagner et al. (1986)
GRL5	Chalkidiki	Mavres Petres	Yes		Gn	18.810	15.6600	38.900	0.0532	0.83254	2.06805	Wagner et al. (1986)
PBS	Chalkidiki	Olympiada	Yes		Gn	18.771	15.6620	38.840	0.0533	0.83437	2.06915	Frei (1992)
AVE4	Chalkidiki	Olympiada	Yes		Gn	18.780	15.6710	38.844	0.0532	0.83445	2.06837	Kalogeropoulos et al.1989
GRL6	Chalkidiki	Olympiada	Yes		Gn	18.780	15.6800	38.900	0.0532	0.83493	2.07135	Wagner et al. (1986)
GRL7	Chalkidiki	Olympiada	Yes		Gn	18.790	15.6800	38.910	0.0532	0.83449	2.07078	Wagner et al. (1986)
GRL8	Chalkidiki	Olympiada	Yes		Gn	18.780	15.6700	38.890	0.0532	0.83440	2.07082	Wagner et al. (1986)
ST-12a	Chalkidiki	Stratoni	Yes		Gn	18.776	15.6570	38.862	0.0533	0.83388	2.06977	Frei (1992)
ST-12b	Chalkidiki	Stratoni	Yes		Gn	18.785	15.6660	38.886	0.0532	0.83396	2.07006	Frei (1992)
TG25	Thasos	Agios Eleftherios	Yes	NHG/ZSG	Gn	18.751	15.6413	38.787	0.0533	0.83416	2.06854	Stos-Gale et al. (1996)
KM3	Thasos	Koumaria	Yes	NHG/ZSG	Gn	18.774	15.6703	38.879	0.0533	0.83468	2.07088	Stos-Gale et al. (1996)
KM2	Thasos	Koumaria	Yes	NHG/ZSG	Gn	18.781	15.6825	38.899	0.0532	0.83502	2.07118	Stos-Gale et al. (1996)
KM1	Thasos	Koumaria	Yes	NHG/ZSG	Gn	18.764	15.6606	38.824	0.0533	0.83461	2.06906	Stos-Gale et al. (1996)
MR1	Thasos	Marlou	Yes	IGME	Gn	18.780	15.6636	38.823	0.0532	0.83406	2.06726	Stos-Gale et al. (1996)
IGME 49	Thasos	Sotiros	Yes	IGME	Gn	18.782	15.6659	38.849	0.0532	0.83409	2.06842	Stos-Gale et al. (1996)
TG28 Sotir	Thasos	Sotiros	Yes	Gale	Gn	18.778	15.6592	38.866	0.0533	0.83391	2.06974	Stos-Gale et al. (1996)
IGME15	Pangaeon	Nikisiani Valley	Yes	NHG/ZSG	Gn	18.707	15.6810	38.810	0.0535	0.83824	2.07462	OXALID unpublished data
PS13	Rhodope	Kirki	No	Papastavrou	Gn	18.729	15.6500	38.770	0.0534	0.83560	2.07003	Stos-Gale et al. (1996)
PS5 (GAMMA)	Rhodope	Kirki	No	Papastavrou	Gn	18.696	15.6583	38.817	0.0535	0.83752	2.07621	Stos-Gale et al. (1996)
PS8 (GAMMA)	Rhodope	Kirki	No	Papastavrou	Gn	18.686	15.6398	38.754	0.0535	0.83698	2.07397	Stos-Gale et al. (1996)
PS9	Rhodope	Kirki	No	Papastavrou	Gn	18.686	15.6387	38.767	0.0535	0.83692	2.07464	Stos-Gale et al. (1996)
PS12 (KA 1)/871	Rhodope	Kirki	No	Papastavrou	Gn	18.728	15.6489	38.747	0.0534	0.83559	2.06894	Stos-Gale et al. (1996)
PS2 (SP 2)	Rhodope	Kirki	No	Papastavrou	Gn	18.690	15.6392	38.764	0.0535	0.83677	2.07407	Stos-Gale et al. (1996)
18	Rhodope	Kalotycho	No		Gn	18.645	15.6940	38.918	0.0536	0.84173	2.08732	Frei (1992)
1	Rhodope	Saint Philippos	No		Gn	18.721	15.6760	38.922	0.0534	0.83735	2.07906	Frei (1992)
PS-2	Rhodope	Saint Philippos	No		Gn	18.701	15.6500	38.806	0.0535	0.83685	2.07508	IGME Xanthi department
PS-3	Rhodope	Saint Philippos	No		Gn	18.704	15.6570	38.834	0.0535	0.83709	2.07624	IGME Xanthi department
PS-9	Rhodope	Saint Philippos	No		Gn	18.686	15.6390	38.767	0.0535	0.83694	2.07465	IGME Xanthi department
PS-12	Rhodope	Saint Philippos	No		Gn	18.730	15.6480	38.753	0.0534	0.83545	2.06903	IGME Xanthi department
PS-13	Rhodope	Saint Philippos	No		Gn	18.729	15.6490	38.769	0.0534	0.83555	2.07000	IGME Xanthi department
2	Rhodope	Saint Philippos	No		Gn	18.730	15.6530	38.772	0.0534	0.83572	2.07005	Frei (1992)
KA-1	Rhodope	King Arthur	No		Gn	18.769	15.6500	38.769	0.0533	0.83382	2.06559	IGME Xanthi department
7	Rhodope	Distrato	No		Gn	18.688	15.6590	38.915	0.0535	0.83792	2.08235	Frei (1992)
8	Rhodope	Distrato	No		Gn	18.716	15.6770	38.976	0.0534	0.83763	2.08250	Frei (1992)
9	Rhodope	Distrato	No		Gn	18.712	15.6900	39.017	0.0534	0.83850	2.08513	Frei (1992)
11	Rhodope	Distrato	No		Gn	18.754	15.7400	39.185	0.0533	0.83929	2.08942	Frei (1992)
KA1	Rhodope	Thermes	No		Gn	18.698	15.6590	38.915	0.0535	0.83747	2.08124	Frei (1992)
MI/2	Rhodope	Thermes	No		Gn	18.695	15.6610	38.934	0.0535	0.83771	2.08259	Frei (1992)
RA/5	Rhodope	Thermes	No		Gn	18.699	15.6600	38.879	0.0535	0.83748	2.07920	Frei (1992)
MI/10	Rhodope	Thermes	No		Gn	18.698	15.6600	38.921	0.0535	0.83752	2.08156	Frei (1992)
MI/11	Rhodope	Thermes	No		Gn	18.698	15.6660	38.926	0.0535	0.83784	2.08183	IGME Xanthi department
MY-4B	Rhodope	Thermes	No		Gn	18.688	15.6600	38.914	0.0535	0.83797	2.08230	IGME Xanthi department

(*continued on next page*)

Table 4 (*continued*)

Sample	District	mine	Ancient Mining	Collected by	Main minerals*	$^{206}Pb/^{204}Pb$	$^{207}Pb/^{204}Pb$	$^{208}Pb/^{204}Pb$	$^{204}Pb/^{206}Pb$	$^{207}Pb/^{206}Pb$	$^{208}Pb/^{206}Pb$	Reference
MY-1	Rhodope	Thermes	No		Gn	18.695	15.6650	38.909	0.0535	0.83792	2.08125	IGME Xanthi department
MY-2A	Rhodope	Thermes	No		Gn	18.690	15.6600	38.907	0.0535	0.83788	2.08170	IGME Xanthi department
MY-12	Rhodope	Thermes	No		Gn	18.689	15.6620	38.909	0.0535	0.83803	2.08192	IGME Xanthi department
MY-2	Rhodope	Thermes	No		Gn	18.689	15.6600	38.913	0.0535	0.83793	2.08213	IGME Xanthi department
MY/13B	Rhodope	Thermes	No		Gn	18.696	15.6700	38.949	0.0535	0.83815	2.08328	IGME Xanthi department
MY-2A	Rhodope	Thermes	No		Gn	18.698	15.6690	38.934	0.0535	0.83800	2.08225	IGME Xanthi department
MY/14B	Rhodope	Thermes	No		Gn	18.686	15.6640	38.912	0.0535	0.83827	2.08241	IGME Xanthi department
MY-1E	Rhodope	Thermes	No		Gn	18.689	15.6630	38.913	0.0535	0.83809	2.08213	IGME Xanthi department
MY-3	Rhodope	Thermes	No		Gn	18.686	15.6610	38.914	0.0535	0.83811	2.08252	IGME Xanthi department
KI/8	Rhodope	Thermes	No		Gn	18.704	15.6690	38.964	0.0535	0.83774	2.08319	IGME Xanthi department
3	Rhodope	Kirki Tris Vryses	No		Gn	18.706	15.6600	38.868	0.0535	0.83716	2.07784	Frei (1992)
MP-41	Rhodope	Boukates Tris Vryses	No		Gn	18.731	15.6620	38.766	0.0534	0.83615	2.06962	IGME Xanthi department
MP-44	Rhodope	Boukates Tris Vryses	No		Gn	18.703	15.6340	38.679	0.0535	0.83591	2.06806	IGME Xanthi department
V-129	Rhodope	Virini	No		Gn	18.713	15.6350	38.690	0.0534	0.83552	2.06755	IGME Xanthi department
21	Rhodope	Aisymi	No		Gn	18.735	15.6590	38.792	0.0534	0.83582	2.07056	Frei (1992)
23	Rhodope	Aisymi	No		Gn	18.725	15.6450	38.768	0.0534	0.83551	2.07039	Frei (1992)
4	Rhodope	Aisymi	No		Gn	18.766	15.6950	38.912	0.0533	0.83635	2.07354	Frei (1992)
5	Rhodope	Aisymi	No		Gn	18.738	15.6680	38.800	0.0534	0.83616	2.07066	Frei (1992)
6	Rhodope	Aisymi	No		Gn	18.773	15.6920	38.932	0.0533	0.83588	2.07383	Frei (1992)
ΓΑ-328A	Rhodope	Aisymi	No		Gn	18.736	15.6600	38.811	0.0534	0.83582	2.07147	IGME Xanthi department
ES-27	Rhodope	Aisymi	No		Gn	18.738	15.6610	38.787	0.0534	0.83579	2.06996	IGME Xanthi department
NK-17	Rhodope	Aisymi	No		Gn	18.740	15.6640	38.804	0.0534	0.83586	2.07065	IGME Xanthi department
BB/15	Rhodope	Thermes	No		Gn	18.707	15.6620	38.913	0.0535	0.83723	2.08013	IGME Xanthi department

* Abbreviations: Apy = Arsenopyrite; Bar = Barite; Ccp = Chalcopyrite; Cer = Cerussite; Conich = Conichalcite; Fe-Mn = Iron-Manganese oxides; Gn = Galena; Gth = Goethite; Hem = Hematite; Jrs = Jarpsite; Lm = Limonite; Mlc = Malachite; Smith = Smithsonite; Sp = Sphalerite; Py = Pyrite; Pyrol = Pyrolusite

concentration in a galena sample from the ancient Moskies mine in Kallianoi is 730 ppm. The most significant mine of the Gialpides gorge is located near the shore with almost 500 m of underground galleries (Fig. 3c). Pottery from the Classical period is found in the inner part of the mine. An extensive, but poorly investigated, metallurgical area at the Archampolis settlement in south Euboea (Keller, 1984) suggests that south Euboea should be considered an important ancient mining area which has been largely, if not totally, ignored in discussions of ancient Greek silver sources.

Central Euboea. There is one minor Ag occurrence in the Almyropotamos mining district comprising three modern shafts and two horizontal galleries with scarce traces of ancient mining. Supergene alteration of the mineralization is major at its higher levels. The supergene mineralization contains 75–91 ppm Ag.

Siphnos. The central part of the island has five mining subdistricts with ancient galleries at Agios Sostis, Agios Sylvestros, Voreini, Kapsalos-Frase, and Xero-Xylo (Fig. 3d and e) exploiting the Ag-rich mineralization pods from the carbonate replacement bodies in marbles. Other mines in the southern part of the island contain very low-grade Ag ore. Wagner and Weisgerber (1985) documented prehistoric (3rd mil. BC), Archaic-Classical (5–4th cent. BC), and modern mining (19–20th cent. AD) in Siphnos. Roman and Byzantine pottery was found at the surface of the mining areas of Kapsalos-Frase and Xero-Xylo. Iron-manganese exploitation during the 19th and 20th centuries has obliterated most ancient traces at Agios Sylvestros, Kapsalos, Frase, and Xero-Xylo, while Voreini has been converted to a landfill. The mineralization from the ancient district of Agios Sylvestros contains high concentrations of Ag up to 4983 ppm.

Seriphos. Nine modern adits with parts testifying to ancient exploitation exist in the Moutoula area in the northern part of the island (Fig. 3f). The mines explore the Ag-rich vein system in the schist-marble intercalations. The mineralization contains 161–470 ppm Ag.

Melos. Two ancient open works were discovered on the island in Triades and one ancient adit at Katsimouti beach. In Triades, Ag concentrations in the galena reach 2473 ppm.

Syros. Silver-rich sulphides are found as disseminations and massive sulfide bodies along the marbles and schists with the most representative ore district being Rozos, an ancient mine with prehistoric rock tools in its interior with high Pb–Zn–Cu–Ag contents. The Ag concentrations in galena vary from 1 to 26 ppm. Ores with higher grades (25 to >100 ppm) are documented in Azolimnos (Voudouris et al., 2014).

Kythnos. In Agios Dimitrios, at the southern edge of the island, Pb mineralization takes place mainly as galena. Ancient galleries of limited length in low-grade (0.2–16.2 ppm) Ag-bearing veins were discovered near the shore of Agios Dimitrios and near the acropolis of Kastellas (Fig. 3g).

Antiparos. Quartz veins in the gneisses and schists at the central and western parts of the island host Ag-bearing mineralizations (2–386 ppm). In the inner parts of modern mines in the Monastiria area, undatable older mining phases have been recorded.

Polyaigos. Modern mining activity was recorded in Ba-rich veins, but ancient traces are absent. The veins contain Ag up to 116 ppm.

Anaphi. Modern mining is located at the central-south part of Anaphi. The Ag concentration is 81 ppm.

Pelion. Ancient mines with Ag-bearing mineralizations are documented here for the first time. Numerous mineralized veins occur at the Pelion tectonic window (Attic-Cycladic Massif) from Zagora to Ksourichti village. Two ancient mines were discovered in Tsagarada and Ksourichti villages, respectively (Fig. 3h). They exploited low-grade Ag veins (3–13 ppm).

3.1.2. Rhodope Massif-Serbo-Macedonian zone-circum Rhodope belt (northern Greece and northern Aegean islands)

Northeast Chalkidiki. The Olympiada mining subdistrict of northeast Chalkidiki comprises several ancient mining shafts and horizontal mines which were used to exploit Ag-rich veins (14.2–2879.6 ppm) (Fig. 3i). At

the Madem Lakkos, Mavres Petres, and Stratoni areas, modern mining activity may have obliterated older phases of exploitation.

Thasos. The Acropolis mine, next to the ancient fortification of Thasos, constitutes the island's most significant ancient exploitation of Ag-bearing veins (Fig. 3j). The mine has 1226 m of underground galleries. The mineralizations are rich in Pb, Zn, and Cu and contain Ag up to 945 ppm and Au up to 60.9 ppm. Modern exploitation of Fe–Mn–Zn-rich mineralizations has presumably destroyed ancient mining traces at areas such as Vouves and Mavrolakas.

Kroussia. This ancient mining district was discovered during the present study. At Koulachli in the northeast, a number of ancient mines were investigated which exploited Ag ore hosted in veins that crosscut the schist (Fig. 3k). The Ag-bearing mineralization at the Agios Markos area contains up to 1364 ppm Ag. Field observations such as the existence of several ancient mines together with the high Ag concentrations point to the importance of the Kroussia mining area. Its location plausibly allows it to be identified as ancient Dysoron, situated on the eastern borders of the kingdom of Macedon under Alexander I (Xydopoulos,

Fig. 3. Selected representative photos from the mining areas where samples were obtained. (a) Esperanza-1 horizontal mine in Lavrion. (b) Dimoliaki mine showing supergene alteration close to the Plaka granodiorite intrusion. (c) Gialpides-1 mine in the Euboean mining district. (d) Ancient adits in the modern trench of the Agios Silvestros mining area on the island of Siphnos. (e) Agios Sostis-1 ancient mine in Siphnos. (f) Modern mine intersected by an ancient gallery in the Moutoula mining area in Seriphos. (g) Ancient mine entrance at the shore of the Kastellas area on the island of Kythnos. (h) Ksourichti mine in the Pelion mining area. (i) Horizontal mine OLY-12 in the Olympiada Chalkidiki mining district. (j) Acropolis mine in the northeast part of the island of Thasos. (k) Koulachli-1 ancient mine in the Kroussia mountains. (l) Koryfis-1 mine in Mt Pangaeon. (m) Ancient Lazarus mine in Palaea Kavala.

2016). It was mentioned by Herodotus (5.17) as providing the king with the huge sum of a talent of silver per day.

Angistron. Two extended mines in the Lechovo subdistrict were recorded. The exploitation followed the carbonate replacement voids and the veins in the marbles filled with oxidized mineralization. Pottery found in the inner parts of the ancient mines dates to the Hellenistic and Roman periods. The ore contains up to 182 ppm Ag.

Pangaeon. Asimotrypes is the most extended mining system on

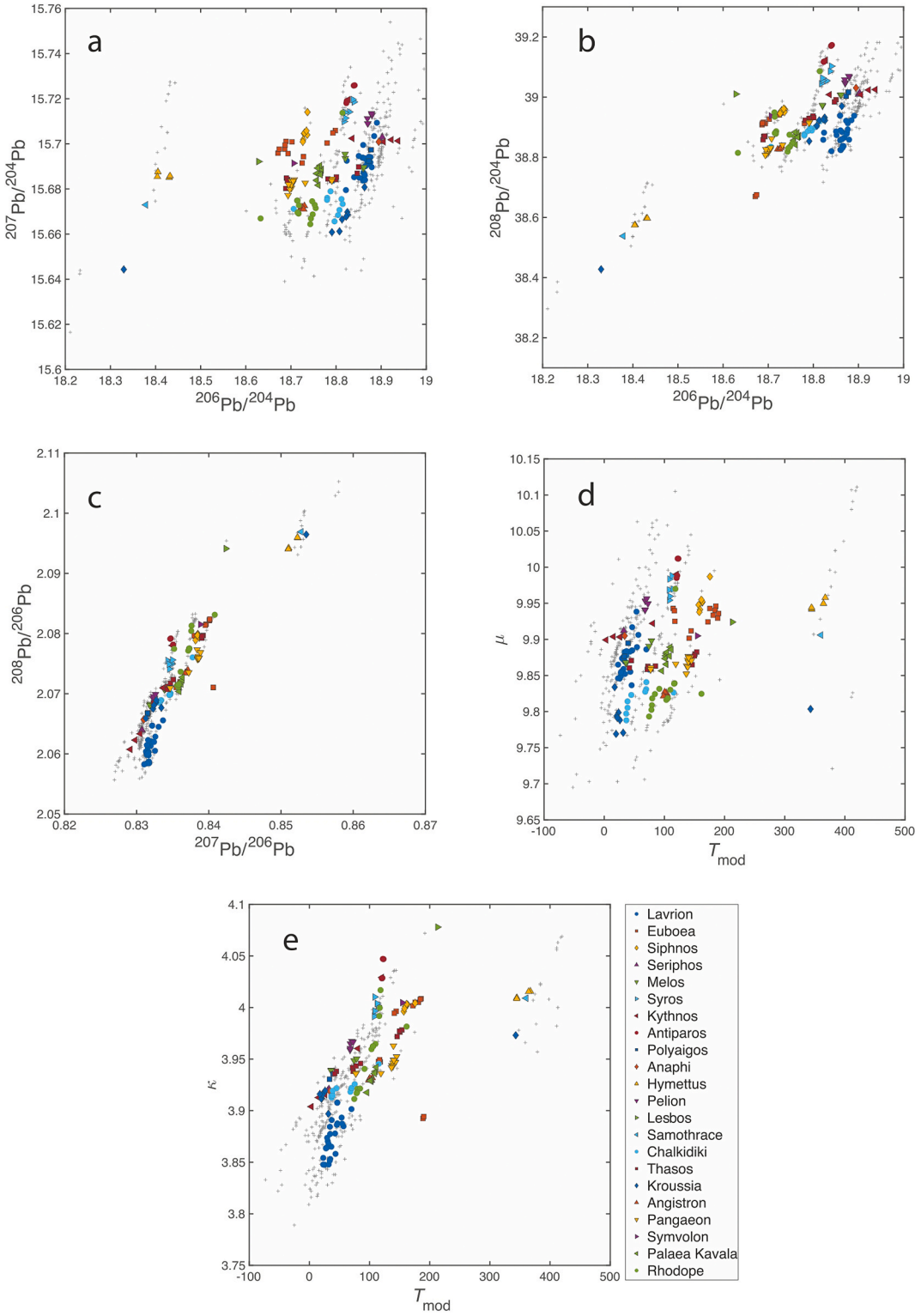

Fig. 4. Measured Pb isotopic compositions of galena, cerussite, and anglesite from ancient Greek mining territories and selected Ag-bearing occurrences in Greece. (a) $^{207}Pb/^{204}Pb$ versus $^{206}Pb/^{204}Pb$, (b) $^{208}Pb/^{204}Pb$ versus $^{206}Pb/^{204}Pb$, (c) $^{208}Pb/^{206}Pb$ versus $^{207}Pb/^{206}Pb$, (d) T_{mod} (Pb model age) versus μ ($^{238}U/^{204}Pb$), (e) T_{mod} (Pb model age) versus κ ($^{232}Th/^{238}U$). Literature data (Barnes et al., 1974; Gale and Stos-Gale, 1981a; Wagner and Weisgerber, 1985; Wagner et al., 1986; Kalogeropoulos et al., 1989; Nebel et al., 1991; Frei, 1992; Stos-Gale et al., 1996; Gale, 1998; Asderaki-Tzoumerkioti et al., 2017; OXALID and IGME unpublished data) provided in Table 4 are depicted with crosses. Lead model ages were calculated according to Albarède and Juteau (1984).

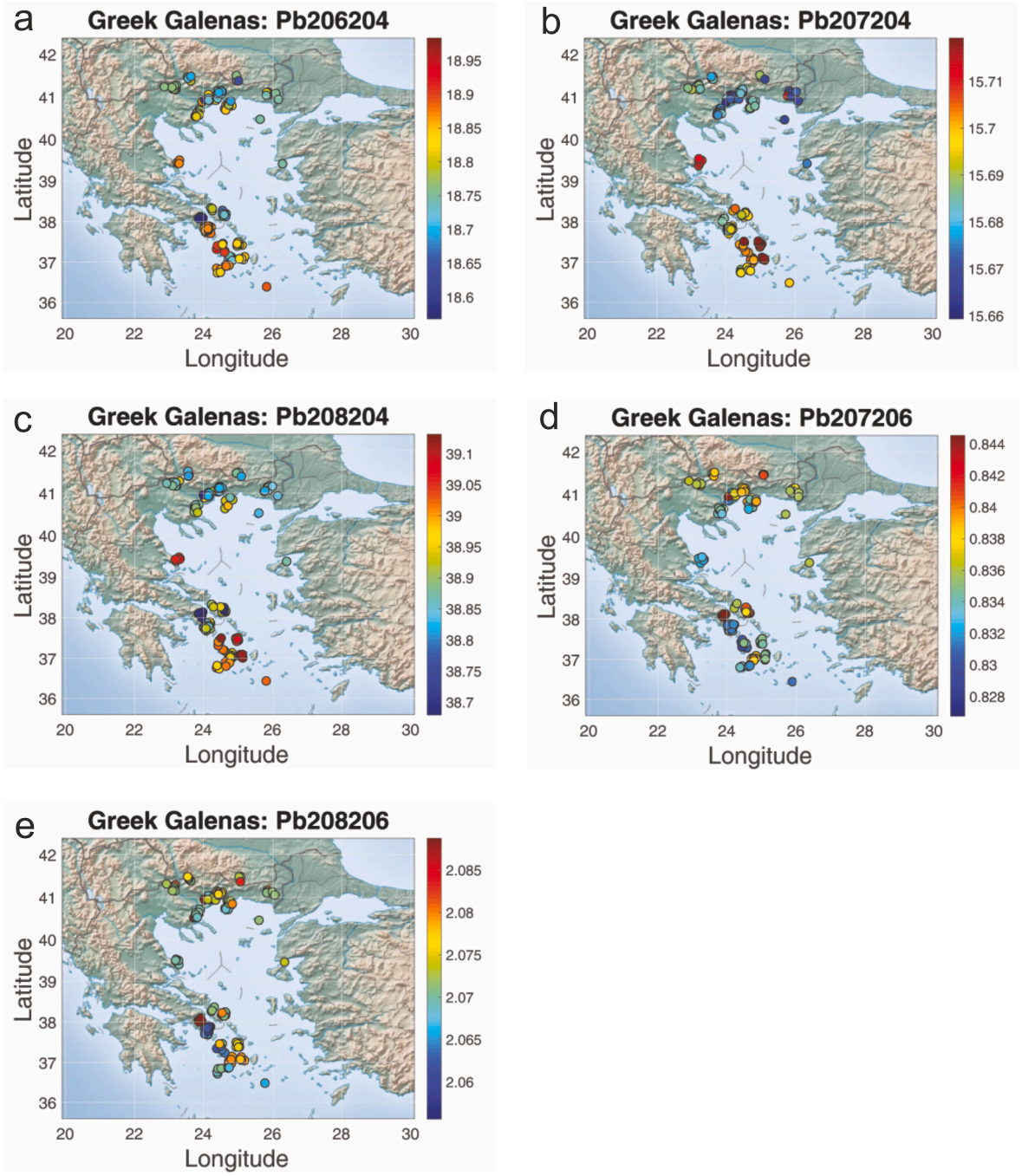

Fig. 5. Maps of (a) $^{206}Pb/^{204}Pb$, (b) $^{207}Pb/^{204}Pb$, (c) $^{208}Pb/^{204}Pb$, (d) $^{207}Pb/^{206}Pb$, and (e) $^{208}Pb/^{206}Pb$. Data from this study only.

Mount Pangaeon and comprises eight ancient galleries (Fig. 3l). The concentration of Ag is higher than any other ancient Greek mining district (up to 9906 ppm).

Palaea Kavala. An extensive mining area with horizontal adits and vertical shafts (Fig. 3m) mentioned in the literature (Koukouli-Chrysanthaki, 1990; Vavelidis et al., 1996) as the ancient "Scapti Yli". Roman pottery is abundant at the surface of most galleries. The analyzed samples from Palaea Kavala contain from 57 to 213 ppm Ag. The extent of the underground works suggests it was a very important mining area for gold and silver which has so far been underestimated.

Lesbos. Modern adits are found at the northern part of Lesbos in the Megala Therma area close to Argenos village. Ancient narrow galleries and shafts have been recorded in the inner part of the modern adits (Pernicka et al., 2003), but during the present study only modern mining activity was documented. The Ag concentration is 154 ppm.

Rhodope mountain range. Thermes, Sappes, Neda, Aisymi, and Pefkos have low-grade concentrations of Ag except for the Kirki ore deposit. The epithermal deposits of Sappes, Neda, Aisymi, and Pefkos contain up to 66 ppm Ag. The carbonate replacement system in Thermes is characterized by similarly low Ag concentrations (4–52 ppm). Although the Kirki area has Ag-rich mineralizations (97–1044 ppm), no signs of ancient mining activity have been found there or in the neighboring areas. Modern mining has taken place in Kirki, and modern prospection trenches and adits exist in Aisymi, Sappes, and Neda. One sample from the epithermal vein system in south Samothrace island contains 471 ppm Ag. Modern prospecting galleries are found on the island.

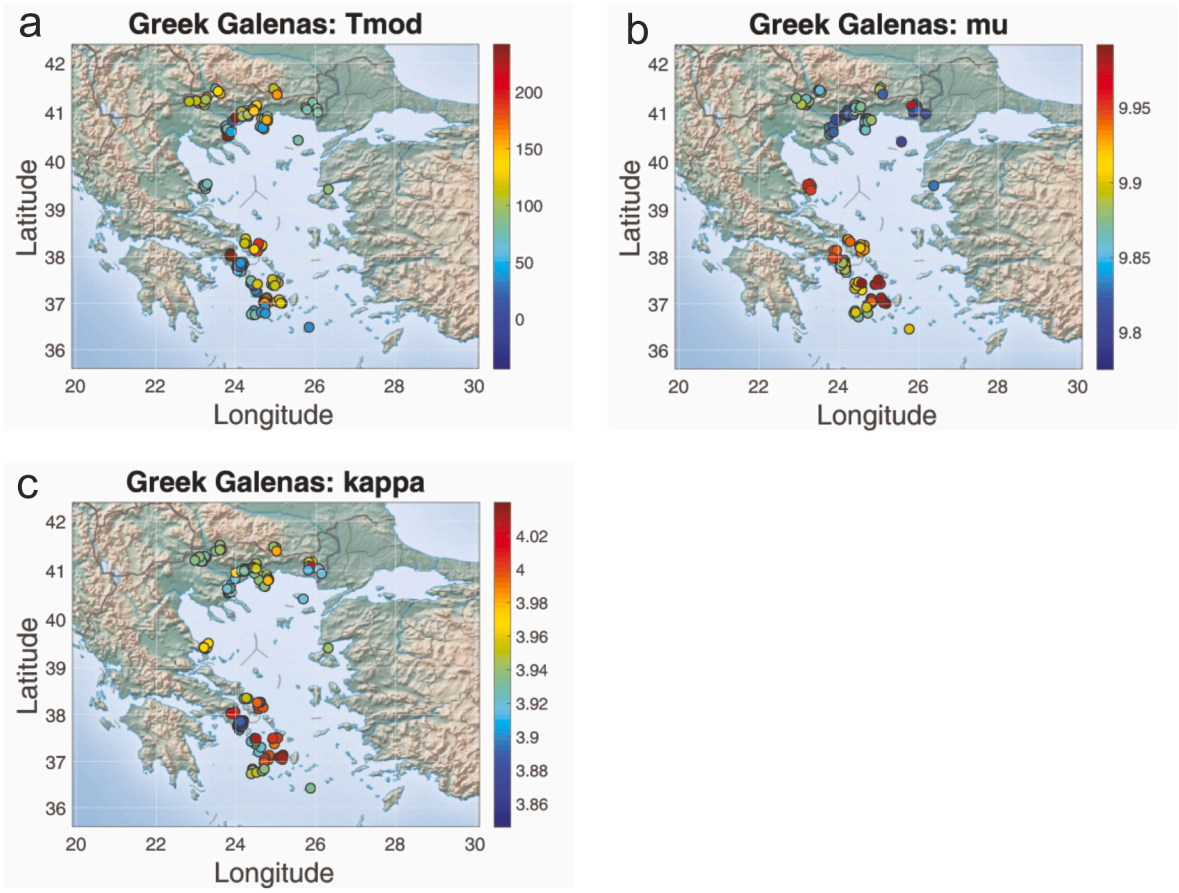

Fig. 6. Maps of (a) T_{mod} (Pb model age), (b) μ ($^{238}U/^{204}Pb$), and (c) κ ($^{232}Th/^{238}U$). Data from this study (Table 3) and literature data (Table 4).

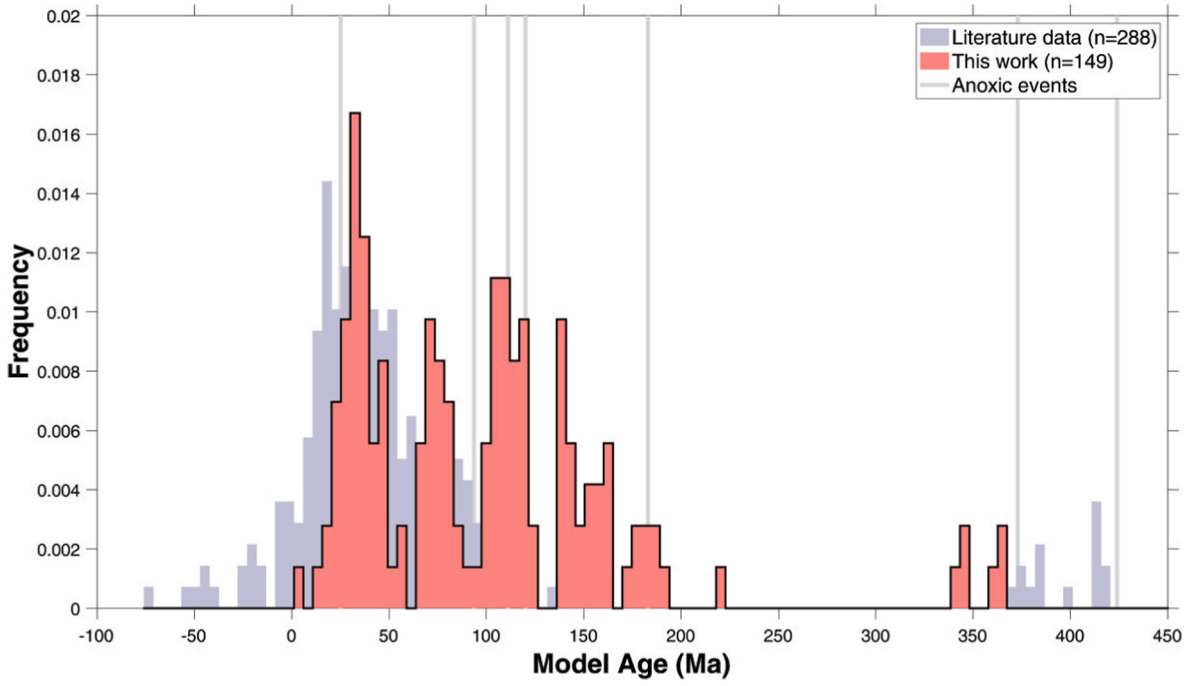

Fig. 7. One-dimensional histogram of Pb model ages from Greek Ag-bearing mineralizations (data from this study and literature data; Tables 3 and 4). Lead model ages were calculated with the assumption of a mixture of five normal populations.

Table 5
Characteristics of the recorded mining and metallurgical activity based on field observations. Extended mining areas are separated in subdistricts.

	Mining Area	Subdistricts	Mining Activity	Dating of surface observed findings	Metallurgy
1	Lavrion	Ari-Dimoliaki-Manoutsos	Over 100 ancient shafts and adits	Prehistoric, Archaic, Classical, Hellenistic, Roman, Byzantine period	Numerous metallurgical establishments with washeries, grinding stones, furnace remains and slag heaps
		Plaka	Over 14 modern shafts and adits		
		Kamareza-Soureza	Over 130 ancient shafts and adits		
		Botsari-Noria-Agrileza	Over 40 ancient shafts and adits		
		Spitharopoussi-Megala Pefka	Over 50 ancient shafts and adits		
		Sounion	Over 30 ancient shafts and adits		
2	South Euboea	Gialpides	2 ancient adits	Classical period	Two metallurgical areas with grinding stones, furnace remains and slag heaps.
		Kallianou Valley	11 modern and 2 ancient adits		
		Schinodavli	3 Ancient adits		
3	Central Euboea	Almyropotamos	3 Modern shafts and 2 adits with ancient horizontal parts		No metallurgical remains
4	Siphnos	Ayios Sostis	Ancient and modern shafts and adits	Prehistoric, Archaic, Roman, Byzantine period	Three metallurgical areas with grinding stones, furnace remains and slag heaps.
		Agios Silvestros	Ancient and modern adits		
		Voreini	Ancient and modern adits		
		Kapsalos-Frase	Ancient and modern adits		
		Xero Xylo	Ancient and modern shafts and adits		
		Aspros Pyrgos	Modern adits and trenches		
5	Seriphos	Moutoula	9 modern adits with ancient parts		No metallurgical remains
6	Melos	Triades	2 ancient open works	Prehistoric, Roman period	No metallurgical remains
		Katsimouti	1 ancient adit		
7	Syros	Rozos	1 ancient adit and 1 modern shaft	Prehistoric times	No metallurgical remains
8	Kythnos	Agios Dimitrios	1 ancient adit and 1 modern shaft		Slags and furnace remains from copper smelting
9	Antiparos	Agios Georgios	2 modern adits and 1 modern shaft		No metallurgical remains
		Prassovounia	4 modern adits		
		Monastiria	Modern adits with ancient parts		
10	Polyaigos	Tris Panagies	Modern adits		No metallurgical remains
11	Anaphi	Kandakospilia/ Doumbaria/Lagada	Modern adits		No metallurgical remains
12	Hymettus	Agios Ioannis	3 modern adits and 1 modern shaft		No metallurgical remains
		Kamini	2 modern adits		
13	Pelion	Agios Konstantinos	5 modern adits and 1 ancient adit	Roman period	No metallurgical remains
		Xourichti	Ancient adit		
14	Lesbos	Argenos (Megala Therma)	Modern adits		No metallurgical remains
15	Samothrace	Megalo Akrotiri	2 modern adits		No metallurgical remains
16	NE Chalkidiki	Olympias	Over 20 ancient shafts and 2 adits	Prehistoric, Hellenistic, Roman, Byzantine, Ottoman period	Metallurgical areas with grinding stones, furnace remains and slag heaps.
		Madem Lakkos	1 ancient adit		
		Mavres Petres	2 ancient adits		
		Piavitsa	1 ancient adit		
17	Thasos	Acropolis	1 ancient adit with modern parts	Prehistoric, Archaic, Hellenistic, Roman period	Metallurgical areas with grinding stones, furnace remains and slag heaps.
		Vouves	Modern adits		
		Kourlou	1 ancient adit		
		Sotiros	Modern adits and 1 ancient adit		
		Marlou	Modern adits with ancient parts		
18	Kroussia	Koulachli	2 ancient adits		Two metallurgical areas with grinding stones, furnace remains and slag heaps.
		Agios Markos	Modern shaft		
		Vathi	6 ancient adits		
19	Angistron	Agios Konstantinos	Modern and ancient adits and shafts	Hellenistic period	Two metallurgical areas with grinding stones, furnace remains and slag heaps.
20	Pangaeon	Agia Triada	3 ancient adits	Hellenistic, Byzantine, Ottoman period	Nine metallurgical areas with grinding stones, furnace remains and slag heaps.
		Nikisiani	5 ancient and 3 modern adits		
		Trikorfo-Avgo-Mavrokorfi	6 ancient adits		
		Ofrynio	3 ancient adits		
21	Palaea Kavala	Kryoneri-Zygos	7 ancient adits and 2 shafts	Roman period	Slags and furnace remains
		Garizo Lofos	4 ancient adits		
		Mandra Kari	3 ancient adits		
		Kokkala	2 ancient adits		
		Giolia	1 ancient adit		
		Chalkero	2 ancient adit		
		Lefki	1 ancient adit		

(*continued on next page*)

Table 5 (*continued*)

	Mining Area	Subdistricts	Mining Activity	Dating of surface observed findings	Metallurgy
		Petropigi	1 ancient adit		
22	Thermes		3 modern adits		No metallurgical remains
23	Sappes		Modern adits		No metallurgical remains
24	Kirki		Modern adits		No metallurgical remains
25	Aisymi		2 modern adits		No metallurgical remains
26	Neda (King Arthur)		1 modern adit and 1 of unidentified age		No metallurgical remains
27	Pefka		1 adit of unidentified age		No metallurgical remains

3.2. Lead isotope analysis

The Pb isotopic compositions of the 149 galena, cerussite, and anglesite samples from the 27 Ag-bearing mineralizations in Greece investigated here are listed in Table 3. Table 4 lists the relevant literature data (Barnes et al., 1974; Gale and Stos-Gale, 1981a; Wagner and Weisgerber, 1985; Wagner et al., 1986; Kalogeropoulos et al., 1989; Nebel et al., 1991; Frei, 1992; Stos-Gale et al., 1996; Gale, 1998; Asderaki-Tzoumerkioti et al., 2017; OXALID and IGME unpublished data). Comments on the existence of ancient mining activity for each Ag-bearing mineralization based on field investigations and literature also are provided.

We first focus on the results of the present work. Fig. 4 shows the standard plots of $^{207}Pb/^{204}Pb$ (a) and $^{208}Pb/^{204}Pb$ (b) versus $^{206}Pb/^{204}Pb$, and $^{208}Pb/^{206}Pb$ versus $^{207}Pb/^{206}Pb$ (c). T_{mod} (Pb model age) is plotted versus μ ($^{238}U/^{204}Pb$) and κ ($^{232}Th/^{238}U$) in Fig. 4d and e, respectively. Fig. 5 also displays the raw Pb isotope ratios but in map view: $^{206}Pb/^{204}Pb$ (a), $^{207}Pb/^{204}Pb$ (b), $^{208}Pb/^{204}Pb$ (c), $^{207}Pb/^{206}Pb$ (d), and $^{208}Pb/^{206}Pb$ (e). The data from the southern Aegean and northern Greece are better separated in Fig. 5a–c (^{204}Pb-normalized) than in Fig. 5d–e (^{206}Pb-normalized).

Fig. 6 shows maps of T_{mod} (Pb model age) (a), μ ($^{238}U/^{204}Pb$) (b), and κ ($^{232}Th/^{238}U$) (c) for the new data of the present study. Except for a few Upper Devonian ages, the Pb model ages calculated for Aegean localities cluster in groups from the Jurassic to the present as observed on the map of Fig. 6a. Although overall regional consistency is observed, the Pb model ages of some ores from the same island, such as Thasos, Kythnos, and Euboea, show a broad range of values. The Pb model ages define different domains in the Aegean. The oldest Pb model ages are recorded in Hymettus (367-345 Ma), Samothrace (360 Ma), and Myriophyto-Kroussia (343 Ma), representing the oldest Ag-bearing mineralization group (Fig. 6a, Table 3). The most recent Pb model ages (15-3 Ma) are recorded at Agios Dimitrios on the island of Kythnos. The μ values of the southern Aegean are higher than those of northern Greece (Fig. 6b). The highest κ values are more frequent in the eastern Cyclades (Fig. 6c) and, in general, μ seems to have a strong potential to discriminate different mining districts (Fig. 6b). The crust systematically has high U/Pb and Th/U in the eastern relative to the western Cyclades and even more so relative to northern Greece. This difference clearly is due to subduction bringing together terranes with very different tectonic histories.

The isotopic field for Lavrion is compact (Fig. 4b and c) and easily distinguished from the fields of other ancient mining areas of Pangaeon, Thasos, Chalkidiki, Euboea, and Siphnos. Samples from the Lavrion mining subdistricts of Kamareza, Soureza, Botsari, and Ari, and even the modern Plaka and Filoni-80 mines have similar isotopic signatures that fall within a well-defined field. Chalkidiki, Pangaeon, and Thasos overlap in most LIA plots not involving ^{204}Pb (Figs. 4c and 5e). The geographical proximity and relative similarities in the geological setting of these mining districts (Rhodope Massif) lead to difficulties in distinguishing between ore clusters.

The partial overlapping of the Siphnos, Euboea, Pangaeon, Thasos, and Chalkidiki fields poses a problem for determination of provenance (Fig. 4c). The Palaea Kavala and Angistron mining districts, which here have been measured for their Pb isotopic compositions for the first time, overlap with Chalkidiki, Euboea, Thasos, Rhodope, and Pangaeon (Fig. 4). The Pb isotopic signature of the Acropolis mine in northeast Thasos is significantly different from that of southwest Thasos Pb–Zn ores (Fig. 4). Analogous segmentation is observed for the fields of Kythnos and Euboea (Fig. 4). The present work also presents the Pb isotopic composition for the Kroussia mining area for the first time. Its isotopic field is close to those of Lavrion, Chalkidiki, and Thasos (Fig. 4). The ore sample D-10 was collected in the northwest part of Kroussia,

Table 6
Mean and standard deviation of T_{mod}, μ, and κ inferred from a 5-group mixing model of the galena samples analyzed in this work. N stands for the number of samples in each group and *s* for standard deviation. Note the differences between the results when literature data are included, which reflect the smaller number and much broader peaks observed in the histogram of Fig. 7. The present groups are compared with the groups identified by Milot et al. (2021) for the Iberian Peninsula. Groups 1 (N = 42), 2 (79), and 3 (N = 22) are the most populated. Note that the very strong Cenozoic peak (35±9 Ma) is absent from Iberia, where late Devonian (395±40 Ma) prevails. The Cretaceous peaks are strong in both provinces, whereas the Early to Mid-Jurassic peak (190±13 Ma) is subdued in both provinces.

Event	T_{mod} (Ma)	*s*	μ	*s*	κ	*s*	N
Aegean galenas (this study)							
1	35	9	9.85	0.04	3.88	0.03	42
2	97	34	9.89	0.06	3.94	0.04	79
3	154	12	9.92	0.04	3.97	0.03	22
4	190	13	9.94	0.01	3.97	0.07	7
5	354	10	9.92	0.05	3.99	0.01	6
Aegean galenas (all data)							
1	31	27	9.89	0.06	3.89	0.04	220
2	77	39	9.80	0.02	3.95	0.04	32
3	107	39	9.89	0.07	3.95	0.04	163
4	198	12	9.91	0.04	3.98	0.10	4
5	403	76	9.95	0.11	4.01	0.03	25
Iberian galenas (Milot et al. (2021))							
1	90	34	9.85	0.06	3.96	0.05	80
2	185	26	9.78	0.23	3.95	0.07	29
3	313	41	9.92	0.12	4.04	0.06	44
4	395	40	9.77	0.12	3.98	0.05	237
5	613	42	9.89	0.20	4.04	0.07	74

deriving from a different mineralization where no mining traces have been found so far in the adjacent area. This difference is depicted in the diagrams as well as observed for the Hymettus and Samothrace samples (Fig. 4a–c). The Pb isotopic signatures of south Euboea mineralizations from Kallianoi, Gialpides, and Schinodavli are different from those of Almyropotamos situated in the center of the island (Fig. 4a–c), a probable expression of the local tectonic complexity (Jolivet et al., 2013; Melfos and Voudouris, 2017).

3.3. Lead model ages and other geologically informative parameters

Although Fig. 5 shows regional differences in raw Pb isotope ratios (in particular for ^{204}Pb-normalized ratios), the differences are regionally more coherent in T_{mod}-μ-κ space, in which northern Greece and the eastern and western Cyclades form well-delineated provinces consistent with local tectonics. In most, if not all cases, Pb model ages are significantly older than the corresponding emplacement ages (Tables 1 and 3) (see Milot et al., 2021). Lead model ages, therefore, cannot be used to date ore deposits or their country rocks. The significance of the multiple but well-defined peaks present in the model age histogram of Fig. 7 thus must be clarified. If the peaks corresponded to different mixtures of Pb from the country rocks, the outcome would be much broader peaks than those observed or even no peaks at all. We will therefore adopt the straightforward model proposed by Milot et al. (2021) which states that, regardless of ore type, ore genesis involves two independent steps: (1) formation of the original Pb stock followed by (2) transport of this stock to its current location. Lead model ages correspond to the last U/Pb fractionation event that formed the current Pb(-Zn-Ag) stock. Whether the current deposit is magmatic, hydrothermal, epigenetic, or other is irrelevant to radiogenic Pb ingrowth. The petrogenesis of Pb ores is in many aspects reminiscent of the petrogenesis of oil fields, which has been pointed out a number of times in the literature (e.g. Sverjensky, 1984).

We calculated Gaussian Mixture Models using the *fitgmdist* function of Matlab™. This function implements the iterative technique called 'Expectation Maximization' which assumes that each cluster has an independent Gaussian distribution, each with its own mean and covariance matrix. We found that a Gaussian mixture of five components provides an adequate description of the present data set. Table 6 shows the results in the T_{mod}, μ, and κ space for the galena samples analyzed in this work with and without literature data included. Comparison with the groups identified by Milot et al. (2021) for the Iberian Peninsula shows that the very strong Cenozoic peak (35 ± 9 Ma) is absent from Iberia, where late Devonian (395 ± 40 Ma) prevails. The T_{mod}, μ, and κ space therefore offers a potential provenance tool allowing a distinction to be made between the Aegean and the Iberian provinces on the condition that three rather than two, not even pair by pair, isotopic variables are used. The Early to Mid-Cretaceous Pb model age peak is present in both the Aegean realm (107 ± 39 Ma) and the Iberian Pb–Zn ores (90 ± 34 Ma; Milot et al., 2021). The Cretaceous peaks are strong in both provinces, whereas the Early to Mid-Jurassic peak (190 ± 13 Ma) is subdued in both provinces.

It has long been known that Pb must be derived from the upper crust, such as the Cycladic basement and Cycladic Blueschist in the southern Aegean, and not from the mantle (Doe and Delevaux, 1972; Heyl et al., 1974; Leach et al., 2005; Wilkinson, 2013; Arribas and Tosdal, 1994; Wind et al., 2020). Explaining the existence of well-defined peaks of Pb model ages under such conditions remains a challenge. Milot et al. (2021) suggested that Pb was originally concentrated in marine sediments during anoxic events, whether global or more local, with sulfur being derived from volcanic activity. Because hydrothermal sulfides are quickly oxidized as sulfate in seawater, the concentration step of massive deposits is unlikely to be possible under normal oxic conditions. As for the second step, hydrothermal activity associated with magmatism or convection of basinal fluids constitute the most probable mechanisms leading to the transportation of Pb(-Zn-Ag) to their current position in the crust.

The arguments presented by Milot et al. (2021) for the Iberian Peninsula to support the initial segregation of large amounts of Pb in sediments during anoxic events are also valid for the Cretaceous Pb model ages in the Aegean. The prominent peak of Cenozoic Pb model ages (35 ± 9 Ma; Fig. 7) is consistent with the ubiquitous accumulation of carbon-rich sediments in the Paratethys during the Oligocene in a broadly east-west trending zone extending from the Panonian Basin to the Carpathian, all the way to Azerbaidjan to a rock formation locally known as the Maikopian group (Pawlewicz, 2007; Hudson et al., 2008; Sachsenhofer et al., 2018; Shnyukov and Yanko-Hombach, 2020). The abundant Cretaceous Pb model ages are reflected by some geological evidence from northwestern Greece (Tsikos et al., 2004). In contrast, the Early to Mid-Jurassic peak (190 ± 13 Ma; Fig. 7) expected from stratigraphic studies (e.g. Kafousia et al., 2011) is subdued.

3.4. A remark on overlapping fields

Possible ambiguities created by fields overlapping in two-dimensional plots, such as ^{207}Pb/^{204}Pb versus ^{206}Pb/^{204}Pb, and sometimes in two of such paired plots at the same time, should not be overemphasized. Cases for which groups of data plotted in the three-dimensional ^{206}Pb/^{204}Pb–^{207}Pb/^{204}Pb–^{208}Pb/^{204}Pb space overlap on their projections onto two 'faces' of the coordinate system, while defining separate volumes in three dimensions, are easy to conceive and visualize. The same situation is also conceivable in the three-dimensional T_{mod}-μ-κ space. Use of three-dimensional plots to represent Pb isotope data is unfortunately uncommon in archeometry (Albarède et al., 2020). In practice, such ambiguities do not often arise in three dimensions as three-dimensional fields, or volumes, rarely overlap. An efficient 'convex hull' technique to assess provenance issues in three-dimensional Pb isotope space is described by Gentelli et al. (2021).

4. Conclusions

Field observations made during this study have led to the conclusion that the most significant ancient Ag mining territories in the Aegean were Lavrion, northeast Chalkidiki, Pangaeon mountain, the islands of Siphnos, Thasos and Euboea, Palaea Kavala, Kroussia, and the Angistron district. This significantly broadens the mining areas from which ancient peoples extracted silver beyond those specifically attested in ancient sources and deduced from numismatic considerations. High Ag concentrations in samples from Lavrion (5872 ppm), Chalkidiki (2880 ppm), Pangaeon (9906 ppm), and Siphnos (4983 ppm) are indicative of the importance of these deposits. The galena sample found in the Poundazeza metallurgical area in Lavrion with 4220 ppm Ag provides information about what was considered to be a profitable yield, though mines with lower yields were also exploited possibly as extraction techniques improved in Hellenistic and Roman times.

We have provided new high-precision Pb isotopic data for samples obtained from the known ancient mining territories in Greece with the intention of providing a useful tool for silver artefact provenance studies. A clear distinction in Pb isotopic composition is observed between the major silver mining territories in the Aegean, such as Lavrion and Siphnos-Pangaeon-Thasos-Chalkidiki. Samples originating from proximate and geologically relevant areas, such as Pangaeon, Thasos, and Chalkidiki, overlap to some extent in lead isotopic plots. We further demonstrate that combining plots of raw Pb isotope ratios with calculated Pb model ages provides more reliable provenance assessment.

An important finding is that the measured Pb isotopic variations and calculated Pb model ages from some closely neighboring mining areas, especially on islands such as Thasos, Kythnos, and Euboea, may sometimes reveal different Pb sources. Thus, northeast Thasos differs from southwest Thasos, north-central Kythnos differs from southwest Kythnos, and south Euboea differs from Almyropotamos (central Euboea).

In contrast to the older, generally more noisy literature data, the Pb

model age histogram of the new high-precision Pb isotope data of this study shows well-defined peaks which further enhance the resolution of provenance assignment. This observation is consistent with that of Milot et al. (2021) for Iberian ores. Lead model ages do not date the formation of the present ore deposits as the two sets of ages are distinctly different, with Pb model ages being systematically older than ore emplacement ages. Regardless of ore type, the isotopic data can be accounted for by a two-stage evolution model, much reminiscent of that of oil-field formation. The first stage accounts for Pb accumulation in sediments during global or local anoxic events, while the second stage corresponds to the remobilization of the original Pb stocks by basinal and metamorphic fluids.

Another important finding is that, until now, ores from Euboea have been neglected in provenance studies but may have contributed more substantially to coinage production than currently realized, especially in the late Archaic period for the island of Aegina, considered to be the earliest Greek minter outside of Asia Minor (Stos-Gale and Davis, 2020).

Likewise, evidence of extensive ancient exploitation from Palea Kavala and exceptionally high Ag yields from Pangaeon (Asimotrypes) in northern Greece suggest that these districts have been underestimated as mining sources, while low yields from the Rhodope mountain range suggest it has been overestimated.

Finally, field investigations combined with Pb isotopic data have revealed two so-far undiscovered ancient mining areas in Mounts Pelion and Kroussia. The geographic location of the mining district in Kroussia and the characteristics of the Ag-bearing mineralization allow it to be plausibly identified with Mount Dysoron described as a silver-rich area during Alexander's I reign (Hdt. 5.17).

Declaration of competing interest

The authors declare that they have no known competing financial interests or personal relationships that could have appeared to influence the work reported in this paper.

Acknowledgements

This work was funded by the European Research Council H2020 Advanced Grant 741454-SILVER-ERC-2016-ADG 'Silver isotopes and the rise of Money' awarded to Francis Albarède. The Archeological Ephorates of the East Attica Cyclades, Euboea, Magnesia, Chalkidiki, Kilkis, Serres, Kavala, and Thasos (Greek Ministry of Culture) kindly gave permission to conduct the fieldwork and ore sampling carried out during this study. Pavlos Tsitsanis, exploration manager of Eldorado Gold Corporation, is gratefully acknowledged for providing galena samples. We thank Philippe Télouk, Jean Milot, and Chloé Malod-Dognin for help with the mass spectrometers and Vasilis Melfos, Panagiotis Voudouris, and James Ross for facilitating sampling by sharing their knowledge and experience. Fieldwork assistance by Zacharoula Papadopoulou, Anna Aslanoglou, Kyriaki Fellachidou, and numerous local people in the ancient mining areas of Greece is also gratefully acknowledged.

Appendix A. Supplementary data

Supplementary data to this article can be found online at https://doi.org/10.1016/j.jas.2021.105474.

References

Albarède, F., Juteau, M., 1984. Unscrambling the lead model ages. Geochem. Cosmochim. Acta 48, 207–212. https://doi.org/10.1016/0016-7037(84)90364-8.

Albarède, F., Telouk, P., Blichert-Toft, J., Boyet, M., Agranier, A., Nelson, B., 2004. Precise and accurate isotopic measurements using multiple-collector ICPMS. Geochem. Cosmochim. Acta 68, 2725–2744.

Albarede, F., Desaulty, A.M., Blichert-Toft, J., 2012. A geological perspective on the use of Pb isotopes in Archaeometry. Archaeometry 54, 853–867.

Albarède, F., Blichert-Toft, J., Gentelli, L., Milot, J., Vaxevanopoulos, M., Klein, S., Westner, K., Birch, T., Davis, G., de Callataÿ, F., 2020. A miner's perspective on Pb isotope provenances in the Western and Central Mediterranean. J. Archaeol. Sci. 121, 105194.

Albarède, F., Blichert-Toft, J., de Callataÿ, F., Davis, G., Debernardi, P., Gentelli, L., Kemmers, F., Klein, S., Malod-Dognin, C., Milot, J., Telouk, P., Vaxevanopoulos, M., Westner, K., 2021. From commodity to money: the rise of silver coinage around the Ancient Mediterranean (sixth–first centuries BCE). Archaeometry 63 (1), 142–155. https://doi.org/10.1111/arcm.12615.

Alfieris, D., Voudouris, P., Spry, P.G., 2013. Shallow submarine epithermal Pb–Zn–Cu–Au–Ag–Te mineralization on western Milos Island, Aegean Volcanic Arc, Greece: Mineralogical, geological and geochemical constraints. Ore Geol. Rev. 53, 159–180.

Arribas, A., Tosdal, R.M., 1994. Isotopic composition of Pb in ore-deposits of the Betic Cordillera, Spain - origin and relationship to other European deposits. Econ. Geol. 89, 1074–1093.

Artioli, G., Canovaro, C., Nimis, P., Angelini, I., 2020. LIA of Prehistoric Metals in the Central Mediterranean Area: a review. Archaeometry 62 (S1), 53–85.

Asderaki-Tzoumerkioti, E., Rehren, T., Skafida, E., Vaxevanopoulos, M., Connolly, P.J., 2017. Kastro Palaia settlement, Volos, Greece: a diachronical technological approach to bronze metalwork. Star: Sci. Technol. Archaeol. Res. 3 (2), 179–193.

Barnes, I.L., Shields, W.R., Murphy, T.J., Brill, R.H., 1974. Isotopic Analysis of Laurion Lead Ores. Advances in Chemistry Series, 138. American Chemical Society, Washington, pp. 1–10.

Bassiakos, Y., Philaniotou, O., 2007. Early copper production on Kythnos: archaeological evidence and analytical approaches to the reconstruction of metallurgical process. Metal. Early Bronze Age Aegean 7, 19.

Brill, R.H., Wampler, J.M., 1965. September. Isotope ratios in archaeological objects of lead. In: Application of Science in Examination of Works of Art. Proceedings of the Seminar: September 7-16, vol. 1965, pp. 155–166.

Brill, R.H., Wampler, J.M., 1967. Isotope studies of ancient lead. Am. J. Archaeol. 71 (1), 63–77.

Bonsall, T.A., Spry, P.G., Voudouris, P.C., Tombros, S., Seymour, K.S., Melfos, V., 2011. The geochemistry of carbonate-replacement Pb-Zn-Ag mineralization in the Lavrion district, Attica, Greece: fluid inclusion, stable isotope, and rare earth element studies. Econ. Geol. 106 (4), 619–651.

Chamberlain, V., Gale, N.H., 1980. The isotopic composition of lead in Greek coins and in galena from Greece and Turkey. In: Slater, E.A., Tate, J.O. (Eds.), Proceedings of the 16th International Symposium on Archaeometry and Archaeological Prosepection, Edinburgh 1976. The National Museum of Antiquities of Scotland, pp. 139–155.

Chiotis, E., Koukouzas, C., Papadimitriou, G., 1996. Old mining and metallurgical activities in Angistron-Serres-Macedonia. In: Proceedings of the 2nd Symposium of the Hellenic Archaeometric Society. Hellenic Archaeometric Society Thessaloniki, pp. 77–89.

Conophagos, C.E., 1980. Le Laurium antique: et la technique Grecque de la production de l'argent (Athens).

Doe, B.R., Delevaux, M.I.-I., 1972. Source of lead in southeast Missouri galena ores. Econ. Geol. 67, 409–425.

Ducoux, M., Branquet, Y., Jolivet, L., Arbaret, L., Grasemann, B., Rabillard, A., Gumiaux, C., Drufin, S., 2017. Synkinematic skarns and fluid drainage along detachments: the West Cycladic Detachment System on Serifos Island (Cyclades, Greece) and its related mineralization. Tectonophysics 695, 1–26.

Fornadel, A.P., Spry, P.G., Melfos, V., Vavelidis, M., Voudouris, P.C., 2011. Is the Palea Kavala Bi–Te–Pb–Sb±Au district, northeastern Greece, an intrusion-related system? Ore Geol. Rev. 39 (3), 119–133.

Frei, R., 1992. Isotope (Pb, Rb-Sr, S, O, C, U-Pb) Geochemical Investigations on Tertiary Intrusives and Related mineralizations in the Serbomacedonian Pb-Zn, Sb+ Cu-Mo Metallogenetic Province in Northern Greece. Unpublished Doctoral dissertation. ETH, Zurich.

Fytikas, M., Vougioukalakis, G., 1992. Volcanic structure and evolution of Kimolos and Polyaigos isl.,(Milos island complex). In: 6th Congress of the Greek Geologic Society, pp. 221–237.

Gale, N.H., 1979. Lead isotopes and Archaic Greek silver coins. Archaeophysica 10, 194–208. Rheinisches Landesmuseum Bonn.

Gale, N.H., 1998. The role of Kea in metal production and trade in the Late Bronze Age. Kea-Kythnos: Hist. Archaeol. 737–758.

Gale, N.H., Stos-Gale, Z.A., 1981a. Lead and Silver in the Ancient Aegean. Sci. Am. 244 (6), 176–192.

Gale, N.H., Stos-Gale, Z.A., 1981b. Cycladic Lead and Silver Metallurgy. Annu. Br. Sch. A. T. Athens 76, 169–224.

Gale, N.H., Gentner, W., Wagner, G.A., 1980. mineralogical and geographical silver sources of Archaic Greek coinage. Metal. Numismat. 1, 3–49.

Gialoglou, G., Drymniotis, D., 1983. Northeastern Greece: mining activities, mineral exploration and future developments. Trans. Inst. Min. Metall., Sect. A 92, A180–183.

Gentelli, L., Blichert-Toft, J., Davis, G., Gitler, H., Albarède, F., 2021. Metal provenance of Iron Age Hacksilber hoards in the southern Levant. J. Archaeo. Sci. 134, 105472.

Gentner, W., Müller, O., Wagner, G.A., Gale, N.H., 1978. Silver Sources of Archaic Greek Coinage. Naturwissenschaften 65 (6), 273–284.

Grögler, N., Geiss, J., Grünenfelder, M., Houtermans, F.G., 1966. Isotopenuntersuchungen zur Bestimmung der Herkunft römischer Bleirohre und Bleibarren. Zeitschriftfür Naturforschung 21a, 1167–1172.

Grossou-Valta, M., Adam, K., Constantinides, D.C., Prevosteau, J.M., Dimou, E., 1990. mineralogy of and potential beneficiation process for the Molai complex sulphide

orebody, Greece. In: Sulphide Deposits—Their Origin and Processing. Springer, Dordrecht, pp. 119–133.
Heyl, A.V., Landis, G.P., Zartman, R.E., 1974. Isotopic Evidence for the Origin of Mississippi Valley-Type Mineral Deposits: A Review. Econ. Geol. 69, 992–1006.
Hudson, S.M., Johnson, C.L., Efendiyeva, M.A., Rowe, H.D., Feyzullayev, A.A., Aliyev, C. S., 2008. Stratigraphy and geochemical characterization of the Oligocene–Miocene Maikop series: implications for the paleogeography of Eastern Azerbaijan. Tectonophysics 451, 40–55.
Institute of Geological and mineral Exploration (IGME), 1965. Metallogenetic Map of Greece (Athens).
Jolivet, L., Brun, J.P., 2010. Cenozoic geodynamic evolution of the Aegean. Int. J. Earth Sci. 99 (1), 109–138.
Jolivet, L., Faccenna, C., Huet, B., Labrousse, L., Le Pourhiet, L., Lacombe, O., Lecomte, E., Burov, E., Denèle, Y., Brun, J.-P., Philippon, M., Paul, A., Salaün, G., Karabulut, H., Piromallo, C., Monié, P., Gueydan, F., Okay, A.I., Oberhänsli, R., Pourteau, A., Augier, R., Gadenne, L., Driussi, O., 2013. Aegean tectonics: strain localization, slab tearing and trench retreat. Tectonophysics 597, 1–33.
Kafousia, N., Karakitsios, V., Jenkyns, H., Mattioli, E., 2011. A global event with a regional character: the early Toarcian oceanic anoxic event in the Pindos Ocean (northern Peloponnese, Greece). Geol. Mag. 148, 619–631.
Kalogeropoulos, S.I., Kilias, S.P., Arvanitidis, N.D., 1996. Physicochemical conditions of deposition and origin of carbonate-hosted base metal sulfide mineralization, Thermes ore-field, Rhodope Massif, northeastern Greece. Miner. Deposita 31. https://doi.org/10.1007/BF00189188.
Kalogeropoulos, S.I., Kilias, S.P., Bitzios, D.C., Nicolaou, M., Both, R.A., 1989. Genesis of the Olympias carbonate-hosted Pb-Zn (Au, Ag) sulfide ore deposit, eastern Chalkidiki Peninsula, northern Greece. Econ. Geol. 84, 1210–1234.
Kanellopoulos, C., Voudouris, P., Moritz, R., 2014. Detachment-related Sb-Pb-Zn-Ag-Au-Te mineralization in Kallintiri area, northeastern Greece: mineralogical and geochemical constraints. In: Proc. 20th CBGA Congress, Tirana, pp. 162–165.
Keller, D.R., 1984. Archampolis, an early iron-age settlement and sanctuary in Southern Euboea. In: American Journal of Archaeology, vol. 88, 2, pp. 249–249). 135 William St, New York, NY 10038-3805: Archaeological inst.
Killick, D., Stephens, J., Fenn, T., 2020. Geological constraints on the use of lead isotopes for provenance in archaeometallurgy. Archaeometry 62, 86–105.
Kontis, E., Kelepertsis, A.E., Skounakis, S., 1994. Geochemistry and alteration facies associated with epithermal precious metal mineralization in an active geothermal system, northern Lesbos, Greece. miner. Deposita 29 (5), 430–433.
Koukouli-Chrysanthaki, C., 1990. The mines of the Thasians' coast, Mélanges D. Lazaridis: cité et territoireen Macédoine et Thrace antiques, Recherches Franco-Helléniques, 1. Greek Ministry of Culture, École francaise d' Athénes, Athens (in Greek).
Leach, D.L., Sangster, D.F., Kelley, K.D., Large, R.R., Garven, G., Allen, C.R., Gutzmer, J., Walters, S., 2005. Sediment-Hosted Lead-Zinc Deposits: A Global Perspective. In: Hedenquist, J.W., Thompson, J.F.H., Goldfarb, R.J., Richards, J.P. (Eds.), Economic Geology 100th Annversary Volume. Society of Economic Geologists, Littleton, pp. 561–607.
Maratos, G., 1956. Brief report on the Taygetos mineralogical research. Unpublished internal report. IGEY, Athens (in Greek).
Marinos, G., Petrascheck, W.E., 1956. Lavrion: geological and geophysical research. Inst. Geol. Subsurf. Res. 4, 1–246.
Melfos, V., Voudouris, P., 2016. Fluid evolution in Tertiary magmatic-hydrothermal ore systems at the Rhodope metallogenic province, NE Greece. A review. Geol. Croat. 69 (1), 157–167.
Melfos, V., Voudouris, P., 2017. Cenozoic metallogeny of Greece and potential for precious, critical and rare metals exploration. Ore Geol. Rev. 89, 1030–1057.
Melidonis, N., Constantinides, D., 1983. The stratabound sulphide mineralisation of syros (Cyclades, Greece). Z. dt. geol. Ges. 134, 555–575.
Menant, A., Jolivet, L., Vrielynck, B., 2016. Kinematic reconstructions and magmatic evolution illuminating crustal and mantle dynamics of the eastern Mediterranean region since the late Cretaceous. Tectonophysics 675, 103–140.
Milot, J., Blichert-Toft, J., Ayarzagüena Sanz, M., Fetter, N., Télouk, P., Albarède, F., 2021. The significance of galena Pb model ages and the formation of large Pb-Zn sedimentary deposits. Chem. Geol. 583, 120444.
Nebel, M.L., Hutchinson, R.W., Zartman, R.E., 1991. Metamorphism and polygenesis of the Madem Lakkos polymetallic sulfide deposit, Chalkidiki, Greece. Econ. Geol. 86 (1), 81–105.
Nesbitt, R.W., Billett, M.F., Ashworth, K.L., Deniel, C., Constantinides, D., Demetriades, A., Katirtzoglou, C., Michael, C., Mposkos, E., Zachos, S., Sanderson, D., 1988. The geological setting of base metal mineralisation in the Rhodope Region, northern Greece. In: mineral Deposits within the European Community. Springer, Berlin, Heidelberg, pp. 499–514.
Pawlewicz, M., 2007. Total petroleum systems of the Carpathian-Balkanian basin province of Romania and Bulgaria. US Geol. Surv.
Pe-Piper, G., Piper, D.J.W., 2002. The igneous rocks of Greece. In: The Anatomy of an Orogen, vol. 30. Beiträge der regionalen Geologie der Erde, Berlin-Stuttgart, p. 573.
Perlikos, P., 1989. Some new aspects on the geology and metallogeny of southern Euboea. Bull. Geol. Soc. Greece 23, 327–344 (in Greek).
Pernicka, E., Eibner, C., Öztunalı, O., Wagner, G.A., 2003. Early Bronze Age metallurgy in the north-east Aegean. In: Troia and the Troad. Springer, Berlin, Heidelberg, pp. 143–172.
Ross, J.R., Voudouris, P., Melfos, V., Vaxevanopoulos, M., 2020. mines, metals and money in Attica and the ancient world: the geological context. In: Sheedy, K.A., Davis, G. (Eds.), Metallurgy in Numismatics 6: mines, Metals and Money: Ancient World Studies in Science, Archaeology and History, 2020.
Sachsenhofer, R., Popov, S., Coric, S., Mayer, J., Misch, D., Morton, M., Pupp, M., Rauball, J., Tari, G., 2018. Paratethyan petroleum source rocks: an overview. J. Petrol. Geol. 41, 219–245.
Schmid, S.M., Fügenschuh, B., Kounov, A., Maţenco, L., Nievergelt, P., Oberhänsli, R., Pleuger, J., Schefer, S., Schuster, R., Tomljenovic, B., Ustaszewski, K., van Hinsbergen, D.J., 2020. Tectonic units of the Alpine collision zone between Eastern Alps and western Turkey. Gondwana Res. 78, 308–374.
Schmid, S.M., Bernoulli, D., Fügenschuh, B., Matenco, L., Schefer, S., Schuster, R., Tischler, M., Ustaszewski, K., 2008. The Alpine-Carpathian-Dinaridic orogenic system: correlation and evolution of tectonic units. Swiss J. Geosci. 101, 139–183.
Shnyukov, E., Yanko-Hombach, V., 2020. Mud Volcanoes of the Black Sea Region and Their Environmental Significance. Springer Nature.
Siron, C.R., 2018. Magmatic, Structural, and Metallogenic Framework of the Kassandra Mining District, Chalkidiki Peninsula, Northern Greece (Unpublished PhD Thesis).
Skarpelis, N.S., 1999. Epithermal type ores in the Aegean. The hot spring mineralization of northern Chios island, Greece. BG 33, 61–68.
Skarpelis, N., 2020. Setting, sulfur isotope variations, and metamorphism of Jurassic massive Zn-Pb-Ag sulfide mineralization associated with arc-type volcanism (Skra, Vardar zone, Northern Greece). Resour. Geol. 70 (4), 311–335.
Stacey, J.S., Kramer, J.D., 1975. Approximation of terrestrial lead isotope evolution by a two-stage model. Earth Planet Sci. Lett. 26, 207–221.
Stergiou, C., Melfos, V., Voudouris, P., Michailidis, K., Spry, P., Chatzipetros, A., 2016. Hydrothermal alteration and structural control of the Vathi porphyry Cu-Au-Mo-U ore system, Kilkis district, N. Greece. Scientific Annals of the School of Geology, Aristotle University of Thessaloniki (Honorary Publication in Memory of Professor A. Kasoli-Fournaraki) 105, 69–74.
Stos-Gale, Z.A., 1998. The role of Kythnos and other Cycladic islands in the origins of Early Minoan metallurgy. Meletimata 27, 717–736.
Stos-Gale, Z.A., Davis, G., 2020. The minting/mining nexus: new understandings of Archaic Greek silver coinage from lead isotope analysis. In: Sheedy, K.A., Davis, G. (Eds.), Metallurgy in Numismatics 6: mines, Metals and Money: Ancient World Studies in Science, Archaeology and History, vol. 56. Royal Numismatic Society Special Publications, London, pp. 87–100.
Stos-Gale, Z.A., Gale, N.H., 2009. Metal provenancing using isotopes and the Oxford archaeological lead isotope database (OXALID). Archaeol. Anthropol. Sci. 1 (3), 195–213.
Stos-Gale, Z.A., Gale, N.H., Annetts, N., 1996. Lead isotope data from the Isotrace Laboratory, Oxford: archaeometry data base 3, ores from the Aegean, part 1. Archaeometry 38 (2), 381–390.
Stouraiti, C., Soukis, K., Voudouris, P., Mavrogonatos, C., Lozios, S., Lekkas, S., Beard, A., Strauss, H., Palles, D., Baziotis, I., Soulamidis, G., 2019. Silver-rich sulfide mineralization in the northwestern termination of the western cycladic detachment system, at Agios Ioannis Kynigos, Hymettus Mt. (Attica, Greece): a mineralogical, geochemical and stable isotope study. Ore Geol. Rev. 111, 102992.
Sverjensky, D.A., 1984. Oil field brines as ore-forming solutions. Econ. Geol. 79, 23–37.
Tataris, A., 1960. Ai flevikai ekrixigeneis emfaniseis kai imetallogenesieis to Anat. Pilion. In Greek. In: I.G.E.Y. Athens, VI, vol. 4, pp. 207–303.
Tombros, S., St Seymour, K., Spry, P.G., Williams-Jones, A., 2007. The genesis of epithermal Au-Ag-Te mineralization, Panormos bay, Tinos island, Cyclades, Greece. Econ. Geol. 102, 1269–1294.
Tsikos, H., Karakitsios, V., van Breugel, Y., Walsworth-Bell, B., Bombardiere, L., Petrizzo, M.R., Damsté, J.S.S., Schouten, S., Erba, E., Silva, I.P., 2004. Organic-carbon deposition in the cretaceous of the Ionian basin, NW Greece: the Paquier Event (OAE 1b) revisited. Geol. Mag. 141, 401–416.
Vavelidis, M., 1988. Geochemistry of trace elements in galenas from Ag-containing lead-zinc ore deposits in Sifnos (Greece). Bull. Geol. Soc. 329–341.
Vavelidis, M., Amstutz, G.C., 1983. New genetic investigations on the Pb-Zn deposits of Thasos (Greece). In: mineral Deposits of the Alps and of the Alpine Epoch in Europe. Springer, Berlin, Heidelberg, pp. 359–365.
Vavelidis, M., Gialoglou, G., Melfos, V., Wagner, G.A., 1996. Goldgrube in Palaea Kavala Griechenland: entdeckung von Skaptehyle. Erzmetall 49, 547–554.
Vaxevanopoulos, M., 2017. Recording and Study of Ancient Mining Activity on Mount Pangaeon, E. Macedonia, Greece. Unpublished Doctoral dissertation. Aristotle University of Thessaloniki, Thessaloniki, Greece, p. 337 (in Greek).
Vaxevanopoulos, M., Vavelidis, M., Melfos, V., Malamidou, D., Pavlides, S., 2018. Ancient mining in gold-silver-copper deposits and metallurgical activity in Mavrokofi area, Pangaeon mount (NE Greece). In: Ben-Yosef, E. (Ed.), Mining for Ancient Copper: Essays in Memory of Beno Rothenberg. Tel Aviv. The Institute of Archaeology of Tel Aviv University.
Veranis, N., Tsamantouridis, P., 1991. Using Panning Method to the Exploration of Auriferous mineralizations of Krousia Metallogenic Province. Institute of Geology and mineral Exploration Internal Report (in Greek).
Voudouris, P., 2006. Comparative mineralogical study of Tertiary Te-rich epithermal and porphyry systems in northeastern Greece. mineral. Petrol. 87, 241–275.
Voudouris, P., Alfieris, D., 2005. New porphyry—Cu±Mo occurrences in the north-eastern Aegean, Greece: ore mineralogy and epithermal relationships. In: mineral Deposit Research: Meeting the Global Challenge. Springer, Berlin, Heidelberg, pp. 473–476.
Voudouris, P., Manoukian, E., Veligrakis, Th, Sakellaris, G.A., Koutsovitis, P., Falalakis, G., 2014. Carbonate-replacement and vein-type Pb-Zn-Ag-Au mineralization at syros island, Cyclades: mineralogical and geochemical constraints. In: Proceedings 20th CBGA Congress, Tirana, Albania, Buletinii Shkencave Gjeologjike Special Issue, vol. 1, pp. 183–186.
Voudouris, P., Mavrogonatos, C., Spry, P.G., Baker, T., Melfos, V., Klemd, R., Haase, K., Repstock, A., Djiba, A., Bismayer, U., Tarantola, A., Scheffer, C., Moritz, R., Kouzmanov, K., Alfieris, D., Papavassiliou, K., Schaarschmidt, A., Galanopoulos, E.,

Galanos, E., Kolodziejczyk, J., Stergiou, C., Melfou, M., 2019. Porphyry and epithermal deposits in Greece: an overview, new discoveries, and mineralogical constraints on their genesis. Ore Geol. Rev. 107, 654–691.
Voudouris, P., Melfos, V., Mavrogonatos, C., Photiades, A., Moraiti, E., Rieck, B., Kolitsch, U., Tarantola, A., Scheffer, C., Morin, D., Vanderhaeghe, O., Spry, P., Ross, J., Soukis, K., Vaxevanopoulos, M., Pekov, I., Chykanov, N., Magganas, A., Kati, M., Katerinopoulos, A., Zaimis, S., 2021. The Lavrion mines: a unique site of geological and mineralogical heritage. minerals 11 (1), 76.
Voudouris, P., Melfos, V., Spry, P.G., Bonsall, T., Tarkian, M., Economou-Eliopoulos, M., 2008a. mineralogical and fluid inclusion constraints on the evolution of the Plaka intrusion-related ore system, Lavrion, Greece. mineral. Petrol. 93 (1–2), 79–110.
Voudouris, P., Melfos, V., Spry, P.G., Bonsall, T.A., Tarkian, M., Solomos, C., 2008b. Carbonate-replacement Pb–Zn–Ag±Aumineralization in the kamariza area, Lavrion, Greece: mineralogy and thermochemical conditions of formation. mineral. Petrol. 94 (1–2), 85.
Voudouris, P., Spry, P.G., Sakellaris, G.A., Mavrogonatos, C., 2011. A cervelleite-like mineral and other Ag-Cu-Te-S minerals [Ag_2CuTeS and $(Ag, Cu)_2TeS$] in gold bearing veins in metamorphic rocks of the Cycladic Blueschist Unit, Kallianou, Evia Island, Greece. mineral. Petrol. 101, 169–183.
Voudouris, P., Skarpelis, N., 1998. Epithermal gold-silver mineralization at Perama (Thrace) and Lemnos island. Geol Soc Greece Bull 32, 125–135.
Voudouris, P., Tarkian, M., Arikas, K., 2006. mineralogy of telluride-bearing epithermal ores in Kassiteres-Sappes area, western Thrace, Greece. mineral. Petrol. 87, 31–52.
Vryniotis, D., 1978. Έκθεση προκαταρκτικών εργασιών για την σκοπιμότητα πραγματοποίσης γεωχημικής έρευνας στην περιοχή Αλμυροποτάμου Ν. Εύβοιας. I.G.M. E. Athens (In Greek).
Wagner, G.A., Gentner, W., Gropengiesser, H., Gale, N.H., 1980. Early bronze age lead–silver mining and metallurgy in the Aegean. In: Craddock, P.T. (Ed.), Scientific Studies in Early Mining and Extractive Metallurgy, vol. 20. British Museum Occasional Paper, pp. 63–86.
Wagner, G.A., Weisgerber, G., 1985. Silber, Blei und Gold auf Sifnos, prähistorische und antike Metallproduktion, Der Anschnitt, Beiheft 3. Deutsches Bergbau-Museum, Bochum.
Antike Edel- und Buntmetallgewinnung auf Thasos. In: Wagner, G.A., Weisgerber, G. (Eds.), 1988. Der Anschnitt: Beiheft 6 (Veröffentlichung aus dem Deutschen Bergbau-Museum Nr. 42). Bochum 1988.
Wagner, G.A., Pernicka, E., Vavelidis, M., Baranyi, I., Bassiakos, I., 1986. Archaeometallurgische Untersuchungen auf Chalkidiki. Anschnitt 38 (H5–6), 166–186.
Wilkinson, J., 2013. Sediment-hosted zinc-lead mineralization: processes and perspectives: processes and perspectives. In: Treatise on Geochemistry. Elsevier Ltd.
Wind, S.C., Schneider, D.A., Hannington, M.D., McFarlane, C.R., 2020. Regional similarities in lead isotopes and trace elements in galena of the Cyclades mineral District, Greece with implications for the underlying basement. Lithos 366, 105559.
Xydopoulos, I., 2016. The Eastern Macedonian border in Alexander I's reign. In: ΗΧΑΔΙΝ. *Τιμητικός τόμος για τη Στέλλα Δρούγου*. Athens. (In Greek).